SHARPP

Solar Heliospheric Activity Research and Prediction Program

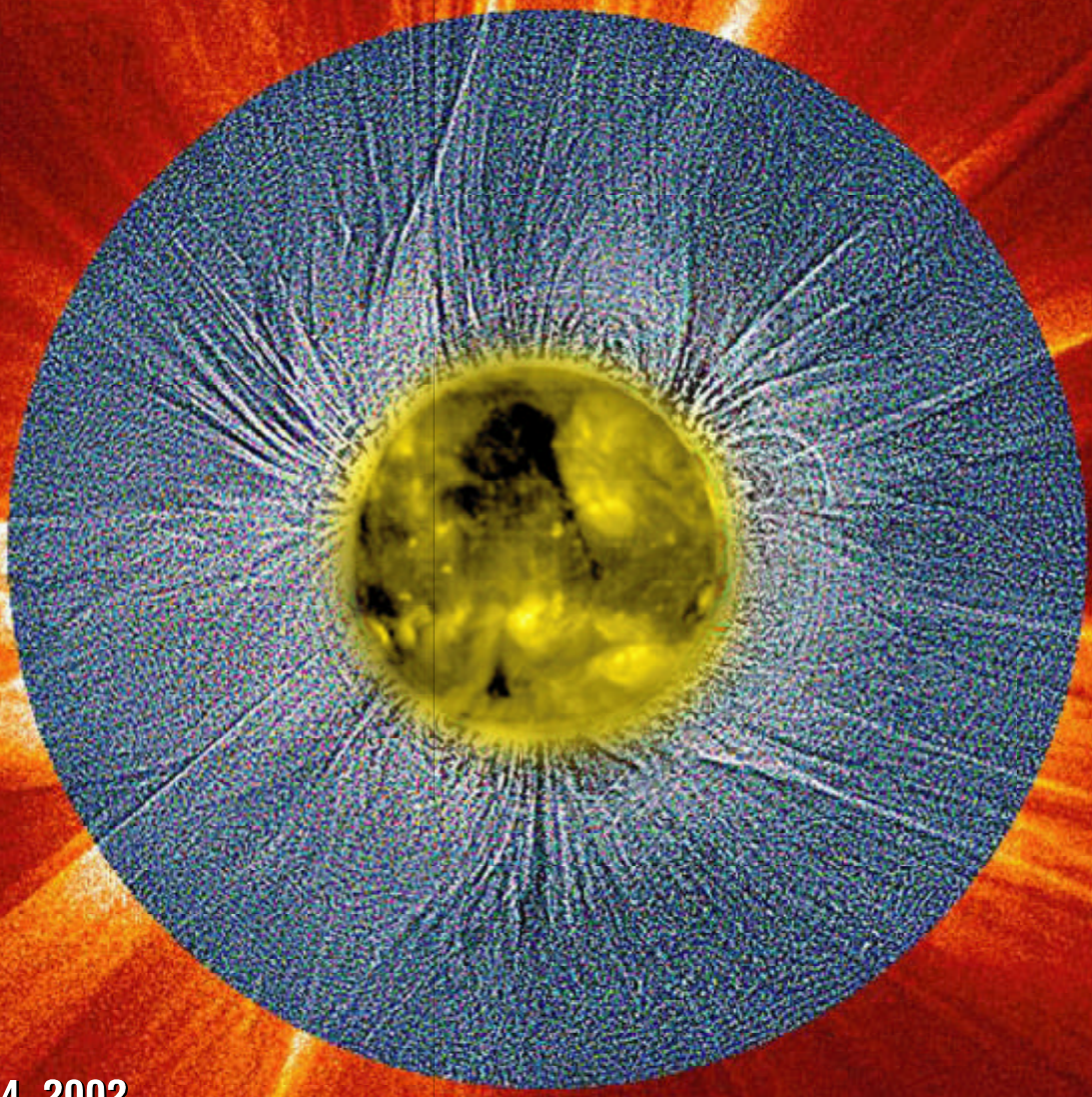

April 24, 2002

Submitted in response to
NASA AO 02-OSS-01
for the Solar Dynamics Observatory

Submitted by the Naval Research Laboratory
Russell A. Howard, Principal Investigator

76-T-581-02

Table of Contents

1. Science Investigation

1.1 Executive Summary. Understanding the Sun and its variation has been the primary goal of many National Aeronautics and Space Administration (NASA) missions over four decades, yielding an ever-clearer picture of the physics behind a wide range of active and quiescent phenomena. During this time, societal as well as scientific needs have evolved in response to this knowledge and to increasing recognition of the importance of global change to life on Earth. International Living with a Star (ILWS) is unique among NASA programs in its dual emphasis on both research and utility - supporting Sun Earth Connections (SEC) research addressing questions with impact to society. To meet this challenge, ILWS must go beyond traditional compartmentalized research to explore the processes and phenomena coupling the Sun, Heliosphere, and near-Earth environment. This systems approach demands an unprecedented level of continuity and integration not only in instrument capabilities but also in theory, modeling, and data analysis. The Solar Dynamics Observatory (SDO), the flagship mission of ILWS, will carry the first instrument package dedicated to deciphering the coupling between the Sun and the Heliosphere.

The Solar-Heliospheric Activity Research and Prediction Program (SHARPP) proposed here provides essential elements of the observational and theoretical suite required to meet the primary goals of SDO: to determine how the Sun drives Space Weather (SWx) and global change, and to understand how and why the Sun varies. The three closely integrated instruments comprising SHARPP are the Atmospheric Imaging Assembly (AIA), Extreme Ultraviolet (EUV) Coronagraph (ECOR)[1], and the white light (Kontinuerlich-corona) Coronagraph (KCOR). Thus SHARPP contains two top-priority instruments in the SDO strawman payload, and provides essential support for a third (Solar Irradiance Experiment, [SIE]). SHARPP has been designed specifically to provide high spatial and temporal resolution observations of the complete solar atmosphere and its coupling to the heliosphere (from the chromosphere to well into the open-field wind) and to deliver state-of-art numerical tools that can model this solar-heliospheric interaction. The development of 3D MHD and visualization Software (S/W) is nearly complete, so these powerful tools will be available at no cost to NASA, the SEC community, and the SHARPP team well before launch.

The SHARPP team has proposed a low risk, low cost (to NASA) approach to satisfy major goals of the SDO program. The international instrument team is highly experienced, having delivered similar instruments for spaceflight since the 1970's. NRL has extensive experience in managing such teams and will be responsible for all interfaces between SHARPP and the SDO project and the spacecraft. The minimal interdependence between the US and European H/W designs facilitates simple interfaces and minimizes ITAR-related issues among the participating institutions.

SHARPP takes advantage of the high telemetry and nearly constant solar viewing to construct an unprecedented program addressing the fundamental objectives of the SDO mission. The high spatial resolution, high cadence AIA corrects the observational limitations of both SOHO/EIT and TRACE. It covers a broad range of temperatures simultaneously with the same spatial resolution as TRACE, but with a view of the whole solar disk and a very high cadence. AIA then is ideally suited to observe the rapidly evolving coronal structures responsible for key components of solar variability. As we demonstrate in this proposal, the specific wavelengths selected for AIA have been optimized to trace the flow of energy from the chromosphere through the corona. The other component of SHARPP is the suite of high cadence coronagraphs called the SHARPP Coronagraph Experiment (SCORE). It consists of a traditional visible light coronagraph, KCOR, and a pioneering EUV coronagraph, ECOR[1]. KCOR is identical to the SECCHI/COR2, itself an improvement on the LASCO/C2 coronagraph. ECOR shows the coupling between the AIA disk observations and the KCOR coronal imaging, and, for the first time, maps the upper extent of the same coronal structures viewed in the local corona by AIA.

We believe that the investigations described in this proposal can successfully meet the ILWS dual-use challenge, in part because NRL has a long history of performing basic research that is required by the Department of Defense (DoD) to demonstrate a direct societal impact. Examples include the Wang-Sheeley model for predicting So-

1. ECOR was not selected for the SDO mission. Modeling (e.g., the Adaptively Refined MHD Solver, ARMS) of the inner corona will be used in place of ECOR observations.

lar Wind (SW) speeds and the LASCO halo Coronal Mass Ejections (CMEs) warnings, which are now used by NOAA as operational tools. A key advantage of SHARPP is that the next generation of modeling tools are being developed—the Adaptively Refined MHD Solver (ARMS). ARMS is a S/W package for SWx modeling that is optimized to run on parallel architectures and uses the latest computational technology. and is integrated with the Heliospace/Geospace packages Air Force Research Laboratory for visualizing and analyzing SWx over the full Sun-Earth domain. ARMS/Heliospace will be the core technology for the SHARPP modeling effort; they represent many work-years that will be available to SDO at no cost to NASA.

SHARPP will also be an invaluable asset to ongoing solar missions, providing synergistic benefits that would not accrue from any one mission alone. SHARPP will contribute to meeting the objectives of Solar-B (given it is still operating) by adding continuous observations of the upper corona and higher cadence, and continuous observations of the lower corona. Secondly, SHARPP will act as the STEREO "third eye", placing a third *identical* coronagraph, KCOR, between the twin STEREO spacecraft. SHARPP will observe from Earth's vantage point, which will be essential for STEREO to reconstruct the 3D structure of Earth-directed SWx. STEREO, in turn, will provide the directivity, velocity and topology of halo CMEs, which SDO will need to determine signatures of potentially geoeffective solar activity.

SDO will also benefit greatly from the coordination and integration with the STEREO mission. Because the same NRL team will be responsible for both SECCHI and SHARPP, NASA will be guaranteed the highest possible level of coordination, consistency, and cost-effectiveness throughout all common aspects of these missions, from instrument building to data handling and reduction, and data dissemination to the community.

Table 1-1. Investigative Strengths of SHARPP

Instruments	• SHARPP: Continuous, simultaneous coverage of overlapping Fields of View (FOV) from the disk to $15R_{\odot}$ • Atmospheric Imaging Array (AIA): UV/EUV imaging of the solar atmosphere at temperatures from 0.02 to ~3 MK (up to ~20 MK during flares) using a suite of individual telescopes for each spectral line. This concept permits simultaneous imaging of the solar disk (to $1.4R_{\odot}$) at 10-s cadence. • EUV Coronagraph (ECOR): Pioneering EUV coronagraphic imaging of ~1 MK plasmas in the middle corona (1.2-$3R_{\odot}$) with 2.8 arcsec pixels and 10 sec maximum (2 min synoptic) cadence. • White Light Coronagraph (KCOR): White-light coronagraphic imaging from 2 to $15R_{\odot}$, with a 8 sec maximum (1 min synoptic) cadence for a full pB sequence. • Slight modifications of the SECCHI main electronics and camera electronics for cost-effectiveness and efficiency. Data compression and packetization is performed within the cameras to offload the computing requirement on a central processor. • Cost-effective data archiving strategy enables efficient and open data access. Automated screening algorithms will identify various activity signatures, such as CME, unusual temperature ratios, etc., create alerts to the operational community, and generate hypertext lists of interesting periods for retrospective studies by the scientific community.
Theory & Modeling	• Adaptively Refined MHD Solver (ARMS): State-of-the-art, massively parallel 3D MHD code with adaptive mesh refinement, being developed as part of DoD Common High Performance computing S/W Support Initiative. • Heliospace: State-of-the-art S/W package for visualization and analysis of SWx data (real or simulated) over the full Sun-Earth domain developed by the Air Force Research Laboratory.
Heritage	• Successful international collaborations including the same institutions to design, build, and fly similar instruments on SOHO (EIT and LASCO) and STEREO (SECCHI EUVI and COR2). • AIA: Built SOHO/EIT and components of SECCHI/EUVI, improved TRACE. • ECOR: Combined experience with Fe XII imaging on EIT/SOHO and extensive coronagraphic experience. • KCOR: Built first space coronagraph, followed by coronagraphs for OSO-7, P78-1/SOLWIND, and SOHO/LASCO; identical coronagraph under construction for STEREO/SECCHI. • Electronics: Most boards already in development for SECCHI or are qualified under X2000 program. • Camera: Modification to boards under development for SECCHI will be able to run the CCDs at 2 MHz and permit simultaneous quadrant readout.
Science Team	• Discoverers of CMEs, EUV waves, halo CMEs. • World leaders in EUV and white light imaging of corona, and end-to-end science based on these data. • Pioneers in using EUV imaging and spectroscopy to measure and determine the sources of solar EUV irradiance. • World leaders in large-scale numerical modeling essential for closure between solar observations and theory. • History of transitioning basic research to meet the needs of DoD and NOAA.

SHARPP Investigations

- *How and why does the Sun vary?*
- *How does the Sun drive the solar wind?*
- *What solar mechanisms lead to global change at Earth?*

SHARPP Applications

- *Significantly improve space weather disturbance predictions*
- *Provide a scientific foundation for irradiance variability proxies*
- *Offer modeling and visualization tool to the community*

The combined ECOR/AIA FOV

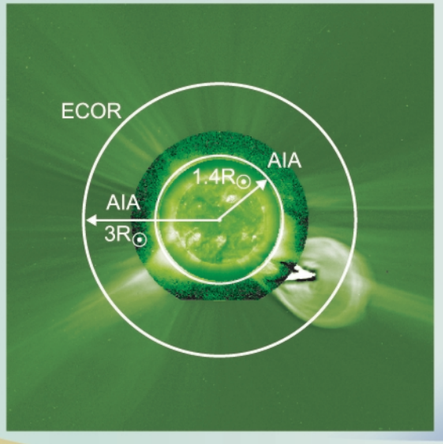

The combined SHARPP FOV

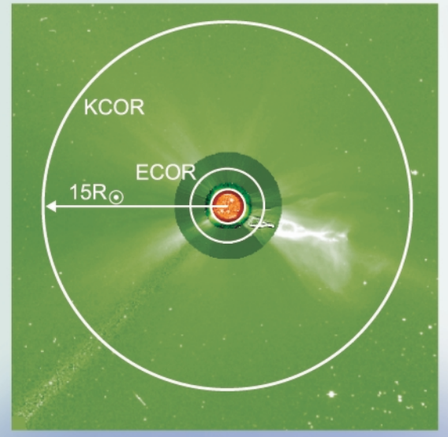

Provide a "third eye" for STEREO

AIA provides complete coverage of the solar atmosphere from the chromosphere to the corona

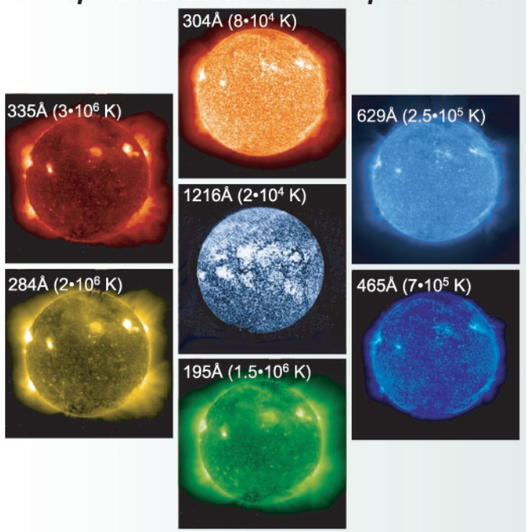

Model the CME initiation process

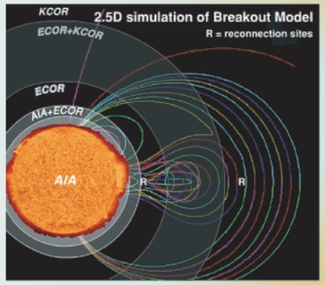

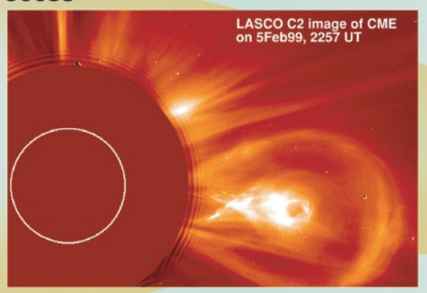

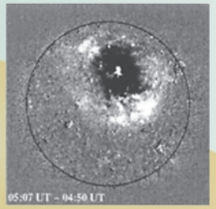

Follow the early evolution of CMEs

Monitor and assess geoeffectiveness of CMEs

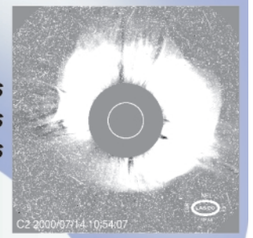

Locate and track the sites of particle acceleration

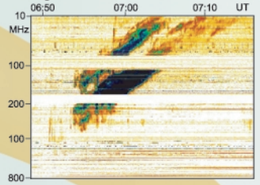

Solar wind variability

Geomagneti Storms

Short-term variability

SEPs

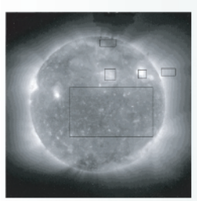

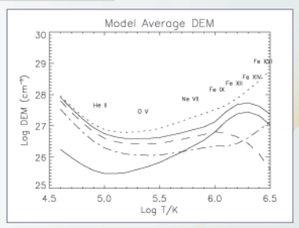

AIA DEM analysis deciphers the thermal structure of the atmosphere

Flare emissions and structure

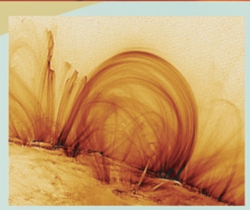

Coronal heating mechanisms

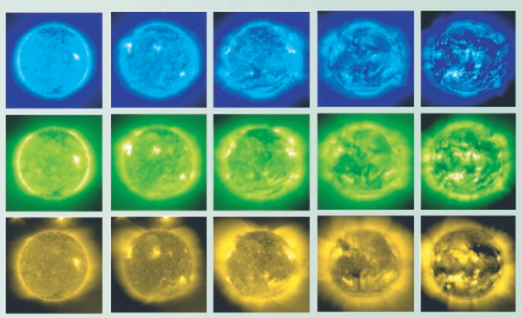

AIA calibrated images determine the sources of irradiance through the solar cycle

Long-term irradiance variability

Global Change

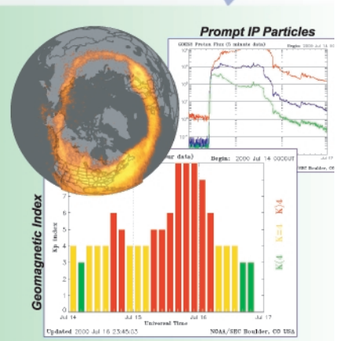

Dramatically improve space weather forecasting

Table FO2-3. SHARPP Mass Summary

Component	Mass (kg)	Included Reserve	Heritage
AIA Assembly			
MAGRITTE Components (5 EUV & 1 VUV Telescopes)	24.26	20%	CSL
Structure, Legs and Thermal Items	7.74	20%	CSL
SPECTRE Components	3.11	20%	CSL
Structure, Legs and Thermal Items	4.08	20%	CSL
Guide Telescope (2 units)	3.29	15%	SECCHI
AIA CEB	6.82	15%	RAL (SECCHI CEB)
Harnesses	3.94		8% of Total Mass
AIA Assembly Mass Subtotal	53.25		
SCORE Assembly			
KCOR	8.53	10%	SECCHI
ECOR Components*			
SCORE Structure & Mounts	6.84	15%	HYTEC (SECCHI SCIP)
SCORE CEB	3.88	15%	RAL (SECCHI CEB)
Harnesses	3.07		8% of Total Mass
SCORE Assembly Mass Subtotal	22.32		
SHEB Assembly			
SHEB Assembly Mass Subtotal	23.86	15%	SECCHI
SHARPP Total	99.43		

Table FO2-4. SHARPP Power Summary

Component	Average Power (W)	Peak Power (W)	Included Reserve
AIA Assembly	73.38	97.96	
Guide Telescope	1.18	1.18	15%
AIA CEB	59.70	84.28	15%
Heaters	12.50	12.50	20%
AIA Assembly Power Subtotal	73.38	97.96	
SCORE Assembly			
SCORE CEB	14.50	20.47	15%
Heaters	12.50	12.50	20%
SCORE Assembly Power Subtotal	27.00	32.97	
SHEB Assembly			15%
SHEB Assembly Power Subtotal	35.29	51.00	
SHARPP Total	135.67	181.93	

Table FO2-5. SHARPP Volume Summary

Component	Length (CM)	Width (CM)	Height (CM)
AIA Assembly			
Magritte	90.2	109.2	12.5
SPECTRE	150.0	50.0	15.0
AIA CEB	19.0	19.0	15.0
SCORE Assembly	137.2	50.7	40.6
SHEB Assembly	58.3	30.5	20.4

Table FO2-6.

SHARPP	Cadence (sec)	Images per Cadence	Compression	Avg. TLM (Mbps)
AIA	10	7	2.3	69.7
ECOR*				
KCOR	60	3	2.3	1.3
			Total TLM (Mbps)	71.0

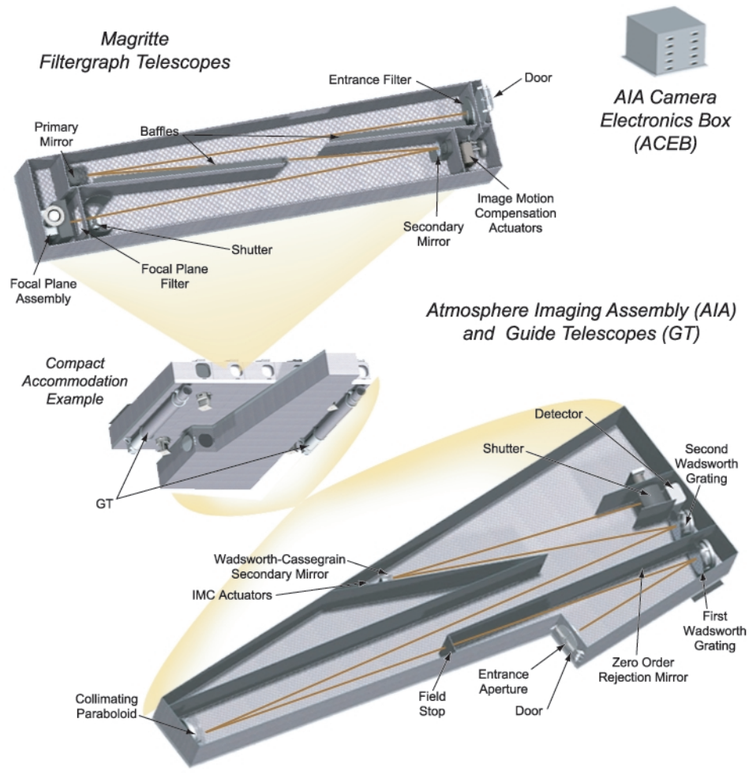

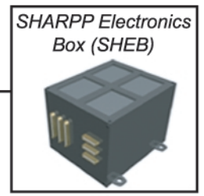

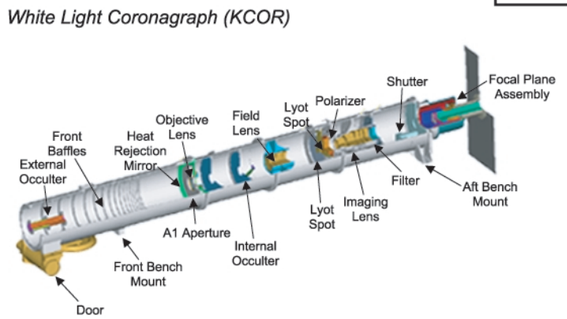

Table FO2-1. SHARPP Instrument Characteristics

	AIA	ECOR*	KCOR
Instrument Type	• 6 Filtergraphs (Magritte) • 1 Spectroheliograph (SPECTRE) • 2 Guide Telescopes for IMC		Externally occulted Lyot coronagraph
Lead Institution	CSL		NRL
Related Projects	SOHO, EIT, SECCHI, XMM OMC		OSO-7, SOL-WIND, LASCO, SECCHI
Observable	Emission Line Chromosphere, Transition Region & Corona		K-corona, F-corona & CMEs
Data Products	Images, Maps of Temperature & EM		pB, B
FOV ($R_\odot$)	• Full disk to 1.4 (Magritte) • Full disk to 1.1 (SPECTRE)		2 - 15
Spatial Scale (arcsec)	• 0.66 (Magritte) • 0.60 (SPECTRE)		14
Focal Plane Array	4096 x 4096		2048 x 2048
Bandpass (Å)	• Magritte - Fe XII 195 - Fe XVI 335 - Fe XV 284 - Ne VII 465 - He II 304 - Ly-α 1216 • SPECTRE OV 629 • GT WL Continuum 6700 Å (500 Å FWHM)		6500-7500
Exposure Times	<8 sec		~3 sec, 3 required for pB
Synoptic Cadence	• AIA 10 sec • GT 50 Hz		1 min
Maximum Cadence (sec)	2.5 sec full disk, full resolution		8 sec
Aperture (mm)	• 45 mm (EUV), 60 mm (Ly-α) (Magritte) • 80 mm (OV) (SPECTRE) • 39 mm GT		30.5 mm
efl	• 3.75 (Magritte) • 4.00 SPECTRE • 1.30 GT		0.19
Straylight/Disk Light Rejection	N/A		10^{-8} $B/B_\odot$
Required absolute pointing	1 arcmin		45″ (occulter positioning)
Required pointing stability	<1.2″ during exposures (8 sec). Requires GT/IMC		1.5″ during pB seq. (25 sec)
Required long term pointing	N/A		50″ over a month (for background model)
Mechanism Count	7 shutters, 7 one shot doors, 6 filter covers		1 shutter, 1 rotating polarizer, 1 door
Camera	4k x 4k, 12 µm, 13 bit/pix		2k x 2k, 13.5 µm, 14 bit/pix

Table FO2-3. AIA Channels With Photon Statistics

Channel Å	Temperature Response (Pk)	QS Response S/N (8 sec)	AS Response S/N (8 sec)
195	1.5 MK	20	100
284	2.0 MK	N/A	50
304	0.08 MK	30	114
335	3.0 MK	N/A	41
465	0.7 MK	8	26
630	0.25 MK	9	26
1216	20,000 K	34	100

*ECOR was not selected for SDO.

1.2 Scientific Goals and Objectives.

Key elements of the SDO Mission are SHARPP primary goals
• How are CMEs triggered?
• Which CMEs cause geomagnetic storms?
• What are the sources of EUV spectral irradiance variability?
• What generates the highly variable SW?

1.2.1 Magnetic Eruptions. Although coronagraphs have revealed much about the nature of CMEs, the largest and most destructive form of solar eruption, we still do not understand these complex events and their relation to other forms of solar activity. Theory and observations clearly indicate that the Sun's magnetic field provides the energy that drives CMEs, but the field structure and the mechanism for eruption remain controversial. These issues must be resolved before we can make substantial progress toward predicting those magnetic eruptions that affect Earth and its environment through geomagnetic storms, energetic particle events, and radiative impact on the upper atmosphere.

Our integrated program will be focused on the three fundamental phases of solar magnetic eruptions: *initiation, evolution/propagation, SWx and near-Earth impact*. For each phase discussed below, we introduce key overarching scientific questions and then discuss specific problems to be addressed by SHARPP. Note, however, that SHARPP will be a broad community facility with enormous research potential, far beyond the research programs described in this proposal that emphasize our team's particular expertise. SHARPP is a complete ILWS investigation, including both basic science and its SWx application. Our goal with SHARPP and ARMS/Heliospace is not only to understand CME initiation and development, but also to develop a prototype for future-generation prediction models.

1.2.1.1 Initiation. A primary focus of SHARPP will be to solve the long-standing problem of understanding CME initiation. The well-established association between magnetic eruptions and regions of strong nonpotentiality highly concentrated around certain segments of neutral lines (Patty & Hagyard 1986; Gary et al. 1987; Schmeider et al. 1996; Martin & McAllister 1997; Canfield et al. 1999; Falconer et al. 2002) confirms theoretical conclusions that the energy for all major manifestations of coronal activity (CMEs, eruptive flares, filament ejections) must be stored in the coronal magnetic field. Prominences/filaments preferentially develop in these regions, giving rise to the term "filament channel" for the entire stressed magnetic configuration regardless of whether a prominence is actually present. For convenience we will use this term in its general sense throughout §1.2.

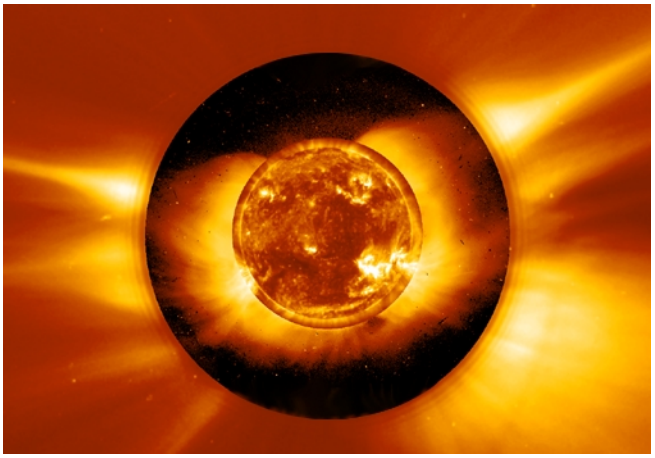

Figure 1-1. LASCO/EIT image on 04/16/98 showing the ~1MK solar disk, the inner E-corona and the outer K-corona

The underlying cause of all magnetic eruptions is the disruption of a force balance between the upward pressure of the strongly sheared/twisted magnetic field of a filament channel and a downward force due either to the magnetic tension of quasi-potential overlying coronal field or the weight of an overlying mass distribution (see Forbes 2000; Klimchuk 2001; Low 2001). The crucial point is that the upward pressure must increase slowly because the magnetic shear/twist is produced by photospheric evolution (shear flows and/or flux emergence). Therefore, fast removal of the coronal downward force is the only way to disrupt the balance sufficiently rapidly to cause a CME. All numerical simulations that have obtained eruption without simply driving the CME in real time use this method (Mikic & Linker 1994; Antiochos et al. 1999, and Amari et al. 2000), but the physics of the downward-force removal is far from understood. In the "magnetic breakout" model, the downward tension is removed by reconnection of the overlying field with neighboring flux systems (Antiochos 1998). In "flux rope" models, the tension is removed by magnetic reconnection of the overlying field with itself, either at the photosphere (Van Ballegooijen & Martens 1989; Forbes & Isenberg 1991) or as "tether cutting" somewhere below the erupting filament (Sturrock

1989; Moore & Roumeliotis 1992). In "mass-loading" models, magnetic buoyancy leads to the collapse of the overlying mass and the release of a rapidly rising flux rope (Low 1996; Wu et al. 1995, 1997; Dlamini & Wolfson 1999; Wolfson & Saran 1998).

These CME models differ significantly in their predictions of the timing and location of reconnection sites before and/or during eruption, the role and distribution of plasma, the amount and distribution of shear or twist in the magnetic field, and the topology and evolution of the flux systems involved. Therefore, the key to understanding and predicting the onset of CMEs is the *observation and modeling of the magnetic field and plasma evolution prior to eruption*. The three instruments comprising SHARPP have been designed to meet this challenge, by delivering fast cadence, high spatial resolution observations of the whole erupting structure, from the bottom of the filament channel to the outermost CME plasma. We describe below a sample research program that illustrates how we plan to attack the CME initiation problem with SHARPP. Note, however, that both SHARPP and ARMS/Heliospace are for the use by the entire community to investigate all CME models.

Sample Research Program: *Which CME initiation model is valid?* The program will consist of two steps: (1) analysis of SHARPP and other data sets for signatures unique to each model to determine which model (if any) is consistent with the observations; (2) simulation of the initiation of actual, well-observed, eruptive events with ARMS using the most viable models. This program will satisfy the dual use requirements of ILWS: raising our scientific understanding of CME initiation through detailed, rigorous comparison between simulation results and observations, and using our new knowledge of the most successful mechanism to create a prototype space-weather prediction tool. If we could accurately reproduce CME initiation *post facto*, we would be a long way towards predicting these eruptions.

The success of the program hinges on identifying a viable model, which in turn requires the specification of unambiguous diagnostics differentiating among competing theories. For mass-loading models, the critical signatures are the presence of a large mass in the corona before eruption, and the downfall of most of this mass during eruption. Due to its comprehensive temperature coverage, SHARPP will be ideal for testing this hypothesis. Coincident SHARPP and STEREO observations (if available) will allow us to view the material both at disk center in EUV and off the limb in white light for CMEs launched over a wide range of position angles. Furthermore, the fast cadence of SHARPP will enable highly accurate measurements of the amount of falling material during eruption. For the flux rope model, the decisive test is whether the magnetic field configuration of the erupting filament channel corresponds to that of a twisted flux rope. We will use two techniques to infer the magnetic topology. First, AIA and ECOR images of the coronal plasma structure, combined with extrapolations of HMI and Solar-B (if available) magnetograms, will reveal whether a flux rope is present. In addition, recent observations (Zirker et al. 1998; Martin 1998) and theoretical work (Antiochos et al. 1999b, 2000; Karpen et al. 2001) have shown that prominence condensations should be streaming constantly along the field, thus outlining the supporting structure. We will trace out the geometry of the field by following the proper motions of filament plasma in emission and/or absorption in all AIA channels. With the advantage of the AIA broad, simultaneous temperature coverage, we will be able to distinguish true motions from temperature changes.

For the breakout model, one key signature is the presence of reconnection in the corona. To look for this signature in a selected set of eruptive events, we must first extrapolate the photospheric fields, (i.e. HMI observations) into the corona and determine the evolving 3D topology of the pre-eruption field. The most crucial task is to identify the location(s) of coronal nulls/separators, if they exist (e.g., Fletcher et al. 2001). Then we will use SHARPP, in coordination with EUV spectroscopic coverage if available, to search for evidence of reconnection dynamics at the null before each eruption. We found evidence for such reconnection flows during one large eruptive flare observed by TRACE, but only a few frames showed these fast motions (Aulanier et al. 2000). High-cadence observations of many candidate events with SHARPP will tell us whether reconnection flows or other signatures (EUV "crinkles": Sterling & Moore 2001, and Sterling et al. 2001), are ubiquitous features of CME initiation. Although we favor the breakout model, the information on the pre-

eruption structure and evolution obtained by SHARPP will be essential for testing and refining any CME initiation mechanism.

1.2.1.2 Evolution/Propagation. After initiation, the passage of a CME through the corona and heliosphere alters both the coronal environment and the CME structure itself (Ostrcil & Pizzo 1999; Pizzo & Ostrcil 1999). On a global scale, CMEs might play a central role in the long-term evolution of the structure of the solar corona and heliosphere (Low 1996), and are the prime link between transient solar activity and large interplanetary and geomagnetic disturbances (Gosling 1993). One profound and controversial issue is whether reconnection is necessary or sufficient to prevent the continual barrage of magnetic eruptions from the Sun from causing steady flux build-up in the Heliosphere (McComas et al. 1991; Gosling 1999; Crooker et al. 2001). Clearly we must characterize and understand the initial magnetic configuration and acceleration mechanism at the Sun, and the processes that modify these as the CME traverses the corona and reaches the heliosphere, before developing reliable geoeffectiveness metrics or resolving the flux build-up conundrum. With SHARPP and the other SDO instruments, we will be able to follow, with comparable cadence, the CME and its surroundings from its initiation in the low atmosphere to its entrance into the SW for the first time. Because the bulk of the flux injected into the Heliosphere to form an interplanetary CME (ICME) probably comes from the large-scale closed coronal field overlying the eruption, rather than the relatively small flux of the erupting filament channel itself (Gopalswamy et al. 1998), the wide-ranging coronal coverage provided by the ECOR and KCOR is absolutely essential for investigating the evolution of CMEs and their coupling to the SW.

Using the low corona ($<2R_{\odot}$) magnetic structure detail obtained at high cadence by SHARPP, we will be able to determine how CMEs are accelerated after birth, and why different patterns for this acceleration exist (Sheeley et al. 1999; Andrews & Howard 2000). Impulsive, fast CMEs (often associated with large flares) travel with uniform or decelerating speeds, while gradual CMEs (often associated with prominence eruptions and streamer blowouts) accelerate gradually over a large distance. However, not all CMEs fit neatly into one class or the other (Plunkett 2001a). Moreover, it is

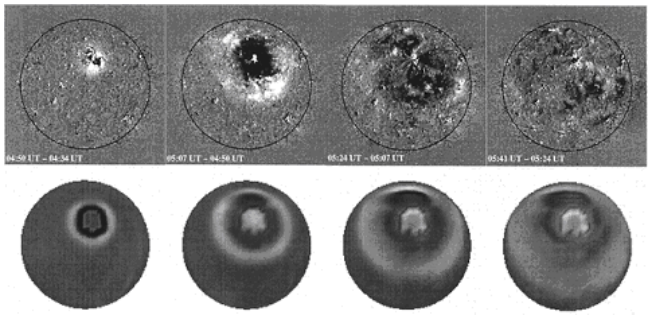

Figure 1-2. MHD simulation of "EIT" wave (Wu et al., 2001).

unclear whether different physical mechanisms trigger and accelerate each type of CME, or whether the same physics operates on different spatial and temporal scales in each case. We have begun to assess the energetics of all classes of CMEs with LASCO data (Vourlidas et al. 2000), but more complete diagnostics of the plasma and magnetic field from the chromosphere to the inner heliosphere are needed to characterize and identify the source(s) of the driving energy. These questions can be answered only through high cadence observations of the region where the initial acceleration must occur - at altitudes less than $2R_{\odot}$, below the occulting disk of all spaceborne white-light coronagraphs (St. Cyr et al., 1999). AIA and ECOR will provide these unprecedented observations for all CME events observed by KCOR. Greater understanding of the acceleration process is an important piece of the geoeffectiveness "puzzle": when our research has identified the most reliable early warning signs of impulsive CMEs, ILWS will be substantially closer to its goal of improving operational space-weather predictions.

We will also use SHARPP to illuminate CME-associated coronal phenomena whose relation to the eruption are still unclear - for example, the EUV "EIT waves" (Figure 1-2) and "coronal dimmings" now known to accompany many CMEs (Thompson et al. 1999; Hudson & Cliver 2001; Biesecker et al. 2002). Coincident EIT and Hα observations indicate that bright EUV waves and Moreton waves are coronal and chromospheric manifestation, respectively, of the same propagating disturbance (Thompson et al. 2000; Warmuth et al. 2001), most likely fast magnetosonic waves (Wu et al. 2001). However, the existence of slowly moving fronts and stationary emitting structures suggests that some EIT "waves" are not waves, but rather trace CME material displaced from the dimming regions (Delanneé & Aulanier 1999; Go-

palswamy et al. 1999). Coronal dimmings are areas that undergo a drop in intensity at times and locations roughly coincident with CME onset (Rust & Hildner 1976; Hudson et al. 1996; Harra & Sterling 2001). A "double dimming" often appears during an eruptive flare in an AR containing an S-shaped or sigmoid structure (Canfield et al. 1999), suggesting in some cases that each dimming is located at a footpoint of an ejected large-scale loop (Webb 2000). In other cases, however, the dimmings are not consistent with flux rope geometries (Hudson & Webb 1999; Kahler & Hudson 2001), thus illustrating the difficulty of deciphering complex eruptive topologies from presently available data. The EIT image cadence and spatial resolution are not sufficient to track the rapid early development of coronal waves and dimmings and higher-cadence observations are usually available only in one coronal emission band. AIA's improved spatial resolution over the full Sun and fast cadence, coupled with the complete, simultaneous temperature and height coverage of the entire SHARPP suite, meet the demands of tracing the flow of energy and mass between the chromosphere and the outer corona during eruptions.

Sample Research Program: *Do coronal dimmings mark the magnetic roots of CMEs?* The exciting discovery of coronal dimmings has raised fundamental questions about the large-scale rearrangement of magnetic flux during eruptions that cannot be answered with SOHO, TRACE, or Yohkoh. Specifically, we will analyze SHARPP data and perform 3D MHD simulations to determine whether dimmings are due to density depletion associated with the overall expansion of the erupting flux system (Hudson et al. 1996). Using AIA's simultaneous high-cadence images of the entire solar disk from 0.02 to 3 MK, we will measure the expansion speeds, areas, and other essential properties of these rapid and widespread events. AIA's observations in the transition-region lines (OV, Ne VII are sorely needed to establish what happens to the local plasma in cooler temperatures (< 1 MK), indicating how far down the magnetic field has been opened and how it closes down again. We will take advantage of the overlap between AIA's Fe XII disk images and ECOR's Fe XII coronagraphy to derive new insights into the 3D magnetic topology involved in the dimmings and their connection to the CME. The Fe XVI channel will also link, for the first time and at the same cadence, the 3-5 MK plasmas typically seen by Yohkoh/SXT and the ~2 MK corona seen by EIT and TRACE.

After our initiation studies (§1.2.1.1) have determined the most successful CME triggering model, the next logical step is to extend our 3D simulations of the eruption until it traverses the corona to $15R_{\odot}$. In particular, we will use these calculations to predict what happens to the overlying field after it is partially opened by a CME and what topological circumstances are needed to generate coronal dimmings. The plasma properties predicted by the ARMS simulations will be used to predict EUV and white-light emission for comparison with AIA observations of dimmings, with ECOR observations of the ~1.5 MK corona, and KCOR observations of the rising density enhancement comprising the white-light CME. Within the context of the breakout model, for example, we expect that specific sequencing of the associated observable manifestations of this process. This groundbreaking investigation will accomplish two important tasks that cannot be achieved with previous missions: to verify whether coronal dimmings indicate mass evacuation in the opening field, and to connect the pre-eruptive magnetic field topology at all heights to the CME topology as it enters the heliosphere. If coronal dimmings accurately map the footpoints of the magnetic field comprising the bulk of a CME, the ILWS program will have gained early indicators of CME strength and orientation, important pieces of the geoeffectiveness "puzzle".

1.2.1.3 Space Weather and Near-Earth Impact.

The interplanetary manifestations of fast Earth-directed CMEs are the major drivers of many SWx phenomena, including large, non-recurrent geomagnetic storms and solar energetic particles (SEPs). The vast majority of moderate and major storms are associated with CMEs originating within a few tens of degrees of the central meridian of the solar disk, as viewed from Earth, thus appearing in coronagraph images as "halo" events (Figure 1-3; Howard et al. 1982; Plunkett 2001b; Zhang at al. 2002). However, not all halo events produce measurable impacts at Earth: some lack critical component(s) that we have only begun to evaluate with LASCO and other existing data sets. The SHARPP coordinated observations from the solar surface to the outer corona will be essential for developing reliable markers of oncoming solar storms.

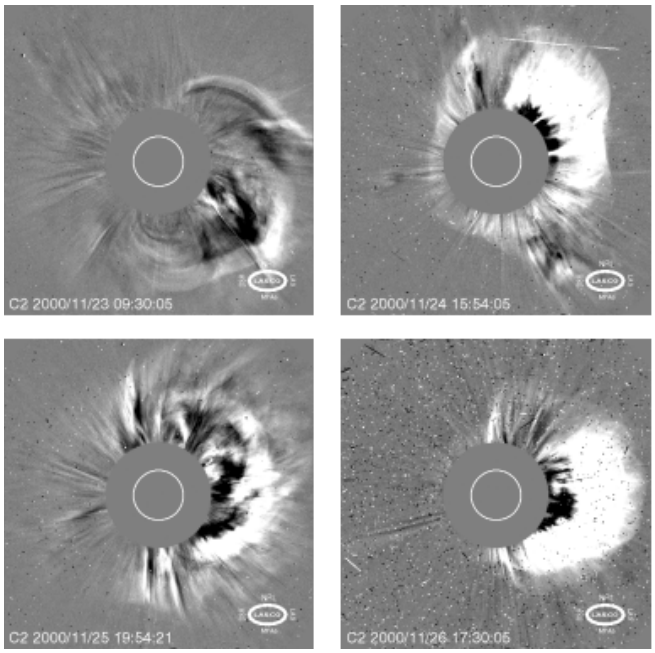

Figure 1-3. Halo CMEs observed by LASCO on successive days in November 2000.

The impact of halo CMEs depends strongly on the radial speed of the ejected plasma, and on the direction and strength of the embedded magnetic field. The most geoeffective CMEs are fast and/or have extended periods of southward magnetic field, either within the CME or in the compressed solar-wind plasma ahead of the CME structure (Gopalswamy et al. 2000, 2001). The radial speed of a halo CME is difficult to measure from coronagraph images alone because of projection effects. Several techniques have been developed recently to relate measurements of expansion speeds in the sky plane to radial speeds (Gopalswamy et al. 2000; Schwenn et al. 2001; Zhao et al. 2002). We will test and refine the utility of these techniques with images from the SECCHI coronagraphs, and we will utilize the resultant procedures to derive radial speeds of halo CMEs from ECOR and KCOR. In addition, the STEREO coronagraphs will measure proper motions of the same CMEs that appear as halo events in the SHARPP FOV, providing rigorous verification of our techniques.

As discussed in §1.2.1.2, the direction, and perhaps the strength, of the magnetic field in a halo CME might be inferred from SHARPP observations of structures in the inner corona both before and during eruption (Webb et al. 1999; McAllister et al. 2001). This, together with a magnetic field extrapolated from photospheric magnetograms (Li et al. 2001), can yield the magnetic structure and direction of the CME core. Another indicator might be the helicity (Leka et al. 1996; Canfield et al. 1999) or nonpotentiality (Falconer et al. 2002) of the pre-eruption flux system, which should be partially carried away with the eruption (Démoulin et al. 2002). We will explore the possibility of using helicity or nonpotentiality measurements as tools for identifying source regions likely to produce geoeffective SWx; with obvious LWS operational benefit.

Although frontside halo CMEs are directly responsible for large geomagnetic storms, fast and wide CMEs from a wide range of longitudes produce the most significant SEP storms (Kahler 1992; Gopalswamy et al. 2002). Impulsive SEP bursts, rich in high-Z ions, have long been observed to accompany impulsive solar flares without detectable CMEs (Reames 1999). Faint, narrow CMEs were recently discovered to be associated with some impulsive flaring and SEP events (Kahler et al. 2001), perhaps providing a useful tool for short-term forecasting purposes. The more intense and longer duration events, known as gradual SEP events, are clearly associated with the passage of a CME-driven shock through the corona and interplanetary space (Reames 1999). When these shocks are generated low in the atmosphere (Richardson & Cane, 1993), ECOR should be able to document their birth and propagation out to $3R_{\odot}$, thus aiding in identifying sites of SEP acceleration. SHARPP will provide new insights into these particle-producing CMEs and the associated shocks as they traverse the corona and enter the SW, the range spanned by KCOR.

Sample Research Program: *Which CMEs generate coronal shocks?* We will search for signatures of CME-associated shocks in the lower and middle corona with AIA and ECOR, augmented by available coincident meter-wave radio and energetic particle observations for additional confirmation of the shock properties. By collecting statistical information on, e.g., shock strength and speed, and testing for correlations with basic CME characteristics (width, speed, direction), we hope to further quantify easily detectable signatures unique to those CMEs with greatest potential for particle storms at Earth. This research program will be strengthened by coordination with STEREO: the SECCHI side views of Earth-directed CMEs, also monitored by SHARPP, will better determine the

geometry of the erupting magnetic field and the shock location within this topology. Moreover, ECOR may be able to detect the hot, dense shock front from limb CMEs viewed face-on by the SECCHI coronagraphs.

The CME models described in the previous two sections are uniquely able to investigate the initiation and propagation of CME-driven shocks in the corona. First, ARMS uses two powerful techniques (adaptive mesh refinement, and Flux Corrected Transport) that are well-suited for computing MHD shocks. Second, we will simulate shocks with the most viable CME model identified by our earlier analyses - a profound shift from previous a priori approaches to this problem. Finally, we will predict observable signatures of the shocks, e.g. velocity and emission intensity in AIA and ECOR passbands, to test whether the model is consistent with SHARPP observations and perhaps identify useful indicators of impulsive SEP output. The powerful combination of SHARPP and SECCHI will greatly enhance the quantity and accuracy of warnings of geoeffective SWx, enabling ILWS to add another key element to its solution of the geoeffectiveness puzzle.

1.2.2 Plasma Dynamics of the Solar Atmosphere. Our Sun affects Earth not only magnetically, as discussed above, but also radiatively. Although the variable EUV radiation from the Sun comprise less than 0.1% of the total solar irradiance, on average, they control the thermodynamics and chemistry of both the neutral and ionized components of Earth's upper atmosphere on timescales from minutes to the solar cycle (Banks & Kockarts 1973; Meier 1991). Solar Ly-α emission alone generates a significant part of the lower ionosphere (Rozanov et al., 2002), while He II 304 Å emission is the dominant source of ionization and heating in the thermosphere (Worden et al. 1999). Important space-weather consequences include the modification of radio signal propagation, which affects long-range communications, over-the-horizon radar surveillance, and positioning and navigation, and the modification of satellite drag, which affects tracking of space assets and debris, mission resource planning, and vehicle reentry.

Despite its importance, our *knowledge* of the solar EUV spectral irradiance - the time-dependent, disk-integrated level of enhancement over the entire EUV range - is fragmented, incomplete, and imprecise (Lean 1997). For example, although limited portions of the EUV spectrum produced by a few flares have been observed by space instruments (Skylab, OSO-7, SMM, SOHO), the flare EUV spectral irradiance, is barely known. While flares and CMEs are the primary short-term drivers of solar EUV variability (Bornmann et al. 1996), they cannot explain the correlations between solar and geospace variability on longer timescales. To answer this important question, we must turn to the spectral irradiance from emitting features on the non-flaring Sun. Full-disk images show that the EUV brightness varies with wavelength, spatial scale, location, and phase of the solar cycle. The most prominent features at all temperatures are the Active Regions (AR), but a varying, significant fraction of the EUV irradiance comes from the fainter but more widely distributed "Quiet Sun" active network (Lean et al. 1995, 1998). We know that this radiated energy comes from the solar interior, through the medium of the dynamo-driven magnetic field, but our current knowledge cannot bridge the gap between this general scenario and the societal need for accurate reconstruction and timely prediction of the EUV irradiance throughout the solar cycle.

Therefore, a primary goal of SHARPP is to develop a comprehensive understanding of the physical processes that structurally differentiate and heat ARs, the network, and the diffuse corona in between. The EUV spectral irradiance calculated from AIA, augmented by theoretical predictions based on relevant coronal-heating models, will be compared with SIE irradiance measurements to evaluate how well, or how poorly, our empirical approach and physical theories account for EUV irradiance variations. Here the strengths of our SHARPP suite become essential: with the continuous duty cycle and high telemetry rates of SDO, the irradiance monitors and magnetograph onboard, and the comprehensive temperature coverage, routine high cadence, and enormous composite FOV of SHARPP, at last we will be able to follow the energy flow sufficiently well to answer fundamental questions about how solar variability affects life on Earth.

1.2.2.1 Flares. At present, we barely know how the solar EUV spectral irradiance changes during a flare (see Meier et al. 2002). SOHO was not designed to observe flares, and TRACE's coverage of the EUV spectral range was not intended to produce irradiance measurements. SDO will be the

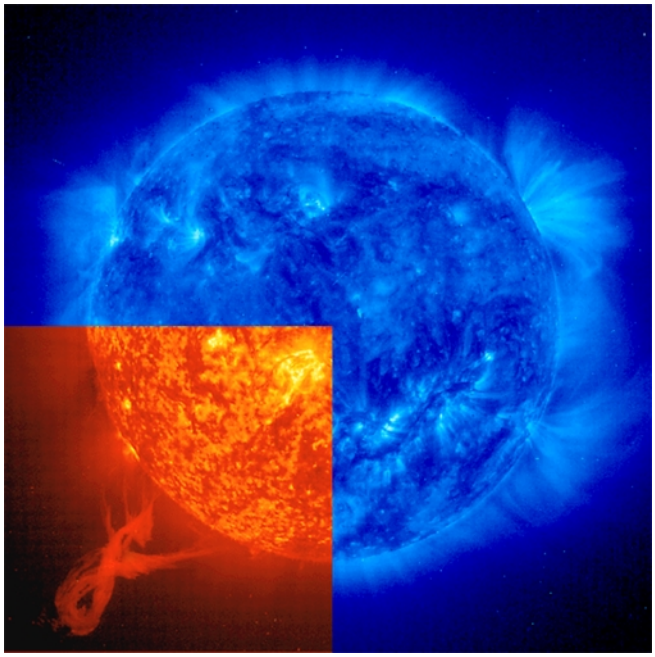

Figure 1-4. Composite of EIT 171 Å and 304 Å

first SEC mission required to measure and explain the Sun's variable spectral irradiance on flare timescales. We have designed SHARPP to meet this challenge on both fronts. Our efforts will be focused on identifying the mechanisms of energy release and transport in flares, and on clarifying the crucial links between flares and magnetic disruptions. With this knowledge we will not only understand how flares affect the EUV emission at 1 AU, but we also expect to provide guidance to the operational community to develop better physics-based indicators of the magnitude and duration of the associated perturbations of the terrestrial ionosphere and neutral atmosphere, meeting the dual-use requirements for the success of ILWS.

Yohkoh and TRACE have provided convincing evidence in support of the standard model for post-eruptive loops (Carmichael 1964; Sturrock 1966; Hirayama 1974; Kopp & Pneuman 1976; Tsuneta 1996), in which reconnection is a consequence of a magnetic eruption (§1.2.1). In this scenario, a flare is the manifestation of the plasma heating and mass motions that result from reconnection along the rising X-line in the current sheet separating the escaping eruption from the underlying growing arcade. As this X-line rises, successively higher loops with larger footpoint separations are activated. The newly reconnected field lines appear as a system of "growing" hot loops visible in both line and continuum emissions in the X-ray, EUV, and UV regimes, comprising the most important source of EUV irradiance during eruptive flares.

Through its ability to obtain simultaneous, high-cadence images of the solar disk in 7 passbands with AIA, and single-band off-limb images in one of these passbands (Fe XII) with ECOR, SHARPP will quantify the key observable characteristics of reconnection and energy transport in flare loops. As shown originally by the NRL S082-A, slitless spectrograph on Skylab and more recently by TRACE, the 195Å passband ordinarily dominated by Fe XII and other "normal" coronal lines can include Fe XXIV emission during flares. Therefore AIA can observe the superhot component (~20 MK) as well as the 0.02-3 MK plasma during flares. Not only will SHARPP flare observations have great value in themselves, but also they will superbly complement observations from Solar-B and RHESSI (if available), thus enabling combined attacks on fundamental problems in flare physics that could not be accomplished by the individual instruments alone. A recent in-depth study of EUV ribbons in one large eruptive flare, combining TRACE, SOHO, and Yohkoh data (Fletcher & Hudson 2001), shows the power of the type of coordinated observations that SDO will routinely obtain. For example, high-cadence AIA and ECOR observations of the Fe XXIV line, bolstered by coincident spectroscopic observations from UIS or EIS/Solar-B (if available), should reveal the reconnection jets formed above the post-eruption arcade - a major breakthrough in our understanding of magnetic reconnection in eruptive flares. In addition, AIA's imaging of impulsive O V and He II footpoint sources will be sufficiently rapid to be compared with cotemporal imaging of HXR (if available) or microwave (Bastian et al. 1998) emissions during impulsive flares, for the first time, providing long-awaited quantitative tests of flare models based on nonthermal electron transport (McClymont & Canfield, 1986; LaRosa & Emslie 1988).

Sample Research Program: *Which magnetic eruptions strongly affect the solar EUV spectral irradiance?* The most basic unanswered flare questions relevant to societal needs are why only a fraction of magnetic eruptions produce intense EUV enhancements, and why the spatial distribution of EUV emission in each flaring topology is so inhomogeneous. We will address these issues with both the observational and theoretical facets

of the SHARPP program. AIA's wide temperature coverage will enable us to trace the magnetic topology and energy distribution of flare loops, from the hottest looptops to their footpoints. We will relate all of the coronal, transition region, and chromospheric flare features to the underlying magnetic field extrapolated from HMI or Solar-B magnetograms.

Observations alone are not sufficient to make progress in elucidating the physics of eruptive flares, however. On the theoretical and modeling front, the standard model has progressed little beyond its initial qualitative 2D depiction. We know from our own reconnection modeling experience that 3D reconnection is significantly different from its 2D counterpart (Dahlburg et al. 1997; Karpen et al. 1998; Linton et al. 2001), and that properly modeling this complex process in the solar environment requires adaptive mesh refinement and other state-of-the-art features of our ARMS code. One well-observed aspect of post-eruptive arcades that can only be addressed in 3D is the inhomogeneity of the EUV and SXR emission (McKenzie & Hudson 1999; Fletcher & Hudson 2001), presumably caused by the patchiness of reconnection along the current sheet between the rising plasmoid and the post-eruptive loops beneath (Klimchuk 1996; Figure 1-5). We can also estimate the time-varying EUV line and continuum emission from post-eruptive loops in the most promising eruption model identified in our studies (§1.2.1.1 & 1.2.1.2). These calculations, based on a selection of observed events, will produce detailed predictions for comparison with the SHARPP observations, thus critically evaluating the viability of the standard model for post-eruption loops. To make these results useful for ILWS, we will collaborate with the SWx community to identify easily observed markers of high geoeffectiveness - e.g., specific magnetic configurations, flux levels, or other indicators that reliably correlate with high EUV output, thus finally quantifying the major transient source of EUV spectral irradiance.

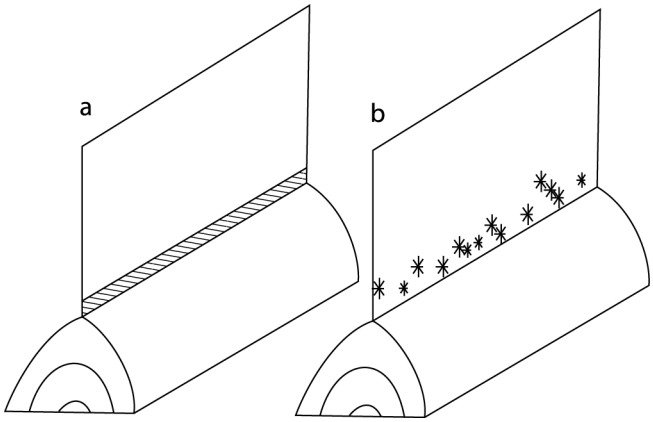

Figure 1-5. Illustration of patchy reconnection in post-eruption loops (Klimchuk 1996).

1.2.2.2 Active Regions (AR). Current observations have gathered stunning and detailed information about coronal loops. Paradoxically, they leave us with a very confused understanding of these fundamental elements of the active corona. Even the most basic questions concerning the internal structure and temporal behavior of loops are still unanswered. These observational characteristics relate directly to the properties of coronal heating in ARs, most notably its variability and distribution in time and space. Only by answering these questions can we hope to understand the physical mechanisms responsible for the Sun's variable EUV radiations.

Coronal imaging and spectroscopy have made great strides to date on this fundamental issue, but further progress has been prohibited by instrumental and telemetry limitations. For imaging observations, the biggest problems have been inadequate temperature resolution and coverage. As a result, loops observed by Yohkoh were found to be equally compatible with two completely different coronal-heating scenarios, steady and uniform heating (Klimchuk & Porter 1995; Porter & Klimchuk 1995) or nanoflaring (see below; Cargill & Klimchuk 1997). One well-studied loop was found to be consistent with uniform heating (Priest et al. 2000), heating concentrated near the footpoints (Aschwanden 2001), and heating concentrated near the loop top (Reale 2002). Clearly we need not only excellent spatial and temporal resolution but also comprehensive temperature coverage from chromospheric values to a few MK if we are to determine whether loop plasmas are static or dynamic (Aschwanden et al. 2000) and how temperature varies along and across loops (Neupert et al., 1998), key determinants of competing heating models. AIA has been designed specifically to match these needs.

Leading candidates for the physical mechanism responsible for heating coronal loops basically fall into two categories: waves and current dissipation/magnetic reconnection. Observational evidence for magnetoacoustic waves propagating

along coronal structures (DeForest & Gurman 1998; Berghmans & Clette 1999; Ofman et al. 1999) has renewed interest in the question whether nonresonant MHD waves can heat coronal loops (De Moortel et al. 2000; Tskilauris & Nakariakov 2001). Coronal loops also might be heated by the resonant absorption of Alfvén waves (Ionson 1978; Davila 1987; Hollweg & Yang 1988; Poedts et al. 1997; Belien et al. 1999; Erdélyi et al. 2001). An important prerequisite for wave heating is, obviously, the presence of waves of the correct frequency and energy flux. Currently available temporal resolution does not allow the detection of oscillations with periods shorter than a few minutes, however, and the sensitivity is marginal even for lower frequency waves within the nominally observable range. Several sources for such waves have been postulated, but observations capable of making such measurements have remained frustratingly out of reach. Furthermore, existing cadence and temperature-range limitations prevent monitoring of temporal variations in the entire multithermal structure.

The second category, relying on small energy bursts in the corona, is often denoted "nanoflaring" because the required energy per event is of order one billionth the energy of a large flare. In this scenario, photospheric motions, coronal turbulence, or other field-line tangling mechanisms (Parker 1983, 1988; Galsgaard & Nordlund 1996; Longcope 1998; Einaudi & Velli 1999) create the small-scale structure responsible for magnetic energy dissipation. However, the rapidity and miniature scale of the underlying current structures make direct detection of nanoflares an extreme observational challenge. Statistical studies of a wide range of transient coronal brightenings in various wavelengths, extrapolated to the low end of the energy spectrum, have been used to test the nanoflare concept, but the present uncertainties are too great to definitively prove or rule out this heating mechanism (Berghmans et al. 1998; Benz & Krucker 2002; Krasnoselskikh et al. 2002). Spectroscopy offers another means to search for distinct signatures of nanoflare heating in loops (Klimchuk & Cargill 2001), but spectroscopy alone will not reveal the heating distribution.

Sample Research Program: *Are AR loops heated by MHD waves or nanoflares?* By combining fundamentally new observations from SHARPP with theoretical modeling of wave and nanoflare heating mechanisms, we expect to finally understand the nature and physical origin of coronal heating in ARs, and hence their contribution to the EUV spectral irradiance (§1.2.2.4). In particular, we will use SHARPP's measurements and modeling, which will not be possible with other solar missions preceding SDO, to build a long-awaited quantitative foundation for critically evaluating heating scenarios that rely on waves and nanoflares.

The high cadence and signal sensitivities of AIA will enable us to detect higher frequency waves in coronal loops than ever before (periods ~20 s) and to evaluate their energetics, while the near-100% duty cycle and high data rates planned for SDO will enable us to obtain markedly better coverage of the pertinent frequency range of the wave spectrum from the chromospheric footpoints to the loop apex. Global resonance periods for coronal loops typically range from ~10-100 s (Ofman & Davila 1996), so our studies of resonance absorption will be focused on the longer (lower global frequency) loops. We will complement this observational program with a 3D modeling effort with ARMS, built upon and extended well beyond our earlier studies (Ofman et al. 1998), that will aid in interpreting the observations and in critically evaluating the viability of wave mechanisms for loop heating.

In parallel, the AIA unprecedented combination of wide FOV, high spatial resolution and fast cadence will extend the observed spectrum of small-scale energy release closer to the true nanoflare level. Furthermore, we will use the temperature diagnostic power of SHARPP to perform a definitive test of the nanoflare heating model. If loops were composed of many unresolved, nanoflare-heated strands, then a wide variety of strand temperatures should coexist within a single loop structure. Detection (or not) of multiple temperatures would therefore provide a definitive test of the nanoflare idea. The 7 AIA channels covering the temperature range from 0.02 to 3 MK will allow us to quantitatively assess the nanoflare model more rigorously than ever before. In particular, OV and Ne VII emission distributed throughout a loop, rather than in the canonical transition region above the footpoints, is a clear signature of nanoflaring. We also will compare the SHARPP loop observations with the results of ARMS simulations of specific nanoflare heating mechanisms, such as the forma-

tion and dissipation of intense current layers in twisted, internally kinking coronal flux loops. Once we understand the heating of individual loops, we will begin to reconstruct the complex, evolving collections of loops that comprise ARs. The large-scale magnetic configuration, extrapolated via ARMS from HMI magnetograms, will provide the framework for testing and refining our plasma emission reconstructions.

1.2.2.3 Quiet Sun. In the so-called "Quiet" Sun (QS), the energetic and dynamic signatures of magnetic energy release and associated heating are present but are more muted in scale and magnitude than in ARs. Building upon earlier EUV spectral observations by rocket-borne instrumentation (Brueckner & Bartoe 1983), SOHO and TRACE revealed a wide spectrum of small-scale structures and energy bursts in the quiet solar atmosphere associated with the evolving "magnetic carpet" discovered by SOHO/MDI (Title & Schrijver 1998): blinkers, network flares, transient loop brightenings, explosive events, and macrospicules, just to name the more common labels (Harrison 1997; Krucker et al. 1997; Innes et al. 1997; Chae et al. 1999, 2000; Seaton et al. 2001). To some extent this apparent diversity reflects the different techniques and instruments with which they were detected (Berghmans et al. 2001). As noted above for AR loops, however, it also may reflect intrinsic differences between the two most likely underlying physical processes: magnetic reconnection and waves (Priest 1999). SHARPP has been designed to clarify how the "steady state" corona outside ARs is generated and why its EUV emissions vary with time. By establishing the spatial correspondence between structures and events at widely different temperatures, and by recording the rapid evolution of these structures simultaneously at those temperatures, we will be able to map the magnetic topologies in which quiet-Sun activity and heating occur. We will establish the connection between the flux tube dynamics of the magnetic carpet and the resulting local coronal response by analyzing cotemporal AIA images together with photospheric magnetograms from HMI.

As a specific example (discussed in more detail below), we will use AIA and ECOR to achieve a better understanding of the wide-ranging family of coronal jets, which have been observed in X-rays (Shibata et al. 1992), in the EUV (Wang et al. 1998; Winebarger et al. 2001), in white-light (Wang et al. 1998; Wood et al. 1999; Wang & Sheeley 2002), and in O VI and Ly-α (Dobrzycka et al. 2000). Only the brightest, longest-lived jets could be detected to the edge of the EIT FOV, and in rare cases, beyond the LASCO C2 occulting disk, so these examples do not necessarily represent the majority. At the other end of the energy distribution, faint, rapid EUV jets have been observed inside the polar coronal holes (Moses et al. 1997). These events exhibit striking similarities to the explosive events and coronal bullets initially identified by NRL's HRTS experiment (Brueckner & Bartoe 1983) and studied further with SUMER (Innes et al. 1997; Winebarger et al. 1999), but their rapidity and small size strain the capabilities of pre-SDO imaging instruments. Unlike previous studies (Dere et al. 1991; Chae et al. 2000), some recent observations suggest that these small-scale events are associated not only with the magnetic network but also with the cell interiors (Krucker & Benz 1998; Benz & Krucker 1998). This is puzzling because the strongest magnetic field outside AR, and hence the largest source of free energy, is in the network. The evolving temperature and density distributions in and around the jets also are poorly known. As a result, we don't know basic facts such as whether the jets become invisible because they are heating up or cooling down. SHARPP will resolve these issues because it will obtain simultaneous EUV imaging over the entire relevant temperature range at the same cadence as HMI, including transition-region temperatures where solar plasmas are most likely to be dynamic.

Sample Research Program: *Does small-scale reconnection heat the quiet corona?* We will use analysis of SHARPP and other SDO observations, coupled with 3D MHD modeling with ARMS, to definitively establish the role of reconnecting flux systems in heating and driving flows in the QS. First, we will locate clear, well-observed examples of coronal jets with different characteristics in AIA images. Simultaneous magnetograms from HMI will reveal the underlying magnetic topology and its evolution (if any) throughout each transient burst. We expect that interacting bipoles, or a small bipole interacting with open field, are the most likely scenarios (Karpen et al. 1998; Yokoyama & Shibata 1999), but only the observations can prove or disprove this assumption. Sequences of

AIA images containing these jets will be calibrated, corrected for solar rotation, and used to create animations showing the evolving jet and its environment. We will derive temperatures for the jets and their source regions from simultaneous images in different emission lines, thus identifying where the heating begins and how the released energy propagates throughout the reconnecting configurations. We will determine the transverse velocity component from proper motions in AIA images, and line-of-sight flow speeds from EUV spectra recorded by UIS or Solar-B/EIS, if available. These observations will clarify how the magnetic topology of the interacting systems dictates the physical appearance of these events, the fraction of energy devoted to heating vs flows, and the important relation between these small-scale bursts, and the larger-scale magnetic topology of the Sun outside ARs.

In parallel, we will model the reconnection process with ARMS, and derive estimates of the resulting mass and energy fluxes injected into the surrounding corona (including wave fluxes). These simulations, which are natural extensions of our 2.5D simulations of reconnecting arcades as drivers of quiet-Sun activity (Karpen et al. 1995, 1996, 1998), will be initialized with the observed pre-event magnetic configurations. In addition, the sophisticated visualization capabilities of ARMS/Heliospace will allow us to present and interpret the physical properties of the model in ways that are most consistent with the AIA. The energetics of the observed and simulated events will be compared, to test and refine our understanding of how magnetic reconnection contributes to quiet-Sun dynamics and heating, and hence to the EUV spectral irradiance discussed next.

1.2.2.4 Source of Spectral Irradiance. The Sun's EUV emission is clearly related to the level of solar activity and varies by factors of 2-10, depending upon wavelength, over the 11-year solar cycle (Hochedez et al. 2002). It would be simple to assume that the EUV irradiance is directly proportional to the total area covered by ARs, but more careful investigations have revealed that the truth is more complicated. As discussed in §1.2.2.2, all AR loops are not alike, so there is no reason to expect the collective EUV spectra of groups of loops to be the same. At minimum, most of the EUV irradiance clearly does not come from ARs. Therefore, both the quiet and active Sun are important components of solar variability. Finally, we note that the very nature of the 11-year solar cycle is not well understood nor reliably predicted. Although some progress was made with SOHO toward linking subsurface processes with chromospheric and coronal activity (Schrijver 2001), many more years of continuous, stable observations are needed to detect, measure, and understand solar-cycle variability.

SDO presents both a challenge and an opportunity to make substantial progress on these problems. SHARPP's contribution to the radiative targets of SDO and ILWS will be two-fold: to measure and identify the sources of EUV irradiance throughout the mission lifetime and to provide essential cross-calibration support for the onboard irradiance monitors (the SIE instruments). In lieu of adequate monitoring to date, semi-empirical models of the variable spectrum have been developed based on proxies such as the Ly-α and 10.7-cm radio fluxes (Hinteregger et al. 1981; Tobiska & Eparvier 1998; Warren et al. 1996, 2001). While this approach has been useful in the short term, the resulting uncertainties are unacceptable for SWx applications (Lean et al. 2002). The SHARPP team has been at the forefront of developing efficient, flexible, quantitative techniques for identifying important solar components, e.g., flares, ARs, coronal holes, and QS areas, and computing their contributions to EUV irradiance (Warren et al. 2001; Cook & Newmark 2002; Hochedez et al. 2002; Newmark et al. 2002; Thompson et al. 2002). Preliminary investigations have established that one approach successfully models the impact of flares on EUV irradiance (Meier et al. 2002). For another highly promising DEM-based methodology, we found excellent agreement between the predicted irradiance history and the SEM/SOHO irradiance observations over the entire test period (Figure 1-6). The SHARPP team continues to pursue these promising proto-operational technologies, as substantial improvements over existing proxies. In addition, AIA will continuously image the Sun in the two most important spectral lines affecting our planetary atmosphere: Ly-α and He II 304Å. Although the physics of chromospheric heating and radiative transport responsible for these emissions is beyond the scope of SHARPP, we will use AIA images to identify and quantify the primary sources of these key lines over a range

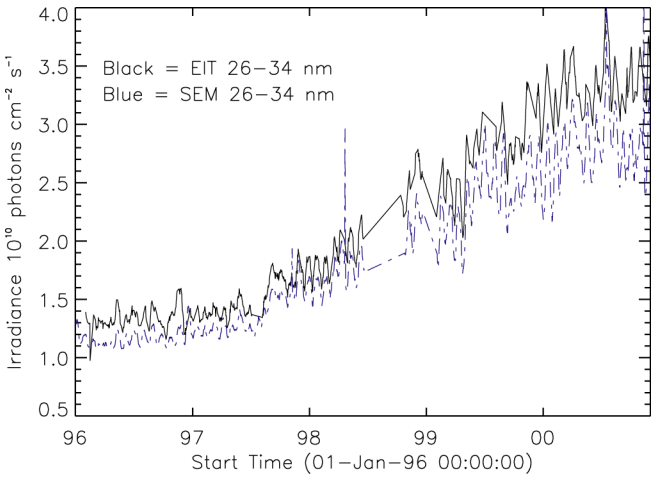

Figure 1-6. Comparison of SOHO/SEM 26-34 nm observations and SOHO/EIT DEM derived model (Newmark et al., 2002)

of timescales and spatial scales inaccessible to previous missions.

By combining the AIA narrow-band imaging with SIE's narrow-band EUV irradiance measurements, SDO also gains another valuable benefit: the two instruments will be cross-calibrated and their radiometric stability will be maintained throughout the mission lifetime, thus avoiding the incompatibilities and discrepancies that have plagued earlier attempts at long-term irradiance monitoring (Baley et al., 2000; Solomon et al., 2001). This crucial task will be aided by specifying the passbands of the SIE to match those of the AIA, as has been done for the proposed EVE experiment (J. Lean, personal communication). We plan to work closely with the SIE team to derive maximum benefit from our complementary irradiance investigations. The leverage and scientific progress to be gained throughout the mission by this coupled approach cannot be overstated.

Sample Research Program: *Are cool AR loops and the QS network significant sources of EUV spectral irradiance?* Accurate real-time specification and advance forecasting of the solar irradiance and its effects at Earth will be accomplished only by applying our comprehensive understanding of chromospheric, transition-region, and coronal heating, gained in part from the studies outlined in earlier Sections, to determining the disk-integrated EUV radiation from the Sun throughout a solar cycle. For SDO, we will work with the SIE team to characterize the primary sources of the irradiance measured by SIE over an unprecedented range of timescales from 10 s to the mission lifetime. Within this large-scale effort, we have identified two unsolved problems that exemplify the dual-use approach at the heart of ILWS: deciphering the contribution of cool solar plasmas to the AR irradiance and establishing the varying source(s) of QS irradiance.

The least understood component of the EUV spectral irradiance from ARs is the emission produced by coronal plasmas below 1 MK. For reasons as yet unknown, the character of the AR appears to change profoundly between 0.2 and 0.7 MK (Feldman et al. 1982; Laming et al. 1995; Brosius et al. 1996; Mason et al. 1997; Matthews et al. 2001). Theory suggests two viable solutions to the static loop equations - low loops entirely occupied by cool (under 0.2 MK) plasma in addition to the standard hot loops (Antiochos & Noci 1986) - but no observations to date have been capable of testing whether cool loops are a substantial component of the active corona. SOHO has shown that cool loop plasmas are highly dynamic (Brekke et al. 1997), so all temperatures must be viewed at the same time to differentiate between the effects of steady flows vs plasma cooling or heating. Therefore, we plan to use SHARPP to sample ARs over the 0.02 - 3 MK range simultaneously, focusing on the important region between 0.2 and 0.7 MK covered by AIA's O V and Ne VII channels, with sufficient spatial resolution and FOV to see both the smallest and largest AR structures. By coupling these groundbreaking cool-loop studies with the first-principles reconstruction of the hot component of AR outlined in §1.2.2.2, we will finally be able to understand and predict the AR sources of EUV irradiance.

SHARPP also offers an unprecedented opportunity to detect, measure, and understand the quiet-Sun contribution to the solar EUV irradiance. The supergranular network (suppressed in ARs) was recognized recently as the most probable source of the non-facular EUV emission (Lean et al. 1995, 1998; Veselovsky et al. 2001), but more work is needed to determine which parts of the network are responsible and how the variations are tied to subphotospheric processes. AIA's high-resolution image sequences will reveal systematic trends in the number, distribution, and topology of small-scale brightenings that contribute to the quiet-Sun EUV emission (§1.2.2.3), while comparison with HMI sequences will reveal the underlying connec-

tions to the magnetic carpet. The computational investigations outlined in §1.2.2.3 (among others) will determine the physical process or processes responsible for converting magnetic energy into heating of the quiet corona, and will yield quantitative measures of the mass and energy fluxes resulting from those processes on scales ranging from elementary flux tubes to supergranules. These observational and theoretical studies by SHARPP are essential for constructing a comprehensive picture of the QS sources of EUV irradiance throughout the solar cycle.

1.2.3 The Sun-Heliosphere Connection. A primary objective of SDO is to relate the structure and dynamics of the corona to the near-Earth structure and dynamics of the SW and SHARPP will be the only SDO component capable of determining this aspect of the Sun-Earth Connection. SHARPP's powerful combination of overlapping observations from the solar surface to 15 $R_\odot$ and 3D numerical modeling and visualization will be focussed on understanding and quantifying two primary issues: the evolution and heliospheric coupling of the large-scale magnetic field in the outer corona, and the origins of the SW.

The coronal streamer belt essentially delineates the Sun's magnetic neutral line and its extension into the heliospheric current sheet (HCS), thus linking the activity belt of the corona with the inner Heliosphere. This structure is constantly evolving on timescales from magnetic eruptions (§1.2.1) to the solar cycle, and is carried to Earth by the supersonic SW (Smith 2001). To date, streamers have been observed only as 2D projections onto the plane of the sky, hence limiting our ability to decipher their evolving 3D magnetic and plasma structure. The upcoming STEREO mission will obtain crucial information on the 3D configuration and slow evolution of streamers, by white-light imaging from two separate vantage points of the associated density concentrations; after the SDO launch, KCOR will provide an unprecedented view from a third vantage point of the same streamers being observed by STEREO. However, we cannot evaluate the full energetics and dynamics of the streamer belt through occulted white-light observations alone. 3D modeling of the corona is becoming more sophisticated (Linker et al., 1999; Mikic et al., 1999; Liewer et al., 2001), but key elements of this ever-changing structure are inadequately observed and exceedingly difficult to compute. The SHARPP suite offers an unprecedented opportunity to tackle these problems, primarily due to its unparalleled cadence and coverage from the closed field regions forming the streamer base to the critical cusp area and beyond, and to its integrated, state-of-the-art theory/modelling component uniquely qualified to interpret and explain these observations. Therefore, a key priority for SHARPP is to decipher how the magnetic topology is formed and modified in the crucial zone between 1.5 and 5 $R_\odot$.

Identification of the source regions of the SW remains a fundamental and controversial issue that can be resolved only through the coordinated observations that SHARPP and the other SDO instruments can provide. Coronal holes are generally considered the primary source regions of the fast wind ($v > 500$ km s^{-1}; Krieger et al. 1973; Nolte et al. 1976), but some have proposed that the fast wind can also emanate from open field throughout the Sun (Habbal et al., 1997; Woo & Habbal 1999). The slow wind is more complex, for reasons still debated: the inner slow wind (closest to the HCS) is highly variable and often has typical coronal abundances, suggesting an origin in closed field regions (Raymond et al. 1997; Li et al. 1998; Schwadron et al. 1999), while the outer slow wind is less filamentary and has poorly determined abundance properties, suggesting an origin at the boundaries between polar holes and the streamers (Wang 1994; Habbal et al. 1997; Ofman 2000). This simple division of the wind into fast and slow components is most applicable at solar minimum, when the dominant coronal holes are large and located at the poles. At maximum, the picture is considerably murkier because coronal holes are smaller, more numerous, and distributed over most of the solar surface (Neugebauer et al. 2002), including transient holes opened by magnetic eruptions (Kahler & Hudson 2001). The characteristics of the SW affect transient and recurrent SWx (Webb 1995), and influence the heliospheric passage and near-Earth impact of CMEs and SEPs (§1.2.1.3). A second key priority for SHARPP, then, is to understand where and how all components of the SW are generated at its base.

1.2.3.1 Streamers and the Slow Wind. SHARPP will be uniquely equipped to thoroughly study and comprehend how both components of the slow wind are generated in the context of large-scale coronal evolution. It will be the first instrument

suite capable of observing the fundamental but poorly understood phenomenon of slow active-region loop expansion (Uchida et al. 1992; Klimchuk et al. 1994). Theory and 2D simulations suggest that this process naturally leads to episodic opening of the outermost closed magnetic flux, once it is elevated to a height where the enhanced gas-to-magnetic pressure ratio exceeds unity, thus providing the inner slow wind (Wang et al. 1998; Suess et al. 1996, 1999).

The opening of the field associated with loop expansion probably involves magnetic reconnection. Support for this hypothesis comes from in situ measurements of variations in the HCS that have been interpreted as evidence for multiple small flux ropes (Crooker et al. 1993), and outflowing "blobs" seen by LASCO in the outer corona near 2-5$R_\odot$ (Sheeley et al. 1997; Wang et al. 1999; Einaudi et al. 1999; van Aalst et al. 1999; Wu et al. 2000). Definitive understanding of active-region expansion, reconnection, and their roles in producing the highly variable slow wind awaits combined observations of the type that SHARPP will obtain. White-light coronagraph images by themselves are not sufficient to address this problem, because the observed electron-scattered emission includes contributions from all plasma along the line-of-sight, regardless of temperature, thus obscuring or confusing foreground and background structures. In contrast, the reconnection site should stand out in ECOR's FeXII images because the associated heating should elevate the local plasma temperature well above the coronal background.

AR expansion is but one aspect of the general problem of how magnetic flux changes from closed to open and vice versa. We know such conversions are commonplace because the boundaries of coronal holes are evolving all the time, partially counteracting the shearing effects of differential rotation, but how this happens is largely a mystery (Wang & Sheeley 1993; Kahler & Hudson 2001). Recent investigations combining LASCO and EIT observations with MDI and ground-based magnetograms have revealed a new phenomenon, coronal inflows (Figure 1-7), with profound implications for the global restructuring of the coronal field (Wang et al. 1999; Sheeley & Wang 2001; Sheeley et al. 2001). These fascinating events have been interpreted as signatures of two long suspected, but previously unconfirmed processes (Nash et al. 1988; Wang & Sheeley 1993; Wang et al. 2000

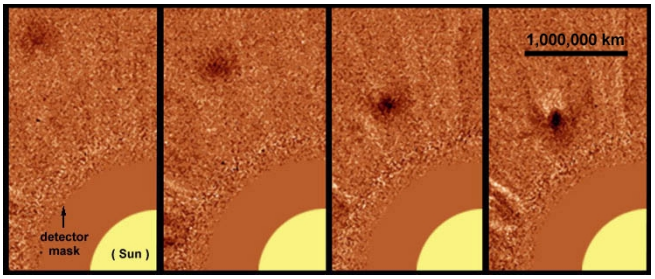

Figure 1-7. Coronal inflow in the LASCO/C2 FOV

a,b): magnetic reconnection between open field lines, closing down flux that was initially opened by AR expansion, reconnection between open and closed flux at coronal hole boundaries, driven by flux-transport processes in the photosphere. Because of the gap between the height at which coronal loops could be seen in EIT and the inner edge of the LASCO C2 coronagraph (2.5$R_\odot$), however, inflows presently cannot be followed as close to the Sun as needed to verify their coupling to changes in the chromospheric and photospheric field.

Sample Research Program: *Does reconnection generate the outer and inner slow wind?* With SHARPP, we will finally be able to test our ideas on the role of reconnection in the evolution of streamers and the generation of the slow wind. We will identify and trace the magnetic and plasma structure of inflows from the upper corona to their chromospheric footprints with simultaneous images taken by KCOR (down to 2.5$R_\odot$) and AIA (below 1.4$R_\odot$). We will also look for key signatures of plasma heating at reconnection sites in ECOR and AIA images (§1.2.1.1), together with UIS or Solar B-EIS velocity diagnostics (if available), thus establishing whether reconnection is indeed the underlying mechanism. For example, AIA images in emission lines of low and high first-ionization potential (FIP) elements (Fe XII and Ne VII) will reveal the origins of plasma observed at different heights, thus indicating whether plasma has been transferred from closed to open field lines. Simultaneous observations of emission lines from low- and high-FIP elements would enable us to confirm and extend these powerful abundance-sensitive diagnostics (Young & Mason 1997; Parenti et al. 2000). We will model this reconnection scenario with ARMS, as described in §1.2.2.3 for QS jets, and will test its viability by comparing the predicted plasma evolution with the same properties extracted or inferred from SHARPP observations.

Coincident HMI measurements of photospheric fields will be used to initialize 3D calculations of their time-varying coronal extrapolation, providing another important test of closure between our model and the data. Note that the SHARPP integrated theory/modeling component will be far superior to existing computational treatments of streamer evolution, due to the ARMS ability to resolve the critical cusp region substantially better than existing fixed-grid codes, to its incorporation of crucial thermodynamical terms, and to its unrestricted 3D capabilities. This research will reveal whether the outer slow wind is indeed formed by reconnection at streamer boundaries, and whether the inner slow wind is indeed the end-product of expansion and reconnection of AR loops at or beyond the streamer cusp.

1.2.3.2 Coronal Holes and the Fast Wind. Coronal holes have long been identified as the primary source regions of the fast SW, but only recently have the fundamental solar roots of this system been explored in detail. SOHO observations have shown that the coronal velocity structure is linked with the chromospheric magnetic network, with the largest outflow velocities occurring along network boundaries and in the darkest (least dense) regions; at greater heights, the fast wind is associated with the darker, interplume regions (Hassler et al. 1999; Landi et al. 1999; Patsourakos & Vial 2000; Wilhelm et al. 2000). EIT observations of the polar coronal holes also have raised the possibility that coronal jets produced by reconnection events in the network not only might heat the quiet corona, as discussed in §1.2.2.3, but also might provide a significant fraction of the SW mass flux (Koutchmy et al. 1997; Wang et al. 1998; Dobrzycka et al. 2002). The precise connection between these important observations cannot be established with existing instruments (SOHO, TRACE) or those planned for Solar-B or STEREO, however, because of this lack of high-cadence, simultaneous imaging and spectroscopy at all relevant temperatures and heights.

SHARPP will be ideally suited to resolve outstanding questions about the mechanism(s) responsible for heating and accelerating the ambient plasma in open-field regions close to the Sun (within the sonic point). In particular, we will explore the possible roles of two processes - MHD waves and magnetic reconnection - in heating and initially driving the coronal-hole plasma that is accelerated farther out to become the fast wind (Parker 1991; Wang 1998). A sample research program geared toward testing the reconnection scenario is discussed below, so we concentrate here on wave-based mechanisms. Slow MHD waves can carry significant energy flux on open field lines, so they may be important for the acceleration of the fast SW. Fast waves, on the other hand, dissipate more quickly, thus contributing to heating at lower heights. Thus far, only long period (10-70 min) intensity fluctuations have been detected in plumes and interplume regions, but nothing is known about higher frequency and/or lower amplitude variations in these structures (Ofman et al. 1997, 2000a.b.; DeForest & Gurman 1998; Banerjee et al. 2000, 2001a,b). To establish the effects of MHD waves on the coronal plasma and possible contributions to the SW, we need to know whether the observed variations are truly due to MHD waves, whether different types of waves are found in different parts of coronal holes, whether they begin at the solar surface or higher up, and how they are generated and dissipated. Although intriguing clues have been derived from the SOHO observations referenced above, these studies have been limited in spatial coverage (slit size), temporal range, and sensitivity. AIA observations will be able to search for waves in coronal holes on a global scale, at frequencies as high as 0.05 Hz, over the entire range from chromospheric to coronal temperatures at once. ECOR and KCOR will extend these observations further into the corona, providing an unsurpassed, comprehensive picture of MHD waves and their effects in corona holes.

Sample Research Program: *Does reconnection heat coronal holes and start the fast wind?* A common thread of this proposal is how magnetic reconnection converts the Sun's magnetic free energy into heating, flows, waves, and nonthermal particle acceleration. To ensure maximum benefits from SHARPP's integrated program, we have designed the SHARPP research program to progress from universally applicable lessons about reconnection to specific applications. In the case of coronal holes, the connection to our QS studies is straightforward: can the effects of the reconnection postulated to drive jets in the lower solar atmosphere extend to the magnetically linked plasmas higher in the corona? A similar mechanism has been proposed to power the fast wind (e.g., Mullan & Ahmad 1982; Mullan 1990; McKenzie et al.

1995; Fisk et al. 1999), but these models have barely progressed beyond the conceptual stage. Plumes - relatively dense structures seen in the EUV in both polar and non-polar coronal holes - offer a superb testing ground for this hypothesis, largely because they are more visible than their surroundings. Observational support for reconnection and associated heating at the base of plumes (Wang 1994; deForest et al. 2001) comes from SOHO (DeForest et al. 1997; Hassler et al. 1997; Wang et al. 1997), but these data fall short of the continuity and spatial and temporal resolution required to confirm this scenario.

Therefore we will employ SHARPP to search for observable signatures of magnetic reconnection at the base of polar plumes, and to assess the effects of this energy release on the energetics and dynamics of the local plasma. AIA will monitor the critical range of heights where reconnection is expected to occur, follow the evolution of plumes and their surroundings at temperatures from 0.02 to 3 MK, and estimate the energy budget. The time-dependent magnetic configuration at the base of the plumes will be derived from HMI or ground-based magnetograms and extrapolated into the corona ARMS, to relate the AIA observations to the magnetic and plasma structure seen beyond $1.2R_{\odot}$ by KCOR. Simultaneous UIS or Solar-B/EIS observations in transition-region lines of plumes on the disk would yield important information on outflows that cannot be derived from off-limb images, enabling improved estimates of the mass flux in these structures. We will use the proposed ARMS calculations of 3D reconnection between an emerging bipole and adjacent open flux (§1.2.2.3) to determine whether the predicted reconnection signatures and evolving plasma properties compare favorably with the SHARPP observations. The ultimate test will require a more complex 3D model of numerous reconnection events, distributed as dictated by SHARPP and HMI data, capable of reproducing a plume from birth to death. We will measure the impact of such reconnection events on the overlying corona and fast wind by determining the mass and energy fluxes - including MHD waves - accompanying the basal heating and dynamics. Although kinetic mechanisms for heating and accelerating the fast wind (e.g., ion-cyclotron waves) are beyond the scope of SHARPP, our studies will reveal the origins of the background conditions in which such important processes must operate.

1.2.4 Traceability Matrix. Table 1-2 summarizes the main scientific goals of the SHARPP suite, and the SDO auxiliary instruments modeling tools that will contribute to reaching these goals.

1.3 Instrument Overview. SHARPP is an instrument suite designed to identify and relate the sources of solar variability from the chromosphere to the outer corona with high spatial and temporal resolution. SHARPP will obtain full sun UV/EUV images of the chromosphere, transition region and inner corona, EUV images of the $1.2\text{-}3.0R_{\odot}$ corona and visible continuum images of the $2\text{-}15R_{\odot}$ corona. The suite can be subdivided into two basic optical packages, the SCORE and the AIA. Each is mounted in its own support structure but under the control of a shared redundant electronics package.

The SCORE will observe the K+F continuum (white light) corona at 7000 Å (1000 Å FWHM) over $2.0\text{-}15R_{\odot}$, and the E-corona at Fe XII 195 Å (10 Å FWHM) over $1.2\text{-}3.0R_{\odot}$ with two coronagraph channels, KCOR and ECOR[2]. The design approach optimizes the trade-offs among the science objectives, scene emission properties, and instrument performance limitations in order to couple the observation of dynamic magnetic structures observed by AIA to the extended coronal structures observed with a white light coronagraph. In particular, the SCORE instrument has been optimized to observe geoeffective halo CMEs throughout its FOV with high cadence.

The AIA package contains seven telescopes to simultaneously image the full solar disk over a temperature range from 0.02 to 3 MK using a carefully selected group of UV and EUV emission lines. The AIA telescopes are designed to obtain high spatial resolution observations (1.3") with very fast cadence (10 sec).

The individual characteristics of the SHARPP instruments and responsible institutions are given in FO2-1. The telescopes will be constructed by experienced teams under the leadership of a senior SHARPP co-investigator at the various participating institutions. The division of labor and clear lines of responsibility greatly simplify the task of managing the SHARPP development effort. Finally, economy and reliability are enhanced by use throughout of standardized subsystem with signifi-

2. ECOR was not selected for the SDO mission. SCORE now consists of only the KCOR.

Table 1-2. SHARPP Traceability Matrix

Science Objectives	Physical Observables	Instruments							
		SHARPP			Auxiliary Observations				Models
		AIA	ECOR*	KCOR	HMI	UIS	Solar-B	STEREO	
SDO Objective: How does the Sun Drive SW and Global Change?									
How are magnetic eruptions triggered? What coronal magnetic field configurations produce CMEs? (§1.2.1.1)	• Mass motions during CME • Erupting field/ filament topology • Timing of flare & CME • Identification of reconnection sites	✓	✓	✓	✓	✓	✓	✓	✓
How do eruptive topologies evolve from the solar surface to the outer corona? (§1.2.1.2)	• CME speed, acceleration, extent, mass, energy (kinetic, potential) • EUV waves	✓	✓	✓	✓			✓	✓
Which CMEs cause SWx disturbances at Earth? (§1.2.1.3)	• Detection of Earth-directed halo CMEs • Magnetic, density topology • CME speed, direction, extent • Identification of candidate sites for particle acceleration	✓	✓	✓	✓			✓	✓
What generates the highly variable slow SW? (§1.2.3.1)	• Tracing inflows, blobs • AR loop expansion • 3D Streamer structure/evolution	✓	✓	✓		✓		✓	✓
How do plumes & other open field structures originate? (§1.2.3.2)	• Plume mass, energy budget • Tracing reconnection at plume base • MHD waves in CH	✓	✓	✓	✓	✓		✓	✓
SDO Objective: How and Why does the Sun Vary?									
How and where are flare arcades heated? (§1.2.2.1)	• Magnetic topology • Energy distribution in flare loops	✓	✓		✓	✓			✓
How and where are coronal loops heated? (§1.2.2.2)	• Loop thermal distribution, Loop MHD waves • Connectivity to photosphere	✓	✓		✓	✓	✓	✓	✓
How does the corona evolve outside AR? (§1.2.2.3)	• Magnetic topology • Reconnection by-products	✓	✓	✓	✓	✓	✓		✓
What determines the solar EUV irradiance at Earth throughout the solar cycle? (§1.2.2.4)	• EUV spectral irradiance from solar sources • Reconstruction of total irradiance for SIE	✓	✓						✓
* Models will be used to partially compensate for the fact that the ECOR was not selected for the SDO mission.									

cant flight heritage. The SHARPP instrument suite satisfies all the requirements of the SDO program for the SCORE and AIA instrumentation within technical and programmatic resources.

1.3.1 SHARPP Coronagraph Experiment. The SHARPP science objectives require close coupling of the full disk magnetic structure activity observed by AIA with the extended coronal density response observed by KCOR. The proposed KCOR, a duplicate of the SECCHI/COR2, will satisfy the 2.5-15$R_\odot$ FOV suggested for the WCI in the AO. However, the KCOR useful inner field cutoff of 2.5$R_\odot$ precludes the observational continuity necessary to relate eruptive magnetic events in the low corona to KCOR observables. With the proposed EUV channel (ECOR), we achieve continuity with the AIA observations of the low corona, explore a largely unknown observational range, and provide context for the outer white light corona.

The classical visible light continuum coronagraph is well suited to the detection of the extremely small K-corona flux at high altitudes because it integrates the Thomson-scattered continuum signal over a broad passband near the peak of the photospheric continuum output distribution. The principle disadvantage of a continuum coronagraph is poor image definition at low altitudes caused by a combination of factors. These include the inability of the instrument to replicate the extremely high photosphere-corona scene contrast in the visible, the linear dependence of the signal on

the line-of-sight integral coronal electron density n_e the lack of temperature sensitivity, and in the case of moderately dimensioned external occultation, poor diffraction limited spatial resolution near the occulter.

1.3.1.1 The White Light Coronagraph. The COR2 coronagraph developed for the STEREO mission is used as the basis for the KCOR. Because the requirement for the SDO white light coronagraph FOV (2.5-15$R_\odot$) is the same as in the COR2 instrument, we are able to duplicate the design for KCOR. Thus, the KCOR concept presented here is a mature design, easily achievable, and meets all of the science requirements. KCOR will obtain total brightness (B) and polarized brightness (pB) images of the white-light corona, and, since it is identical COR2, provide a usable third eye for the STEREO mission.

❒ ***Optical Design***: The KCOR is a traditional externally occulted Lyot design (Instrument Fold-out). A coronagraph is a relatively simple telescope with the added complexity of extreme stray light rejection techniques. The triple disk external occulter, D1 completely blocks direct sunlight and minimizes the total diffracted light ultimately falling on the entrance aperture A1. For KCOR, we calculate the attenuation to be 10^{-5} for a triple disk occulter with 50 mm spacing between the disks and 400 mm from the last disk to A1.

The doublet objective, O1 at A1, is made of super-polished, low scatter glass and anti-reflection coated to minimize unwanted inter-reflections between the lens surfaces. Laboratory tests conducted at NRL during SECCHI/COR2 development have shown no increased scattering from optics with an anti-reflection coating. O1 images the corona on the field stop and also images the third occulting disk of D1 onto an opaque axial disk, D2 intercepting residual diffracted light originating at the edges of D1.

A short distance behind D2 is a field lens O2, which collimates the primary coronal image and presents it to a relay lens which forms an image of the corona on the 2048x2048 pixel CCD camera at the image plane. The main function of the field lens is to form an image of the light diffracted by A1 at a circular stop known as the Lyot stop.

The heat rejection mirror reflects solar disk flux passing into the instrument through A0 back out through A0. The rotating polarizer provides K-corona polarization analysis capability. Successive

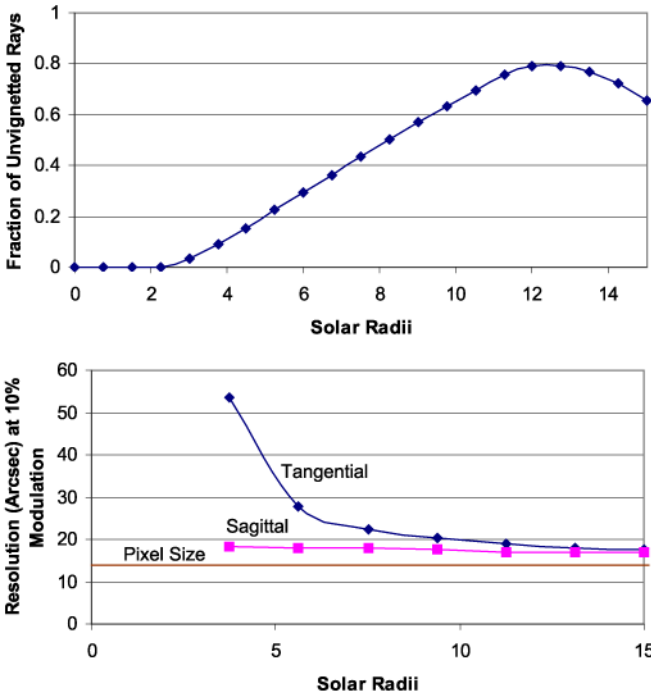

Figure 1-8. Vignetting function and spatial resolution (including CCD sampling effects) for KCOR.

images are acquired through the polarizer at -60, 0 and +60 degree positions respectively.

The total stray light rejection is computed to be about $3x10^{-11}$ $B/B_\odot$, well below the coronal brightness. Figure 1-8 shows the resolution of the optical system. The difference between the radial and tangential resolution is a result of the vignetting caused by the external occulter which creates a lune-shaped entrance aperture. The usable photometry does not begin until the vignetting rises above 0.02, at an altitude of about 2.5$R_\odot$. The roll-off after 12$R_\odot$ is due to the small A0 aperture and compensated for by a larger A1 to keep the overall cross section of the instrument as small as possible.

❒ ***Mechanical Design***: The instrument envelope and basic structural element is a segmented tube with a maximum diameter of 132 mm and a length of 1220 mm from A0 to the focal plane. The KCOR requires the following mechanisms: recloseable aperture door, rotating polarizer, shutter. To maintain the operating temperature for the CCD camera, the focal plane package will transfer its heat to an external radiator. KCOR must complete a pB sequence of three images before CME motion introduces significant polarimetric error. A CME moving at the average speed of 1270 km/s

will move across the 14 arc second pixel in about 8 seconds. Thus, the sequence of three images must be completed within that time. To accomplish this objective, KCOR is designed to allow exposure times that are ~3% of LASCO/C2. The KCOR polarimeter consists of a rotating Polacor polarizer mounted inside a hollow-core motor.

❒ ***Calibration***: The KCOR stray light levels will be evaluated in the NRL coronagraph stray test chamber developed for the SOHO program and refurbished for the STEREO program. A source 10 m away simulates the spectrum and angular size of the Sun. At the aperture door, a diffuser window will be used for in-flight brightness calibrations. The calibration lamp will be used to calibrate the CCD camera both on the ground and in flight. In addition, we have developed many procedures for LASCO flat-field calibration and for in-flight calibration against the stars. Together these procedures determine the stray light, geometric distortion, vignetting, absolute photometry and the instrument pointing and roll.

❒ ***Observing Strategy***: KCOR will complete an 8 sec pB sequence of three images on a 1 min cadence. The high KCOR cadence combined with the AIA and ECOR observations will generate excellent velocity profiles for even the fastest CMEs. The KCOR will be used to determine the presence of a halo or other out of the sky plane CMEs by summing up the three polarized images of a sequence into a single total B image and performing an image motion analysis. It is necessary to convert to total B for this purpose because pB favors observations on the limb.

Having obtained images with the necessary precision, the essential analysis problem is to distinguish the strongly time varying signal of the K-corona with its streamers, plumes and transient structures from the relative bright and static background comprised of the F-corona, planetary/stellar sources and instrumental stray light. This will be accomplished with two well-established techniques that have been successfully used to analyze coronagraph images for the past three decades: polarization analysis and background model subtraction. The background model will be created from the KCOR images over a period of several weeks surrounding the date of interest.

1.3.1.2 The Extreme UV Coronagraph. ECOR was not selected for the SDO mission.

1.3.1.3 SCORE Structure. Because ECOR was not selected for the SDO mission, the SCORE structure is no longer needed in the proposed configuration.

1.3.2 Atmospheric Imaging Assembly. The primary goals of the AIA are to characterize the dynamical evolution of the solar plasma from the chromosphere to the corona, and to follow the connection of plasma dynamics with magnetic activity throughout the solar atmosphere (§1.2.2). A global understanding of the energy balance (conductive/radiative) and energy flux can only be attained by observing emission from VUV and EUV lines that represent the full range of temperatures present in the solar atmosphere: chromosphere (20-80k K), lower Transition Region (TR) (~250k K), upper TR (~700k K), corona (1-2 MK), hot corona (3-4 MK), flares (e.g., 20 MK). This investigation places particular importance in the high cadence imaging of the highly variable TR (§1.2.2.3, 1.2.2.4).

Analysis of Differential Emission Measure (DEM - as described in more detail in sections 1.2.2.4 and 4.0) is a powerful tool to organize the study of solar atmospheric plasma with simultaneous, multi-temperature remote observations. In order to constrain the DEM model of a given line of sight in the solar atmosphere, the observations must be made in such a way as to determine the local minimums, maximums, and inflection points of the DEM curve. As can be seen from Figure 1-9, more than five temperature regimes (five VUV & EUV lines) must be observed in order to constrain the DEM curve over the variation range of solar atmospheric plasma.

The selection of EUV and VUV lines for the AIA filtergraphs, from the lines observable in the solar spectrum, is further complicated by the limitations of instrumentation that can be built in a robust, low risk, resource constrained spaceflight program. The success, over the last decade, of normal incidence, multilayer-coated optics in EUV filtergraph solar telescope applications is one of the prime motivations for the SDO mission. From the EUV filtergraph technology that has been demonstrated to date and that is within the technological resources of the SHARPP consortium, we can confidently use this technique in the SDO AIA application over the wavelength regime from 500Å to 170Å. The short wavelength limit follows from our self-imposed restriction, on the basis of reli-

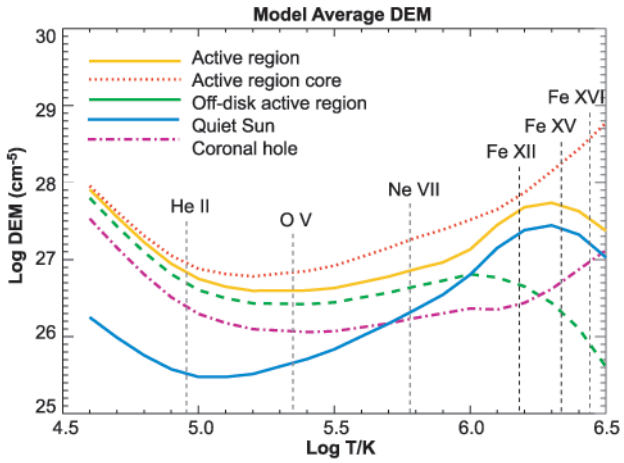

Figure 1-9. EIT Derived Differential Emission Measures, showing AIA ions.

ability over a 5-year mission, to aluminum visible-light rejection filters. The extension of the long wavelength limit to a regime beyond the commonly accepted 300Å limit is achieved on the basis of recent measurements of **robust** Sc-W-Si-W coatings developed for a NRL laser fusion program.

Among the appropriate emission lines in the solar spectrum that are available in the170Å to 500Å wavelength regime, there are three important temperature regimes that are not well characterized: the ~20,000K chromosphere, the ~250,000K lower transition region, and the 5-10MK active region core.

a. The low chromosphere will be observed in AIA with a vacuum ultraviolet (VUV) filtergraph tuned to 1215Å Ly-α emission line. The techniques demonstrated in the CNES Transition Region Camera (TRC) program two decades ago provide a robust system for this filtergraph.

b. The ~250000K lower transition region poses a larger problem in that there are no lines in even the VUV that are available to use in a robust filtergraph. Thus, we must resort, to spectroheliograph techniques. The 629Å OV line was chosen for its relative intensity and isolation from adjacent lines. The ~0.1Å broadening typical of lines in the turbulent transition region requires a low dispersion system to prevent the line width from destroying the high spatial resolution in the direction of dispersion. However, the proximity of the 609Å MgX line and the need for a FOV of a solar diameter, requires a high dispersion system. These dual requirements eliminate the use of a simple Cassegrain-Wadsworth design (e.g. Moses et al. 1996) and require a more complex system derived from the zero net dispersion system of Prinz (1972). Current technology, as demonstrated by our gratings source (Jobin-Yvon), in an extremely conservative proof-of-principle design, described below, can provide OV observations with the cadence required for the SDO science.

c. We have chosen to follow the specific temperature range described in the SDO AO (20,000 K to 4 MK) and not observe the temperature characteristic of the high temperature peak of active region cores, relying instead on the limits placed by observations of Fe XVI and Fe XXIV. The restriction to aluminum visible-light rejection filters prevents the observation of EUV line candidates for this temperature regime. The envelope restriction of the SDO mission prevents the use of a grazing incidence system for observing AR core plasma. We plan to intensively evaluate visible-light rejection filters during Phase A – with a particular emphasis on elimination of grid support diffraction using new approaches pioneered by J. Underwood. Should confidence emerge in a filter with bandpass short of 170A, we will substitute the Fe XVI channel for one of higher temperature.

The SHARPP/AIA consist of 7 telescopes imaging the following bandpasses: 1215 Å Ly-α, 304 Å He II, 629 Å O V, 465 Å Ne VII, 195 Å Fe XII (includes Fe XXIV), 284 Å Fe XV, and 335 Å Fe XVI (Table FO2-2).

The telescopes are grouped by instrumental approach: (1) Magritte Filtergraphs: five multilayer "EUV channels", with bandpasses ranging from 195 to 500 Å and one Ly-α channel; (2) SPECTRE Spectroheliograph: one "soft EUV channel" O V at 630 Å.

These two instruments, the electronic boxes and two redundant Guide Telescopes (GT) constitute the AIA suite. They will be mounted and co-aligned on a dedicated common optical bench. The GTs will provide pointing jitter information to the whole SHARPP suite through an Image Motion Compensation System. The CCD cameras for the AIA are common to the seven telescopes and described in section 1.6. The seven AIA cameras will image the Sun simultaneously at a 10 second cadence with a 0.66"/pixel resolution in a field of view extending from the Sun center to 1.4 $R_{\odot}$. The extended FOV is required to have sufficient over-

lap with the complementary EUV coronagraphs observations.

1.3.2.1 Magritte: Filtergraph Telescopes.

(R. Magritte, famous 20th Century Belgian Surrealistic Artist)

The wavelengths for the filtergraph telescopes were selected according to science criteria and technical considerations and all are based on a common conceptual design. An off-axis optical design (Figures 1-10 and 1-11) was chosen as compromise between the optical performances, the large field of view and the baffling characteristics. The telescopes will image a 45 arcmin FOV with an effective focal length of 3.75 m.

The initial baseline for the 5 EUV channels is 195, 284, 304, 335 and 465 Å, that will use multilayers developed by Institut d'Optique Theorique et Appliquee (IOTA). While 195, 284 and 304 have a very good flight heritage (SOHO/EIT, STEREO/EUVI), the Ne VII (465 Å) channel will require the use of new materials such as scandium and a specific preparatory program.

The Ly-α channel is based on the rocket-borne Transition Region Camera (Bonnet et al. 1980 - TRC) design which uses narrow-band interference filters to isolate Ly-α. It has been adapted for compactness by using a scheme nearly identical to the multilayer instruments: an off-axis Ritchey-Chretien design with a 60 mm (resized for throughput and diffraction) aperture.

❒ ***Optics***: The optics for all the filtergraph channels will be procured and polished by IOTA. After reaching a spherical shape, the off-axis figuring will be obtained with ionic beam polishing at the IOTA facility - Orsay (F). Multilayer EUV coatings will be deposited by IOTA and will be optimized for the off-axis system, with non-normal incident angles. The 195, 284 and 304 Å channels will be similar to the STEREO/EUVI coatings (also heritage and significant improvements from SOHO-EIT). New developments will be conducted to define, prepare, optimize and test coatings for 335 and 465 Å. For Fe XVI (335 Å), standard materials (Si, Mo) or recently tested materials (B_4C, Si; baseline) will be used, while the Ne VII (465 Å) line will require the use of a multilayer originally devised by Seely (Seely et al., Private Communication) consisting of scandium-silicon with a thin tungsten barrier layer to prevent interdiffusion at the Sc-Si interfaces and improve stability of the multilayers (Sc-W-Si-W multilayer).

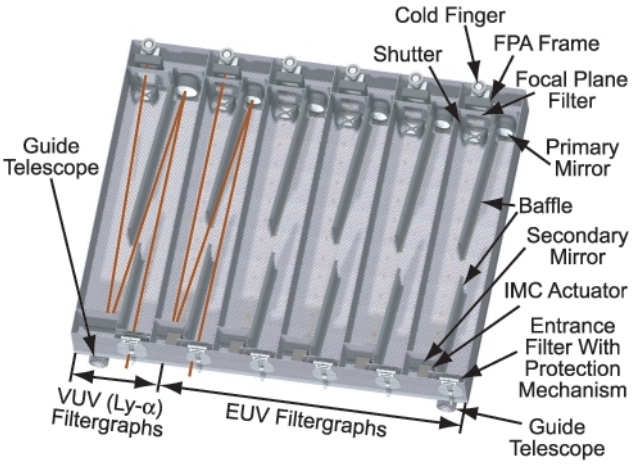

Figure 1-10. Opto-mechanical rendering of Magritte elements.

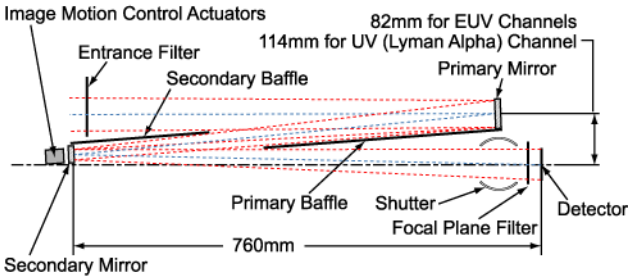

Figure 1-11. Optical layout of Filtergraph off-axis Ritchey-Chretien telescopes. Due to the diffraction limit and throughput, the Ly-α channel will be slightly larger.

This multilayer has been successfully applied on a replica of the Skylab grating in order to obtain laboratory measurements of the optical constants for Scandium. These new optical constants, plus the stabilizing tungsten barrier, form the basis for our reflectivity calculations for this channel.

The Ly-α channel has multilayer coatings on the primary and secondary of $Al/MgF_2/B_4C$ (Larruquert and Keski-Kuha 1999) optimized for reflectivity at 1215 Å. In order to reduce the overall size and keep the Ly-α within the similar mechanical envelope as the EUV channels, the Ritchey-Chretien off-axis telescope will be slightly tilted. This increased incidence angle is not critical.

The filtergraph system is fully baffled with two internal, planar baffles. The compact, off-axis design provides high throughput with straightforward baffles and no obstruction by a mirror support spider. The design has been optimized for easy to achieve baffle tolerances while simultaneously avoiding any vignetting in the FOV.

❒ ***Filters***: The EUV light enters the instrument through an aluminum filter, that suppresses most

of the UV, visible and IR counterparts of the solar radiation. Standard Luxel filters with 1500 Å thick aluminum layer supported by a nickel grid are considered for the baseline. The grid will provide mechanical strength and adequate conductive path for heat excess. A single filter will be mounted at the entrance of the telescopes and one in the focal plane, protected between the CCD and shutter. The second filter will provide adequate redundancy. Alternate solutions will be vigorously investigated in Phase A to either reduce the diffraction effects or improve the mechanical strength. Wider mesh grids or composite filters (stack of Al layers with spacer material such as boron or silicon) may offer superior solutions. Alternative locations for the second filter will be considered, taking into account diffraction and shading effects that the opaque supporting grid may produce.

Two narrow-band interference filters will be used to achieve the spectral purity for the Ly-α channel. Acton Research is fully capable or producing these filters as specified. One filter will be placed at the entrance aperture (where it will reject X-rays and protect the secondary mirror coating with a visible light rejection of 10^{-4}). The second filter will be placed in front of the focal plane. The combination of these filters yields a spectral purity of 87% for Ly-α in the quiet sun and higher purity in active regions.

It is instructive to contrast this instrument with the Ly-α channel on TRACE that was also based on the TRC design. In order to observe both 1550 Å C IV and Ly-α with a single mirror, TRACE used a coating optimized for C IV combined with a Ly-α filter, resulting in a double-peaked response (Handy et al. 1999). The TRACE filtergrams therefore consist of only ~50% Ly-α with the bulk of the residual a mixture of continuum and C IV. Our design, fully optimized for Ly-α, will produce significantly spectrally purer images, similar to the original Bonnet TRC.

❒ ***Instrument Performance***:

❒ ***Optical Performances***: The optical performances were studied by ray-tracing analyses. Figure 1-12 shows the RMS spot diameter as a function varying in the field of view, and the diameter including 70% of the spot energy for the filtergraph channels. The optical performances have been optimized inside the solar disk. Using realistic mirror figuring properties (WFE λ/20 ptp and λ/100 rms), with mounting and alignment tolerances, we estimate the 70% encircled energy diameter to be increased by 6 μm. It means that the 70% encircled energy disk will be included in a single pixel everywhere within the solar disk and for all channels. This plot indicates that the Ly-α channel is diffraction limited, but is still compatible with the 12 μm pixel size.

Table 1-3. Optics Definition Magritte Telescopes

Element	Curvature (mm)	Conic	Distance (mm)	Remark
Primary Mirror (EUV, Ly α)	1730.5 1731.6	-1.0 -1.1	690	Circular (45mm EUV) (60mm dia. Ly-α) Off-axis: 82mm
Second-ary Mirror (EUV, Ly α)	455.5 456.9	-2.7 -4.1	760	Circular (25mm) Off-axis: 16.5mm, 16.23mm
Detector	Flat	N/A	N/A	Plate Scale: 0.66 arcsec/pixel EUV tilted around θ_x by -0.62°

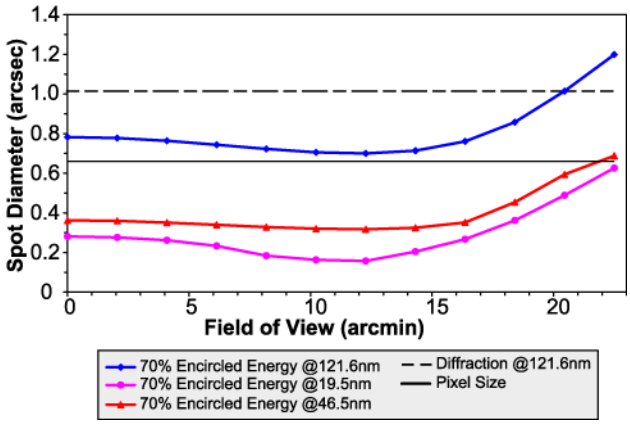

Figure 1-12. Optical performance of Magritte, 70% encircled energy diameter.

1.3.2.2 SPECTRE Zero-Dispersion Spectroheliograph: OV Channel 629 Å. The AIA instrument suite includes the SPECtroheliograph for the Transition Region (SPECTRE). This channel is optimized for imaging the soft EUV 629.7 Å OV line. The zero-dispersion design is evolved from the full disk Ly-α spectroheliograph flown on an NRL rocket on July 10, 1972 (Prinz, 1972), modified to achieve a 0.6 arcsec/pixel spatial resolution in a 41 arcmin FOV. The telescopes will image a 41 arcmin FOV with an effective focal length of 4.0 m. Typical operation schemes will use 2x2 binned exposures for high cadence variability and summed exposures for lower cadence studies.

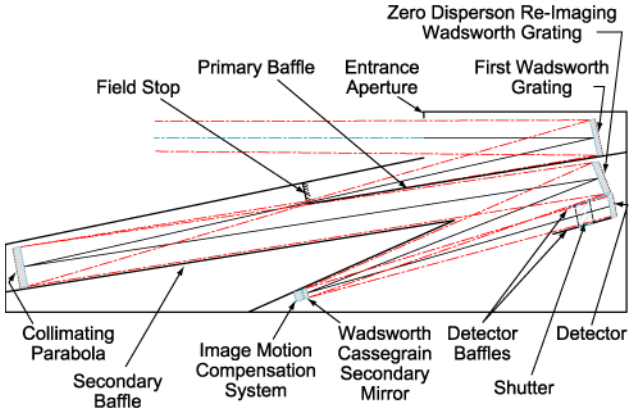

Figure 1-13. Conceptual design of the OV instrument.

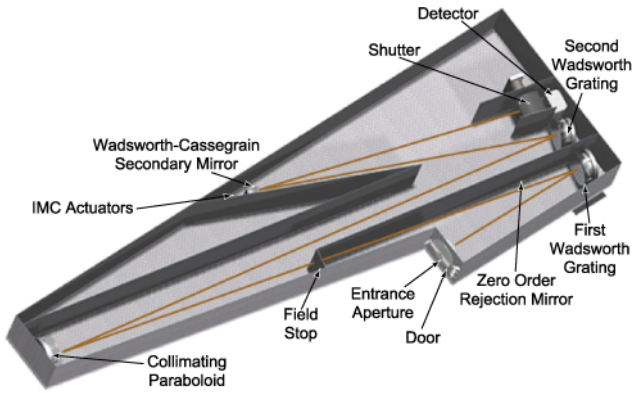

Figure 1-14. Accommodation of the opto-mechanical elements of the SPECTRE (bottom view)

❒ ***Optical Design***: The SPECTRE design is driven by two main factors. First, since 629.7 Å is too long a wavelength to be accessible with the multiplayer optics available to date, the spectral selection has to be made through a spectroheliograph. Second, a zero dispersion configuration is required to compensate the blurring that the ~0.15 Å natural width of the OV line would otherwise produce.

The instrument basically consists of two spectrographs with opposite dispersion placed in tandem (Figure 1-13 and Figure 1-14). An optical prescription is given in Table 1-4. A first parabolic Wadsworth mounted 3500 lines/mm holographic grating focuses a dispersed image of the Sun onto a field/wavelength stop. Besides OV, the main line emission around 630 Å is the 609/625 Å Mg X doublet, with 609 Å the most intense component. The stop isolates a 19 Å bandpass and admits the whole OV 630 image while cutting off 83% of the 609 Å Mg X radiation. After this spectral selection, an off axis parabola re-collimates the resulting quasi-monochromatic beam, and the wavelength dispersion is then nearly perfectly compensated by a Wadsworth-Cassegrain re-imaging system. The 17% Mg X transmission results in a slight contamination of the limb on one side of the OV image. It is hoped to orient the spacecraft roll to have this contamination on one of the polar holes. If this orientation is not available, the field stop can be resized to suppress the entire 609 Å Mg X radiation at the expense of a slight loss of the field of view of the OV image. The predicted intensity ratio of the 625 Å Mg X to OV is 0.1 in the quiet Sun and up to 0.3 in active regions. This contamination can be characterized using the DEM technique (Magritte will obtain images that well sample the formation temperature of Mg X) to produce a synthetic Mg X image that is subtracted off the observed OV.

Table 1-4. Optics Definition of SPECTRE Telescope

Items	Curve (mm)	Conic	Characteristics
Wadsworth Grating	1450	-1	Circular (90 mm) Tilt: 12.73˚ 3500 l/mm
Field Stop	N/A	N/A	Circular (7 mm)
Collimating Parabola	1450	-1	Circular (98 mm) Off axis: 51.29 mm
Wadsworth Grating	1900	0	Circular (90 mm) Tilt: 12.73˚ 3500 l/mm
Cassegrain Secondary	473.03	-2.43	Circular (24 mm) Off axis: 17.78 mm
Detector	Flat	0	Plate scale: 0.6 arcsec/pixel Tilt: +10.3˚

As shown on Figure 1-15, the RMS spot diameters, including the 1.6 Å /pixel dispersion, are just over a pixel in the whole FOV. Preliminary calculations show that the stray residual visible and EUV radiation will be sufficiently suppressed by the holographic gratings and dark SiC surfaces that additional filtering will not be required. The 0th order of the first grating is damped through the entrance aperture after reflection on a mirror placed on the primary baffle. Ly-α in the first order is rejected directly through the entrance aperture. In this way, the secondary mirror is protected from degradation effects such as the loss of reflectivity due to photo-polymerization of contaminants.

Figure 1-16 shows a synthetic spectroheliograph image computed using the DEM technique as de-

Figure 1-15. SPECTRE RMS spot diameters are below or just above the pixel size across the whole FOV. The size of the diffraction is shown for comparison.

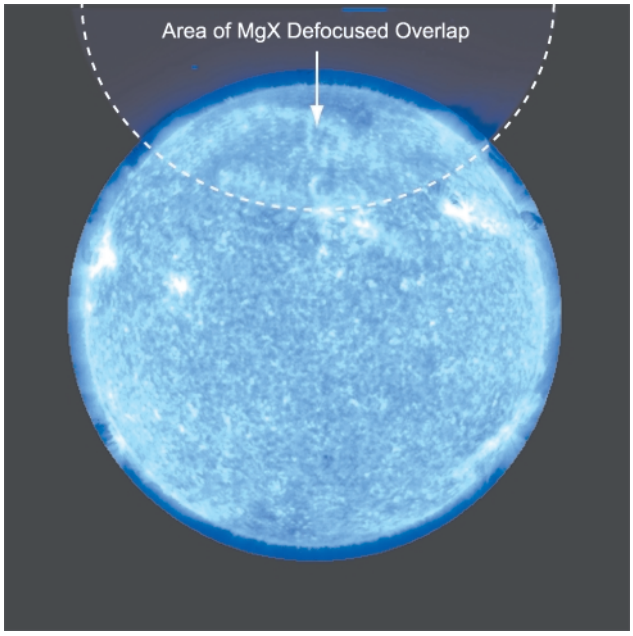

Figure 1-16. Synthetic OV SPECTRE image. The Mg X overlap area enclosed by the dashed line is limited to a single polar region by the field stop. The effect of the overlap is limited to the polar hole and easily removed.

scribed in section 4.0 (note as this was based upon EIT data, the cool temperature was derived using HeII and therefore shows a coronal hole while the AIA OV image will not display such a strong coronal hole).

❒ ***Gratings and Optimization***: The constant line-spacing (SCLS) pattern of 3500 lines/mm is produced holographically on the spherical SiC-blank of the grating. The grooves' shape is then ion etched directly on the substrate. This manufacturing process is routinely used for the production of gratings to be used in synchrotron sources, where the optics has to sustain, with little degradation, high fluxes of XUV radiation. The SCLS grating will be produced by Jobin&Yvon (J&Y), France. J&Y has extensive expertise in producing such high-frequency, holographic gratings for space use. As an example of these gratings' heritage, NASA's FUSE-Lyman is successfully flying two large (27 x 27 cm^2), SiC, holographic gratings with high ruling-frequency (i.e., 5767 l/mm) that have been manufactured by J&Y. J&Y has calculated a reflectivity of 35% for direct etching on SiC. The proposed design should be considered a feasibility study of the general concept. During Phase A, the use of Variable line spacing gratings will be investigated. Careful optimization in collaboration with J&Y should result in an expected 30% volume reduction.

1.3.2.3 AIA Responses and Effective Areas. The efficiency of all the elements of the AIA has been measured in previous programs or extrapolated from component measurements. The 195, 284 and 304 Å multilayers reflectivities are based on recent measurements (CALROC/EIT, SECCHI/EUVI mirrors); the 335 and 465 Å values are theoretical estimates based on measured optical constants. The 335 Å coating will use B_4C/Si layers, while the 465 Å will require Sc/Si layers for which recent measurements have been performed (Seely, NRL). Peak reflectivity for the EUV mirrors range from 15-40% depending upon the particular band. The aluminum filter data are using Luxel filter properties for 1500 Å aluminum layer, including the grid transmission (82%) and an oxide layer. The CCD quantum efficiencies were derived from the Marconi CCD42 performance and range from 80-90% for the EUV lines, to 55% at 630 Å and 15% at 1215 Å.

❒ Those data were convolved with the Solar input spectrum from the Chianti database (identical spectrum to that used in the NRL NEXUS spectrograph proposal), to derive the overall instrument response, as detailed in table F02-3. This table shows the predicted signal-to-noise (photon statistics) achieved in an 8 second exposure and indicates that the AIA design is compatible with a 10 s cadence (8 second exposure plus 2 second CCD readout) for all the channels. The exact exposure time will be optimized for each channel with the goal of having active regions intensities no more than 1/3 full well, in order to allow for flare detec-

tion. The effective area is defined as the product of the optical efficiencies (geometric area, mirror reflectivity, filter transmission, and quantum efficiency) and is shown Figure 1-17.

❒ ***Overall Accommodation***: The baseline AIA packaging concept is a combined Magritte and SPECTRE instrument to be installed as a single unit on the S/C. The instruments are assembled and tested as individual units prior to integration. This concept minimizes volume required on the S/C. However, Magritte and SPECTRE can both be individually placed upon the S/C as separate instruments. A honeycomb panel optical bench serves as the mounting platform for optical component and mechanical H/W brackets, and a removable cover adds to the structural stiffness. Kinematic mounts attached to the optical bench support the instrument and minimize thermal distortions in the structure. A set of four mounts provides optimum support conditions for the near square shape of the Magritte optical bench, while a set of three mounts is adequate for SPECTRE. The optical benches are fastened back to back for the combined instrument structure and utilize the Magritte mounts. The combined instrument configuration does not require the additional set of three mounts, however some of the mass savings is offset by the additional H/W mass used to connect the optical benches.

The CFRP (Carbon Fiber Reinforced Plastic) optical bench facesheets, baffles, and structural panels ensure that the stiffness and thermal stability requirements are met while achieving a low mass structure. Component brackets will also be fabricated from CFRP for compatibility with the structure. The low thermal expansion coefficient of CFRP ensures that the mirror interdistance will remain stable in the 30 mm range under all imposed thermal load conditions. Coalignment of the instrument optics will be achieved by precision mounting of all the mirrors and maintained under on-orbit thermal conditions due to the stable CFRP structure.

▫ *Finite Element Analysis and Models*: Our design study included finite element analysis to support design solutions for the Magritte and SPECTRE instruments and support structures. A modal analysis was performed on a FEM of the individual instruments as well as the combined instrument system (Figure 1-18). Component masses were included and the results show a fundamental mode exceeding 90 Hz for both the individual and combined instruments due to the high stiffness provided by the material selection and box type structural system. The structure will be studied in greater detail during Phase A to optimize for mass and other considerations.

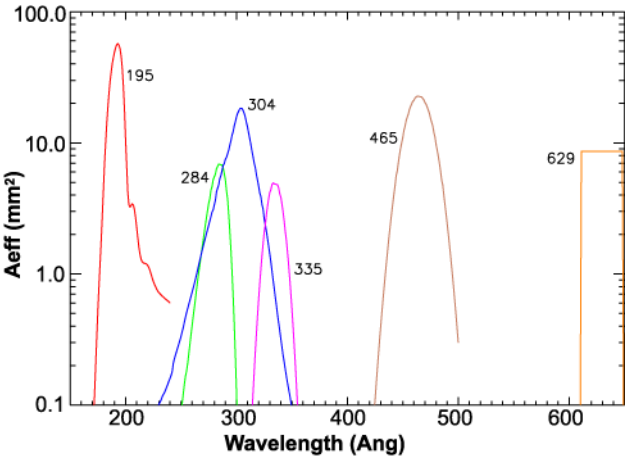

Figure 1-17. Magritte EUV channels instrument efficiencies.

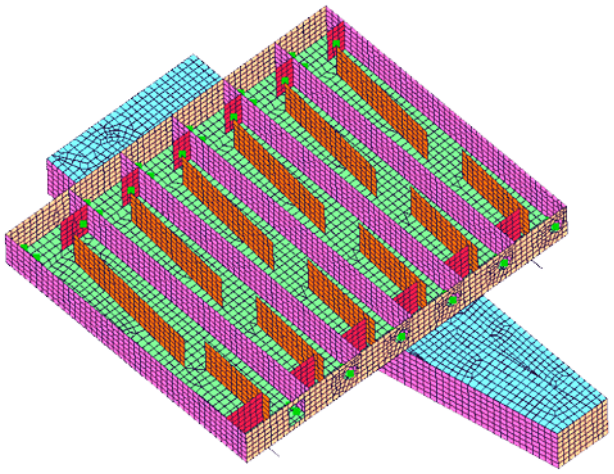

Figure 1-18. AIA Finite Element Model (FEM)

▫ *Contamination Control*: In order to obtain our desired instrument performance, it is essential to develop a detailed Contamination Control Plan. We build on procedures from our extensive heritage with LASCO and SECCHI to limit particulate and molecular contamination. Enclosed volumes must be vented in such a manner as to prevent damage due to pressure differentials during ascent and to provide a path for molecular escape. Venting design will be derived from the advanced contamination control processes derived from SECCHI. Many of the instrument surfaces are sensitive

to humidity or depositions of molecular contaminants. Consequently, it is required that the most of the instrument apertures/detectors be continuously purged with nitrogen. Purging may only be stopped for very limited periods during certain tests and operations. Thermal control is an important part of contamination control. Temperatures of sources should be kept as low as possible. Temperatures of contamination sensitive optical surfaces should be kept as warm as possible. During operations, all the CCD radiators are individually connected to their respective cold fingers, which will allow independent baking sequences. The focal plane filters on Magritte serve as an additional contamination barrier.

❒ ***Calibrations***: Calibrations are essential for AIA to obtain physical measurements and quantitative results from the SDO observations. As SDO must operate over a 5-year solar cycle time scale, we have to guarantee long term stability and provide for adequate in-flight calibration. For AIA a Calibration Plan will be developed in Phase A to address constraints in design, schedule, and management. The Calibration Plan will encompass the many lessons learned and subtleties gathered through the heritage of past instruments (SOHO/LASCO, SOHO/EIT, STEREO SECCHI, etc.).

At the sub-system level, each mirror, grating and filter will be fully characterized in terms of its averaged efficiency over its working bandpass, as well as over an extended UV and EUV range. The detectors will be tested in detail to physically model the QE and flat field. End-to-end testing at the NRL synchrotron light beam line at Brookhaven National Laboratory will validate the computed throughput and modeled quantities such as: baffling efficiency, PSF, scattered light, distortion, and filter mesh diffraction.

In-flight calibration will be verified with onboard calibration lamps that will monitor any drift of the absolute detector QE and flat field in a manner analogous to the SOHO technique (Newmark et al 2002). In AIA, LED cal-lamps will enhance the in-flight calibration over that achieved in EIT with monochromatic illumination. Given the high stability of modern CCDs, we anticipate tracking even minute changes in sensitive volume, the surface oxide, and possible contaminants (water or hydrocarbon). As a consequence, we aim at the unprecedented precision of <5% at launch, and <10% along the mission lifetime.

Table 1-5. SHARPP GT Performance Requirements

Accuracy (1 hr.)	<1" over a 50" motion
Accuracy (10 min)	<0.25" over a 50" motion
Noise Equivalent Angle	<0.1"
Max. Expected Operating Range	300"
Bandwidth	Updating at 100Hz

❒ ***Design Heritage and Procurement Sources***: See the discussion contained in Section 5.3.

1.4 SHARPP Image Motion Compensation System (IMCS) and GT. The AIA instruments have a tight pointing stability requirement (Table 1-5) of 1.2 arcsec over their image exposure time, which is estimated to last for a maximum of 8 sec. The spacecraft attitude control system will not be able to easily meet this demanding pointing stability requirement, assuming that it is using reaction wheels to point the SHARPP telescopes at the Sun to satisfy the required spacecraft pointing accuracy. The noise characteristics of reaction wheels will transfer energy to the flexible body dynamics of the spacecraft that will lead to instrument jitter. The IMCS is designed to overcome the jitter of the S/C and ensure sub-arcsecond pixel resolution. The AIA secondary mirrors are controlled over 2 rotational axes by three piezoelectric transducers (PZT) at the mirror mount driven by the SHEB IMCS interface with pointing information from the AIA Guide Telescope (GT).

The IMCS for AIA is directly derived from the NRL SECCHI system. A pair of GTs, described below, is mounted on the same optical bench as the AIA telescopes, providing redundant fine pointing measurements at ~100 Hz. The SHEB converts the GT output to a pointing error signal and provides it to the spacecraft. For the AIA, the SHEB will use this error signal to generate the appropriate PZT commands at ~20 Hz. This system attenuates the image motion to < 10% of the original instrument jitter over the frequency range of 0.08-10 Hz. Assuming that the spacecraft can satisfy the pointing stability requirements listed in the AO, the AIA pointing stability requirements will be satisfied.

The GT performance requirements are given in Table 1-5 and the GT design requirements are given in Table 1-6. As in the SECCHI GT, sunlight enters the GT through a moderate bandpass, optical interference filter, constructed of radiation-hardened glass (Andover Corporation). A radiation hardened, air-spaced doublet lens combined with a

matched Barlow lens, produces a diffraction limited solar image at the field stop. The field stop selects four small areas of the solar limb to pass through the system onto a quadrant detector. The output of each quadrant is conditioned in a local preamplifier card. International Radiation Detectors (IRD) will provide the radiation hardened, ultra-stable UVG-600 silicon p-n junction photodiodes quadrant detectors. IRD has a long successful history of providing diode detectors for space missions synchrotron applications, and are recommended for use by international standards organization such as NIST and PTB.

The usable range of the preamplifier and corresponding ADC range in the electronics box will be sufficiently large to accommodate any responsivity degradation, radiation induced dark current and drift errors occurring over the duration of the mission. Thermally insensitive, radiation stable electronic parts will be selected for use in the signal processing chain. The digitized quadrant output will then be corrected for linearity, limb darkening, overall sensitivity and offset prior to calculating the centroided solar pointing position. With a 0.2 ppm 1°C thermally stable structure, a structure fundamental frequency of >100Hz and a thermally benign environment, no serious difficulties are anticipated in meeting the GT/instrument optical axis in-flight coalignment requirement. The GT performance testing will include a test using actual solar illumination from a Heliostat system. The removal of the field stop and installation of a "test" field stop with wider slots will also allow performance testing of the system using a sun simulator telescope under normal laboratory conditions.

1.5 SHARPP Electronics Box (SHEB). The SHARPP instrument suite consists of nine telescopes, each with its own CCD and CCD camera readout electronics, a guide telescope and the SHARPP electronics box (SHEB). Figure 1-19 provides a SHEB block diagram and all major interfaces. To achieve the 6-year operational life, the electronics are fully redundant using a cold spare philosophy. The electronics are extensively derived from the STEREO/SECCHI electronics. Every computer circuit assembly (CCA) is either qualified on a previous flight program or slightly modified from a qualified SECCHI design. The camera readout electronics and their power circuits are housed close to the CCDs to minimize mass, power and noise.

Table 1-6. GT Design Parameters

Optical Characteristics	
Filter	570nm (50nm FWHM)
Lens	Aperture 39mm, focal length 1300mm
Solar Image Angular Radius	Annual range: 944 - 976" (5.95 - 6.15mm)
Field Stop Slot Radial Extent	744 -1144" (4.69-7.21mm)
Field Stop Slot Width	200" (1.26mm)
Typical UVG-600 Quadrant Diode Characteristics	
Linearity Error	<0.02% below 3mA (Associated error of 0.01" over 50")
Uniformity	<0.25% over slot areas* (Associated error of 0.125" over 50")
Nominal Electronic Readout Characteristics	
Nominal Sensitivity	1.28mV/arc-second
Elect. Noise Rqmt.	<0.128mV @ 50Hz**
* requires quadrant diode selection to achieve this uniformity level (typical is <0.5% over 1mm) ** noise floor well above shot noise, resistor Johnson noise and preamplifier chain-related noise	

❒ *Overview*: The SHEB consists of a control computer, interfaces to the cameras and CCDs, interfaces to the GT, jitter control electronics, mechanism control electronics, a housekeeping data acquisition system, S/C interface for commands and HK telemetry, and power conversion.

❒ *Single Board Computer (SBC)*: The control computer is built using a British Aerospace RAD750 133 MHz RISC-based SBC that was developed for the JPL X2000 program and is also used on SECCHI. It will be used without change for SHARPP. The SBC uses a cPCI bus to control the SBC CCAs. Built on 0.5 μm technology, the SBC has 128 Mbytes of SDRAM, 256Kbytes of EEPROM, programmable H/W timers, a watchdog timer and a JTAG and serial ports for ground testing. The SBC is faster than required, but it permits the heritage S/W and other assemblies to be used, saving considerable development cost and lowering risk.

❒ *Spacecraft Interface CCA*: The SHEB utilizes a MIL-STD 1553 interface card to provide a redundant interface to the spacecraft for receiving commands, sending and receiving status messages to/from the spacecraft, and for sending CCSDS formatted telemetry records to the spacecraft. The 6U SECCHI CCA also has 3MB of EEPROM that is used to store the flight S/W. For SECCHI the

digitized GT pointing information output is sent to the spacecraft via the 1553 at 50Hz.

❒ *Camera Interface CCA*: The camera control interface is a bi-directional I2C card developed and qualified under the JPL X2000 program. It will be used without change. The SECCHI CCD cameras currently use this I2C interface for control. The CCD readout waveforms, readout control commands and image compression and CCSDS packet ID information are uploaded to the cameras via this interface. Status is received from the cameras on this interface.

❒ *Housekeeping CCA*: The SHEB collects, digitizes, and sends selected voltages, currents, and thermal sensor monitors to the SBC via the HK CCA. It also contains the interface circuitry to control the redundant sensors on the GT and to digitize the sensor signals. The interface to the jitter control PZTs for the AIA telescopes is on this card. It is similar to the SECCHI card, but will be different in some detail because of the differing number of interfaces, but they are the same types of interfaces as on SECCHI.

❒ *Mechanism Drive CCA*: The drive electronics for the 9 shutter mechanisms, 2 recloseable doors, 6 filter mechanisms, 1 deployable boom, and 1 rotating polarizer are contained on two 6U CCAs. The mechanism drivers are identical to the Solar-B/EIS driver, just replicated for each mechanism to enable simultaneous mechanism operation. In addition to these drivers, paraffin actuators for 9 one-shot doors with redundant drivers are included on these CCAs.

❒ *Power Supply*: The Power Supply Subsystem is comprised of a Power Switching and Control card and Power Converter cards. As in SECCHI, we will use flight qualified, radiation hardened, modular converters rather than custom designs, as these save mass and development costs. The requirement is to handle a range of input voltages (21-39 V) and output +3.3V, +5V and +/-12 V. In contrast to STEREO, the EMI/EMC specification is not extensive.

1.6 SHARPP Camera System. The SHARPP camera system uses existing 2kx2k detector designs from Marconi Applied Technologies (formerly EEV) for the ECOR and KCOR. The AIA will use a new 4kx4k CCD detector design from Marconi. These are not standard designs but are simple modifications from the CCD42 series. The camera readout electronics are directly based on

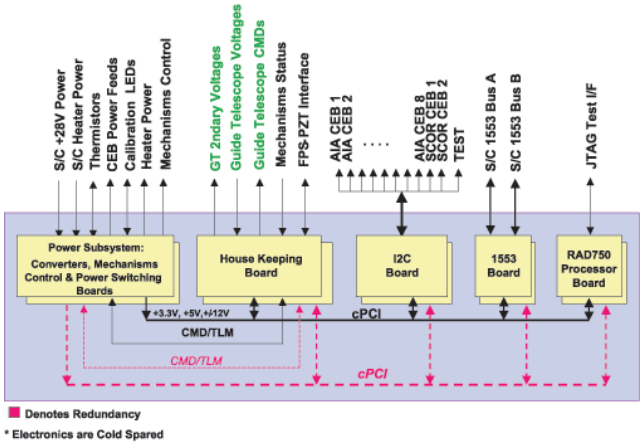

Figure 1-19. SHARPP Electronics (SHEB) Block Diagram

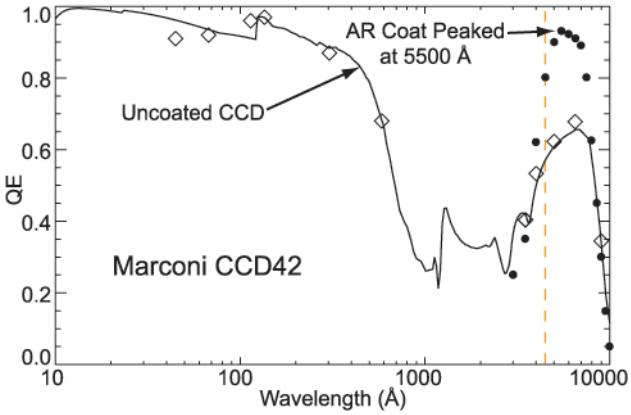

Figure 1-20. CCD QE response.

the SECCHI design The boards for the AIA will be identical for all seven CCDs. The boards for the SCORE CCDs are similar to those, except that 2 analog processing ASICs are included rather than 4. This heritage and commonality minimize schedule and design risk for the mission. CCD development is always a concern, so that the development of the 4K devices will be started in Phase A.

❒ *CCD Detectors*: The CCDs for the ECOR and KCOR are thinned, back-illuminated, low dark current variants of the standard Marconi CCD42-40 (2k x 2k, 13.5 μm pixels) and are identical to those used on SECCHI. The package design developed for SECCHI will be used here. The KCOR uses a standard anti-reflection coated CCD, whereas the ECOR will use a bare (non-coated CCD) with excellent response at EUV wavelengths (Figure 1-20). The SHARPP CCDs operate in a non-inverted mode as did the SECCHI CCDs, enabling large full wells, which have been measured at about 200k electrons. This large full well permits a large SNR.

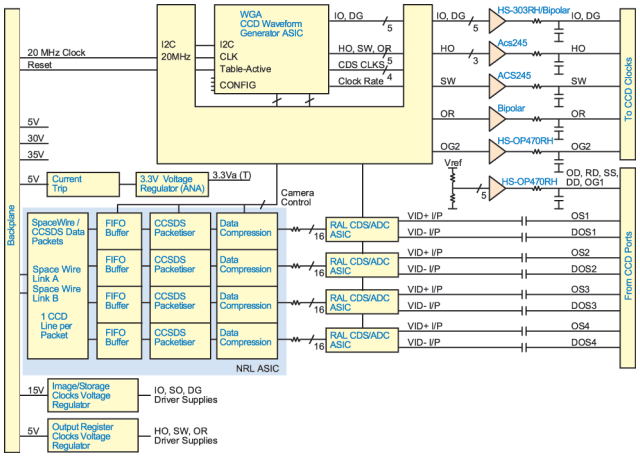

Figure 1-21. CCD Interface Card

The AIA CCDs will be a new Marconi chip with 4k x 4k pixels of 12μm pitch. The six EUV imagers will employ thinned, back-illuminated chips, whereas the VUV imager will employ a front-illuminated chip with lumogen coating. The AIA CCDs will be designed for 4-phase clocking and operate non-inverted to ensure good full well capacity (150k to 200k electrons). They will also allow low-voltage clocking of the serial output register to minimize power dissipation in the clock driver electronics without sacrificing full well capacity for 2 x 2 pixel binning.

❒ *Camera Readout Electronics*: The CCD camera readout electronics (Figure 1-21) are required to read out at 2 Mpixels per second through four/two ports simultaneously for the AIA/SCORE CCDs. The resultant video signals will be digitized to 14 bits accuracy. The digital signal will then be compressed, formatted into CCSDS packets, and routed to the S/C using the serial IEEE-1355 spacewire protocol with LVDS line drivers. The high cadence requirement plus the fast readout (up to 8 Mpixels/s) requires that compression and packetization must occur separately. We propose to do this in the camera with a new ASIC development.

Multiple ASIC and surface-mount electronics packaging technologies will help minimize the size, mass, and power requirements of the cameras. Controlling all AIA and SCORE CCDs from two camera controller boxes (Figure 1-22) will minimize the overheads arising from secondary power converter inefficiencies, and thus the overall size, mass, and power of the respective camera controllers.

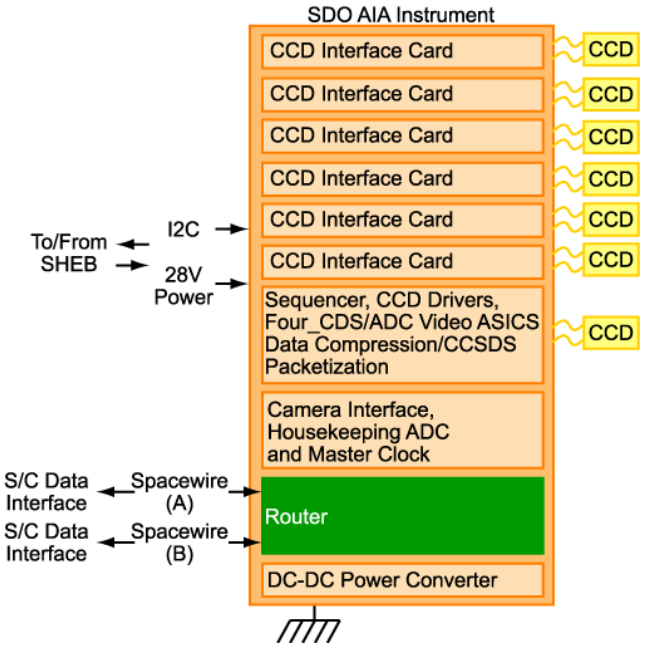

Figure 1-22. AIA CCD Camera Architecture

The camera electronics will exploit the same basic waveform generator ASIC and CCD clock driver circuit topologies designed for the STEREO/SECCHI CCD cameras, but optimized for the faster pixel readout rate for SHARPP. Each CCD will be clocked from its own dedicated sequencer and clock drivers, and will be read out through up to four 14 bit CDS/ADC video processors operating in parallel. The CDS/ADC video processor design will be implemented in an ASIC. We will use a specially designed, radiation tolerant chip developed at RAL for the STEREO/SECCHI program, but re-optimized for the 2 Mpixels/s readout rate of the new 4k x 4k pixel CCD.

A new development from the STEREO/SECCHI cameras will be the addition of an ASIC to apply image compression, CCSDS packetization, and FIFO data buffering on the CCD video data prior to transmission. We will implement a lossless Rice compression and the wavelet compression developed for LASCO/EIT and also used on SECCHI. Timing analyses show that we can perform the compression line-by-line (200 ms) in the CCD parallel shift time (500 ms). This eliminates the need to do double buffering on the input stream. Each CCD readout port will have unique packet identifiers (APIDs), enabling the images to be reconstructed on the ground. The ASIC functionality will be developed using a XiLinks FPGA. A back-up to the ASIC fabrication is the FPGA with a

Universal Source Encoder for Space (USES) device from ICs, which performs a lossless compression at a sustained rate of 20 Mpixels per sec.

CCSDS packets will be transferred directly to the spacecraft bus over a redundant high speed LVDS serial link, operating up to 200 Mbits/s, and employing the SpaceWire protocol (as used in STEREO/SECCHI). We propose to use SpaceWire, because it is a standard interface, with simple protocol and with readily available COTS interface boards for ground testing. A router is provided within the SCORE and AIA cameras to combine the separate camera outputs into two separate redundant SpaceWire streams to the S/C. Flow control enables a constant stream of data to the S/C without requiring a burst capability on the S/C. A breadboard system has demonstrated such routing up to 300 Mbps, well above our requirement. This concept permits a full redundancy in the camera (other than the CCD and CCD drivers themselves). By changing the readout pattern we can direct the readout to be through any CCD port and processing chain.

Exposure timing for each CCD will be controlled directly from the SHEB. Appropriate programming and control of the camera waveform generator ASICs will enable updating of CCD readout waveform patterns and readout tables, and the initiation of various readout modes e.g. clearing, exposure, full-frame, windowed, or continuous readout. Pixel binning, programmable video gain, and programmable video DC offset level will also be supported.

Each camera controller will contain a DC-DC power converter that will convert the incoming 28V power to the required +5V, +15V, and +30V, and +36V secondary supplies. The design will be based on the ART2815T converter from Lambda Advanced Analog with additional circuitry to generate the +36V rail.

❒ *Focal Plane Assembly (FPA)*: This FPA provides the SHARPP CCDs with physical mounting, optical positioning, electrical connection, and thermal cooling. The interaction of these four requirements makes the FPA an engineering challenge. The SHARPP FPA design for the SCORE (Figure 1-23) is virtually identical to the STEREO/SECCHI design. The same FPA front end design up to the cold finger will be used on all nine SHARPP telescopes. The AIA cold finger support sleeve will come out at right angles to the optical axis.

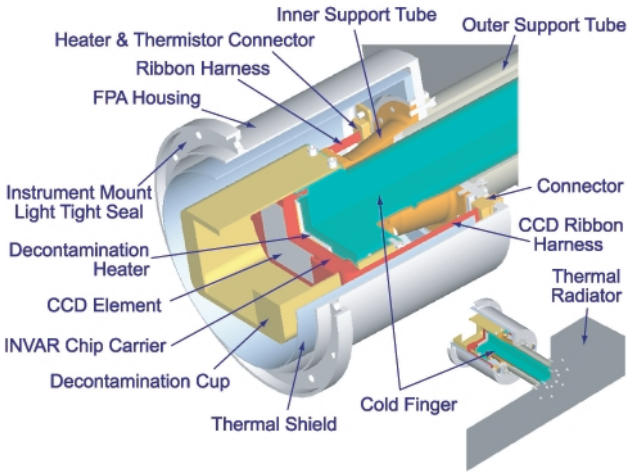

Figure 1-23. SHARPP Focal Plane Array Design

The FPA includes the CCD package, a cold plate, the cold finger, a thermally isolated cold finger sleeve, and the radiator mount. The estimated mass of the current design is 0.6 kg for the FPA and 0.2 kg for the radiator support. The design goal for the CCD temperature is about -80C. Initial thermal modeling shows that the CCD will be cooled to below the maximum operating temperature of -65C with the current FPA design.

1.7 Mechanisms.

1.7.1 AIA Mechanisms. To increase the reliability of the AIA program, the internal mechanisms have been limited to the minimum: a one shot aperture cover, one acoustic cover protection for filters, an image motion compensation system and a shutter mechanism per unit.

The aperture cover will open only once in orbit, and will be maintained open during the entire mission. The design of the mechanism is based on the INTEGRAL/OMC (to be flown end 2002) and COROT (under development) aperture systems. It uses a spring-loaded hinge with plain bearings, and a paraffin actuated launch lock device (Starsys RL-50C) that was implemented in the SOHO/EIT and INTEGRAL/OMC aperture mechanisms. The RL-50C devices will be custom modified by Starsys to allow an easy resetting, as presently done for the CSL COROT aperture system, currently under development.

Aluminum filters require special protection to avoid acoustic damage during tests and launch ascent. The filter will be mounted in a bulkhead and protected by 2 doors that retract in flight driven by a DC brushless motor. This will allow reclosing operation to provide means for calibration se-

quences (dark current and calibration lamps) and contamination protection during S/C maneuvers. A DC brushless motor will be used. Venting around the filters will be possible trough labyrinths designed to avoid stray-light (as implemented in SOHO/EIT). This solution is preferred to the vacuum compartment option, which requires regular pressure monitoring and risky pumping operations.

The secondary mirror will be mounted on an image motion compensation system (IMS), to overcome the jitter of the S/C and ensure subarcsecond pixel resolution. This device will use 3 piezoelectric transducers driven in open loop with the information from the AIA Guide Telescope. There is no hysteresis compensation. The small mass of the mirror allows avoiding a launch lock. A specific mount for the secondary mirror will be implemented to allow tilt movements with the piezo actuation. This piezo mechanism will also provide possibilities for specific flat-fielding techniques (as initiated with SOHO/EIT during the SOHO off-pointing sequences). This latter option will be considered during Phase A.

Each unit will be equipped with a shutter mechanism described below. However, preliminary studies showed that the AIA could be operated in shutterless mode, as experimentally done in specific sequences with the SOHO/EIT instrument. The shutterless option will be considered and evaluated during Phase A.

1.7.2 SCORE Mechanisms.

❒ *Reclosable Doors*. The baseline design will be a duplicate of the doors build for the STEREO/SECCHI telescopes (Figure 1-24) derived from the SOHO/LASCO doors. The doors use a 1.8º stepper motor to drive a cam follower. A paraffin wax-actuated fail-safe device pulls a pin that opens the door completely. The only difference between the two SCORE doors is the diameter of the lid covering the telescope aperture. The interface between the lid and the tube is a series of concentric groves. The purpose of the door is to maintain the cleanliness of the optical system against external contaminants. During the launch, the door mechanism must keep the lid tightly pressed against the aperture without generating particles. The LASCO doors were designed to accomplish these objectives and did so extremely successfully.

❒ *Shutters*. All SHARPP telescopes are equipped with shutters in front of the CCD cameras (Figure 1-24). The seven AIA units use a cylindrical shutter for accommodation reasons and inertia reduction. The two SCORE telescopes use a blade shutter. All shutter mechanisms use the same brushless DC motor with an integral, optical, shaft angle encoder that provides position feedback for commutating the motor and measurement of the actual exposure. An operating time of less than 20 milliseconds is provided. The bearings will employ ceramic balls and will be lubricated with ultra low outgassing fluorinated grease to assure reliable operation for in excess of 20 million open/close cycles. The motor is based on the MDI, SECCHI, and Solar-B design. The MDI prototype underwent a life test of 67 million exposures, and the flight unit has taken more than 20 million images. The Solar-B/EIS shutter prototype is undergoing a life test and has completed 10 million cycles so far.

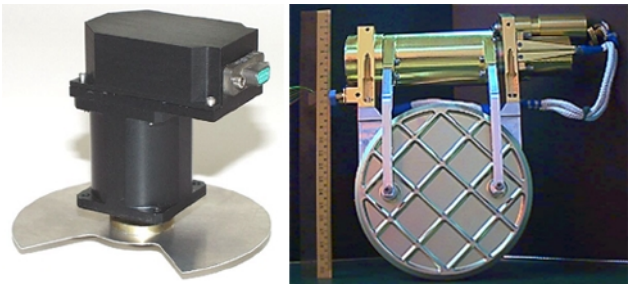

Figure 1-24. SECCHI Shutter (left) and Door Assembly (right)

❒ *Rotating Polarizer*. SCORE/KCOR contains a rotating polarizer mechanism. It is the same mechanism used in the two SECCHI/COR2 coronagraphs. They are evolved versions of motors presently flying on MDI and TRACE, and very similar to the Polarization Modulator unit that will fly on Solar-B. They are brushless DC motors built by SWALES. The MDI prototype motor underwent a life test of 100 million cycles and the pair of units on MDI has made over 20 million moves on orbit. As with the shutter motor, an integral, optical, shaft angle encoder is used for commutation and for identifying the position.

❒ *ECOR Occulter Boom*. After evaluating several deployable concepts, a previously qualified telescoping boom was chosen to place the ECOR occulter 2.4 meters forward of the entrance aperture. The boom was developed by AEC-ABLE Engineering Co, Inc. as an astronaut tool used to build the International Space Station. The boom was life tested to 10,000 deployments and retractions. The boom consists of a number of nested tube segments, a lead screw to deploy the tubes,

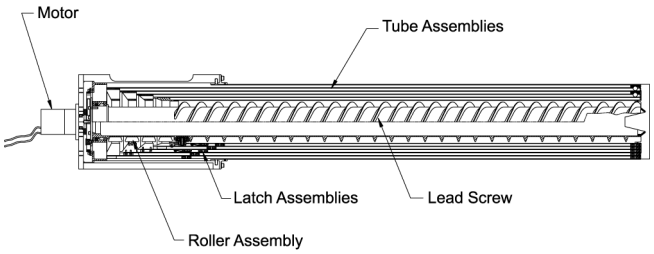

Figure 1-25. ECOR boom cross section

and latches to fasten the tube segments together (Figure 1-25). A stepper motor is used to drive the lead screw. Rollers at the base of the innermost tube are engaged in the lead screw, and each tube segment deploys sequentially. Each tube segment interface is aligned via a preloaded cup and cone design and the joint is locked by a number of spring-loaded latches. Preliminary analysis shows this joint design will provide the required deployable repeatability and stiffness to maintain occulter positioning relative to the ECOR entrance aperture. Further work in Phase A will focus on modifying the existing design (5.5 meter boom) to meet the 2.4 meter length requirement and minimizing the mass of the boom while maintaining its repeatability, deployed stiffness, and reliability.

❒ *ECOR Filter Mechanism*. The thin-film filters used in the ECOR are fragile and sensitive to acoustic loading during the launch phase of the mission. A light tight filter wheel design protects the filters during integration, test, and launch, and provides a redundant filter set in the event of damage to the primary set of filters. An aluminum shroud encloses the filter wheel and provides mechanical protection for the filters and a light seal for the ECOR camera compartment. A CDA Intercorp stepper motor will rotate the primary filter out of the shroud and into the optical path before the science portion of the mission. If there is a problem with both of the primary filters, the wheel will rotate again to bring the back-up filter set into the optical path. The stepper motor will provide for remote operation of the filter wheel during instrument testing. The Phase A work will focus on meeting the light tightness requirements around the rotating filter wheel, a tractable problem with external occultation, while minimizing contamination concerns.

1.8 Thermal Control System (TCS). SHARPP uses a passive TCS to maintain unit temperatures within chosen limits. The design incorporates the same principles implemented on LASCO, EIT, and SECCHI. The individual units will be thermally isolated from the S/C. The CCDs will be passively cooled to -60˚ C with a ~250 cm^2 radiator per chipset (similar to LASCO's camera design). All SHARPP CCD radiators will have a clear view to space. The SHARPP TCS will maintain the optical box to ~10˚c during normal operations. Dissipated heat and absorbed solar energy will be matched by radiative losses through the front aperture and blankets. The dissipated energy will be spread through the box with radiative and conductive coupling. About 3W heater power is required to offset SHARPP uncertainties in MLI, BOL/EOL properties, and variations during the eclipse seasons. The SHEB will be cooled using a radiator that views deep space. A thermal balance test will be conducted to validate the thermal design.

Table 1-7. Flight S/W Requirements

• Control the telescope
• Prepare and provide HK data to the S/C
• Monitor health and safety and take corrective action
• Accept, validate, and distribute CMDS from the S/C
• Control GT, transmit pointing information to S/C, command jitter control mechanisms

1.9 SHARPP Flight Software. The SHARPP instrument suite flight S/W builds on the flight S/W developed for the STEREO/SECCHI instrument suite. High-level requirements for the SHARPP flight S/W are listed in Table 1-7. The flight S/W uses the proven COTS VxWorks multi-tasking real-time operating system with the C and C++ programming languages. This real-time operating system was used with the JPL Mars Pathfinder, LMSAL SXI/GOES and the GSFC SMEX among others. The payload control S/W being developed for STEREO/SECCHI is derived from the payload flight control S/W for the Triana payload.

❒ *Memory Margins*: The flight S/W executes from the 128 MB of system RAM. Code is loaded from the 3MB of EEPROM. Roughly 256kB of the EEPROM will be the VxWorks runtime kernel. About 75% (400kB) of the flight S/W exists as reusable SECCHI S/W; the remaining 25% (100kB) will be developed specifically for SHARPP. This results in a 50% margin for fitting within 1.5 MB of EEPROM and allows a redundant copy of all S/W.

❒ *CPU Utilization*: The heritage RAD750 has fewer tasks than on SECCHI, because all the image compression and packetization tasks are being

performed in the cameras. The current usage is less than 25%.

❒ *S/C Interface and Control*: An IEEE 1553 command and housekeeping bus will handle the communication between the S/C and SHARPP. GT attitude information and housekeeping will be sent from SHARPP to the S/C over this bus. The data manager task will also be able to dump at a high cadence housekeeping, memory, or other data into the science channel for diagnostic purposes.

❒ *Health and Safety*: The instrumentation voltage, S/C pointing, and temperature limits are monitored to ensure safe conditions. The SHARPP flight S/W has the capability to safe the instrument if an error is detected or a self-test fails. If the GT error exceeds a designated threshold, the SHARPP payload will also be safed, and error flags will be set in the housekeeping telemetry. SHARPP will further safe itself if it is sent event flags from the S/C that require action (closing doors for thruster firings or a controlled power-off).

❒ *Heritage*: The flight S/W architecture is based on the SECCHI multi-tasking design being developed by NRL with flight heritage from Triana and SMEX-lite code developed at GSFC. A major difference in the requirements between SECCHI and SHARPP is that here the image compression and packetization will be performed by ASICs within each camera. The full image header information will be sent down separately from the image data with a tag being included in both the header and the science image to associate the two. However, we envision only a slight evolution from the SECCHI flight S/W since all of the other requirements are also the SECCHI requirements.

❒ *Task Concept*: The major S/W tasks and their functions are described in Table 1-8. The tasks are further divided into sub-tasks, not shown here. The tasks and sub-tasks are separate modules, which can be tested independently. The individual modules are kept small so that in the event of a S/W problem a new module can be uploaded with a small number of commands. The tasks communicate with each other using message queues and semaphores that are part of the VxWorks operating system. Two-step commanding is utilized for critical commands such as opening or closing a door. "One-time" commands will be doubled commands and password-protected and may require special ground commanding. For diagnostic purposes, commands understood by the mechanism control task can be issued from the ground and passed to the mechanism control module as well as being issued under observation schedule control. Individual instrument processing will be table driven. Tables will contain the necessary information to position mechanisms, setup the cameras (number of clears, pixel summing, region of interest), do camera exposure and readout, and process the image. Actual observation time and exposure time are added to the header template after an image is taken.

❒ *Experiment Science (ES) Processing*: One task example is the ES, which configures the telescopes for each exposure and issues the camera commands to clear, expose, and readout the CCDs and then controls the compression and formatting into CCSDS packets. ES also generates the science header for each image. It processes status information received from each exposure, which includes information on the number of pixels above some threshold for automatic exposure control.

1.10 Spacecraft Accommodations.

❒ ***Volume, Mass, and Power:*** The SHARPP volume, mass, and power are listed in Tables FO2-3 to FO2-5. Mass and power contingencies are explicitly listed and were based on heritage.

❒ ***Interfaces****:* There are three primary mechanical and thermal interfaces with the S/C (AIA, SCORE, and SHEB). S/C power, commands and status interface through the SHEB, but science telemetry pass to the spacecraft directly from the two camera boxes to the spacecraft. We recommend the use of a redundant, serial SpaceWire link from each camera. Commands and HK telemetry are passed over the redundant MIL-STD 1553 link. All inter-instrument electrical interconnects are provide by a SHARPP flight harness. Interfaces between all the various components (inter-instrument and intra-instrument) will be defined in Phase A and finalized in Phase B. The location on the S/C of the three units is constrained only by the interconnect harness.

❒ ***Thermal Interfaces***: The AIA and SCORE are thermally isolated from the S/C. Passive radiant coolers with a view to deep space are required to cool the CCD detectors to below -40ºC, with a goal of -80ºC. The SHEB can either be thermally isolated or conductively coupled, depending on the S/C desires. This decision will be made in Phase A. The nominal operating temperature range for

Table 1-8. SHARPP S/W Tasks

Subsystem	Function
Task Manager	Add/Destroy S/W tasks
Scheduler	Handles timing of all tasks such as image acquisition, housekeeping collection, etc.
Housekeeping Manager	Issues status requests to other S/W subsystems. Formats status into specific format. Health and safety monitoring and safing. Watchdog timer reset.
S/W Manager	Load (from ground commands) or dump (to telemetry) various system tables or memory locations
Self Test	Built in tests that are executed at least during power up
Data Manager	Transfers data to spacecraft
Command Handler	Receive and route ground commands
Instrument Control	Controls all aspect of a telescope data acquisition. One control task for each telescope
Mechanism Control	Controls operation of each mechanism. Simultaneous operation (Shutter motions) are possible. Accepts commands from other tasks or from the ground
Experiment Science Processing	Performs exposure evaluation, image header formatting.
Experiment Housekeeping	Acquires and formats housekeeping data from the telescopes in response to requests from Housekeeping Manager task
Guide Telescope Manager	Controls redundancy within GT, acquisition of data from GT detectors, formatting for spacecraft

AIA and SCORE is 0-40ºC. The ±0.5ºC thermal stability is acceptable.

❒ ***Alignment***: The SCORE and AIA must be pointed to Sun center to 50" and 2" respectively. The SCORE (KCOR) requirement is less than the AO stated capability. We request that the bias due to launch and thermal shifts be offset to accommodate the KCOR requirement.

❒ ***Pointing Control***: The minimum required pointing stability of 5" is determined by the need to have a constant stray light pattern in the coronagraph. A jitter control is included in the AIA telescopes to achieve better stability than the S/C can deliver. The SHARPP provided GT supplies this. If this GT is descoped, then the SHEB must receive the GT output over the 1553.

❒ ***Commanding***: SHARPP can accept CCSDS command packets over the 1553 link. A S/C stored command capability is not required. A heartbeat status message from SHARPP to the S/C is available to enable the SHARPP instrument to be powered off in case of trouble.

❒ ***Reliability Assurance***: All EEE parts, CCDs and optics are selected so that the susceptibility to total radiation dose and single event upsets are consistent with the mission lifetime. EEE parts are Grade 2 or better (see Sect. 5.6.3).

❒ ***Cleanliness and Contamination***: Both particulate and volatile contamination will degrade the science of SHARPP. A stringent materials selection process is required, with bakeouts. Contamination control practices are required for all I&T activities involving the instrument suite. SHARPP will be designed to accept a 10,000 class clean room with an instrument purge using dry N2.

1.11 SHARPP Science Team. Tables 1-9 through 1-11 list the co-investigators and collaborators for the SHARPP suite of instruments. Over half of the Co-Is are from European institutions and, of course, receive no NASA funding, but contribute significantly to SHARPP. This validates the international aspect of ILWS, enabling the best science for the least amount of funding within a given funding entity. The tables identify the funded Co-Is, those Co-Is funded from non-NASA SHARPP funds, and collaborators. Almost all of the science team listed in these tables will be involved in some aspect of the data analysis tasks, and so this role has not been explicitly identified.

Table 1-9. SHARPP Co-Is Funded by NASA in Phases A-E

Name	Org.	SDO Mission Role
F. Auchere	USRA	CCD Detector Scientist
D.A. Biesecker	L-3 Com Analytics	CME WG/Comets, EPO
J.M. Davila	GSFC	3D WG, Multilayer Consultant, Detector consultant
R.A. Howard	NRL	SHARPP PI
J.T. Karpen	NRL	SHARPP Mission Scientist, MHD Modeling (ARMS)
J.A. Klimchuk	NRL	MHD Modeling (ARMS)
P.C. Liewer	JPL	SHARPP Data Systems Consultant, MHD modeling
D.J. Michels	CUA	EPO
J.D. Moses	NRL	SHARPP Deputy PI
J.S. Newmark	NRL	AIA US Project Scientist
S.P. Plunkett	USRA	I&T Lead Scientist
J. Seely	NRL	Multilayer Design Consultant
N.R. Sheeley	NRL	CME WG, Coronal Structures
D.G. Socker	NRL	SCORE PI
O.C. St. Cyr	CUA	Operations Scientist, CME WG, SCORE calibration
A. Vourlidas	NRL	KCOR Project Scientist, CME WG, SCORE Calibration
D. Wang	NRL	SHARPP Flight S/W, Ground Systems, Polarization Calibration
Y.M. Wang	NRL	CME WG, Coronal Structures

Table 1-10. SHARPP Co-Is Funded Otherwise

Name	Org.	SDO Mission Role
S.K. Antiochos	NRL	MHD Modeling
E. Antonucci	Torino	SPECTRE PI
G. Artzner	IAS	AIA optical design, 3D WG
D. Berghmans	ROB	Data analysis, data reduction algorithms
K. Bocchialini	IAS	Data Archive
V. Bothmer	MPAe	EPO, 3D WG, CME analysis
F. Clette	ROB	AIA program scientist (Phase E- AIA PI)
P. Cugnon	ROB	AIA Program Management
L. Culhane	MSSL	CCD Design and Screening, flares and CME
J.M. Defise	CSL	AIA Deputy PM
J.P. Delaboudiniere	IAS	AIA optical design, data analysis
S. Fineschi	Torino	SPECTRE Program Scientist
A. Fludra	RAL	UK Project Scientist, Data analysis, operations
R.A. Harrison	RAL	UK Program Scientist, Data analysis, operations
J.F. Hochedez	ROB	AIA Technical and Scientific Consultant
M. Idir	LIXAM	AIA Calibration
P.L. Lamy	LAS	SCORE Optical Consultant, Comets, F-corona, Polarization
J. Lang	RAL	CCD Camera PM
M. Malvezzi	UP	EUV Coatings
E. Marsch	MPAe	Data analysis, data reduction algorithms
R. Mercier	IOTA	AIA Multilayer fabrication
S. Poedts	KUL	MHD Modeling
M.F. Ravet	IOTA	AIA Multilayer coatings
M. Romoli	UF	SPECTRE Instrument Design, Calibration Test
P. Rochus	CSL	AIA PI
N. Waltham	RAL	CCD Camera Specialist

Table 1-11. SHARPP Collaborators

Name	Org.	SDO Mission Role
D. Banerjee	KUL	MHD Modeling
J.W. Cook	NRL	3D WG
K.P. Dere	NRL	CME WG
F. Delmotte	IOTA	AIA Multilayer fabrication
D. Gardiole	INAF	SPECTRE Instrument Design, Calibration Test
N. Gopalswamy	GSFC	CME Analysis
E. de Jong	JPL	SHARPP Data Systems Consultant
C.M. Korendyke	NRL	GT Project Scientist, SCORE Calibration, Contamination
A. Llebaria	LAS	SCORE Optical Consultant, Comets, F-corona, Polarization
J. Luhmann	UCB	Magnetic origins of CMEs
R. Vanderlinden	ROB	AIA Data Analysis
E. Verwichte	ROB	AIA Data Analysis, mission operations
T. Zurbuchen	UM	Interplanetary manifestations of CMEs
C. Foullon	ROB	Space Weather

2. Education & Public Outreach

2.1 Abstract. The SHARPP Education and Public Outreach (E/PO) program capitalizes on exciting science and existing infrastructure to bring the maximum impact to the public. The SHARPP instruments will be central to the NASA ILWS Program and thus to the understanding of the utility and societal impact of Sun-Earth Connections. The focus of this E/PO effort is to empower the teachers of today and the future through a variety of outreach efforts such as direct education of future teachers, teacher internships, workshops, and development of educational tools, all designed to meet or exceed National Science Education Standards.

2.2 SHARPP Approach to E/PO. The SHARPP outreach approach focuses on empowering educators from all subject areas to use the latest results of scientific research in the field of Sun-Earth Connections. By establishing programs in which current teachers and teachers in training interact with working scientists, the SHARPP approach will instill in them the knowledge and confidence to teach science and the scientific method. This effort will reach all of K-14+ education, either directly or indirectly. The SHARPP team has already developed E/PO programs as part of the SOHO and STEREO missions, in which the team is a major participant. Starting with existing infrastructure and partnerships, this E/PO effort will work to ensure that programs being developed and field-tested locally can be extended to a wider audience. Most importantly, the goal of empowering teachers will provide the broadest reach for the SHARPP E/PO effort. The average teacher will interact with dozens, if not hundreds of students each year. By focusing on teachers in training, the SHARPP program will establish lifelong relationships with educators, allowing them to stay in touch with the latest in Solar and Earth science research. SHARPP is just a small part of the ILWS program, so the E/PO outreach effort will be coordinated with ILWS and SEC Educational Forum (SECEF) activities.

2.3 SHARPP Experiment. The SHARPP instrument package consists of 3 telescopes. These telescopes will provide images and movies of the dynamic Sun and solar atmosphere out to 15 $R_{\odot}$. The images will show CMEs, from their dramatic and explosive beginnings, through their evolution in the low corona, and finally their passage into interplanetary space. CMEs, one of the main drivers of space weather, provide an ideal, visual tool to illustrate the utility of the SHARPP mission and routine workings of the scientific process. The full solar disk will be imaged with high spatial resolution at an unprecedented cadence of 10 seconds per image by the AIA, and at a range of plasma temperatures from 20,000 K to 3,500,000 K. The broad temperature coverage ensures that a wide variety of phenomena will be well observed. The FOV of the AIA extends into the solar atmosphere to a height of 1.4 $R_{\odot}$, thus showing the early development of CMEs. As they move outward, an entirely new instrument, the ECOR, will follow the CMEs from 1.2 to 3.0 $R_{\odot}$. The ECOR instrument will produce images of plasma at a temperature of 1,600,000 K (Fe XII). CMEs are readily revealed at this high temperature. The ECOR will allow the early evolution and propagation of CMEs to be followed. Finally, a visible light coronagraph, KCOR, will be used to show CMEs and the extended corona at heights from 2.5 to 15 $R_{\odot}$. The visible and polarized light images taken by KCOR will allow for determinations of the shape and speed of CMEs as they begin their journey through interplanetary space, toward Earth.

2.4 Implementation and Evaluation. The SHARPP E/PO program is structured into two types of outreach: formal and informal education. It is designed to bring the latest in Sun-Earth research to educators, students, other scientists, and the general public. Use of existing programs at the Naval Research Laboratory (NRL) helps to maximize reach with minimal effort and duplication. In addition, the pre-existing relationships the SHARPP personnel have are used to ensure efficiency and that the E/PO effort fits in to the overall SDO and ILWS education and outreach efforts.

2.4.1 Formal Education (K-14+). Teacher training and empowerment is the main focus of this effort. Through strengthened training of teachers, the maximum number of students of all ages, races, and ethnicities will be reached.

❒ *Sun-Earth-Centered Program for Teachers in Training*. A joint endeavor between the Catholic University of America (CUA) and NRL is being developed under the STEREO E/PO effort. This

will be part of the regular Education Department program for Bachelor's or Master's Degree with concentration in Science Education. It will be coordinated by NRL and the Center for Solar Physics and Space Weather of the CUA Department of Physics. Preliminary discussions with the Departments of Physics and of Education at CUA have already taken place. Development of curriculum requirements and definition of program administrative parameters are underway. Both pre-service and in-service teacher training will be part of the curriculum. It is expected that all students in the Education Department will take a 1-semester course in Solar and Earth Sciences. Math and Science Education teachers will take an additional 2 semesters. The SHARPP E/PO effort will work intimately with this program, with the view of bringing the curriculum to a wider audience. This will begin by reaching out to other colleges and universities in the Washington, DC region, with an emphasis on institutions committed to the service of underserved and underutilized populations and to the Washington Area Consortium of Universities. These efforts would lay the groundwork for making this program available nationally.

❒ *Summer Intern Program*. Both in-service teachers and teachers in training will be involved in this effort. Teachers will be brought to NRL or to the Goddard Space Flight Center for a period of several weeks each summer where they will work on-site with NRL scientists. Depending on the desires of the teachers, these experiences can be in an area of current research or be used to assist in the development of curricula and educational materials.

a. Select students from the CUA Education Department who have taken part in the Sun-Earth-Centered Training course will have the opportunity to work one on one with individual scientists for six weeks. This time will serve to give the students confidence in their science education and to foster life-long relationships with researchers.

b. Washington DC teachers who participate in the SUNBEAMS program at GSFC, will be hosted by SHARPP personnel. SUNBEAMS provides DC teachers, who represent an underserved population, with the time and resources to develop educational materials and lesson plans based on the latest science and technology. It establishes long-term partnerships between scientists and engineers and grade 6 math and science teachers. The teachers will work one on one with SHARPP scientists for 5 weeks in the summer. Then in the school year, 1-week student workshops take place for students selected by the teachers. The whole community is involved through a Family Night where the school community, as well as parents and siblings can share in the students' experiences.

c. The on-going Goddard In-Service Professional Development Programs for science teachers provides teachers to work at NRL one on one with SHARPP scientists for 6 weeks. NRL has hosted teachers in the past under this program and will continue to do so as a part of the E/PO effort.

❒ *Master Teacher Workshops*. The teachers who participate in the Summer Intern Program at NRL will be integral to the hosting of an annual one-week Master Teacher Workshop. A diverse population of master teachers, not limited to math and science, will be recruited each year. This program will cover the expenses of teachers participating in the Master Teacher Workshops. The teachers will be trained to use the tools developed in the Teacher in Training and the Summer Intern programs. The summer intern teachers, who know best how to communicate with other teachers and how to deal with typical classroom problems, will work jointly with SHARPP scientists to give the teachers a first hand look at the process of conducting science.

❒ *Planetarium Show*. A planetarium show currently in development will be incorporated into the SHARPP E/PO program. NRL scientists will work with the show to ensure it stays up to date with the latest in Sun-Earth science. In addition, they will work to ensure the show can be packaged for distribution to other planetariums. Integral to the theme of educating the educators, it will be critical to bring planetarium directors into the one week Master Teacher Workshops so they will be comfortable with presenting the show and the science behind it.

2.4.2 Informal Education. The informal education aspect of the SHARPP E/PO program is very similar to activities NRL already has in place for the STEREO program. The theme of the STEREO mission is very similar to that of SHARPP; an investigation of CMEs with respect to Sun-Earth

Connections. Overlap between the two programs is natural and cost-effective.

Visits by SHARPP scientists to local classrooms and groups with a general interest in solar physics and astronomy will be an important part of the E/PO effort. The SHARPP web page will play an important role in reaching the general public as well, not being limited by geography. A well-developed page like the SOHO mission page (http://sohowww.nascom.nasa.gov) has the potential to reach and educate thousands of people every day. The SHARPP team will model its web page after the successful SOHO page. The pages will include interactive instructional tools, real-time data displays, and a place for interaction between SHARPP scientists and the public. The SHARPP web pages will run in concert with the STEREO mission pages, providing a continuous resource reaching across NASA missions.

Education materials meeting National Science Education Standards will be developed by teachers participating in the Formal Education part of this proposal. Additional tools, such as CD-ROMs, videos, and posters will be produced. These tools serve several purposes as they can be: used by NRL and other scientists when giving talks to the public; used in the classrooms of the educators from the Formal Education part of the E/PO effort; and delivered directly to the general public who request them.

The SHARPP E/PO team will create displays featuring computers which when connected to the Internet will show real-time movies of data from the SHARPP telescopes. Accompanying the computers will be display posters describing the SHARPP mission and the SEC theme. These exhibits will be on display at NRL, for presentations to Laboratory visitors, and will be road-ready for transportation to conferences and museums for temporary exhibit. As much as possible, these exhibits will be staffed by SHARPP scientists.

2.5 Dissemination of E/PO Products. Random dissemination of E/PO products and materials does not effectively serve any community. Certainly, these products will be available to any teacher who requests them. However, the primary SHARPP E/PO distribution outlets will be the educators who have engaged in the formal E/PO activities and other scientists. These are the educators who are empowered to fully understand the materials and to make effective use of them.

2.6 SHARPP E/PO Management. SHARPP Co-I Dr. Biesecker (L-3 Com Analytics) will coordinate the proposed E/PO activities, within the team, with other missions at NRL, with the GSFC ILWS E/PO program and with the SECEF. His experience with SOHO E/PO efforts and solar eclipse outreach will benefit the SHARPP E/PO program. He will work extensively with the Summer Intern and Master Teacher workshops.

SHARPP Co-I Dr. Michels (NRL/CUA) has extensive experience in E/PO for SOHO, ISTP, and STEREO, and will continue to work closely with CUA to develop the Teacher-in-Training portion of the SHARPP E/PO program and to work with other DC area colleges and universities to expand the CUA program. He will work to ensure the planetarium program is kept current and is packaged for wider distribution.

2.7 Budget Explanation. Costs associated with SHARPP team member participation in informal education efforts are not included. E/PO activities will be a regular part of SHARPP science team meetings beginning with Phase B. Coordination with ILWS and SECEF will also begin in Phase B. In Phase C, web page development and preparation for Master Teacher Workshops will begin. Beginning one year before launch through the five-year mission, Student Teacher Interns will be hosted at NRL and one Master Teacher workshop per year will be held. Development of educational materials will take place throughout this period. During Phase E, the traveling exhibit will be developed and be displayed.

3. Technology and Small Disadvantaged Business/Minority Institution Plan

3.1 New Technology. The SHARPP mission concept extensively uses heritage instruments. Our mission cost constraints and operational complexity provide little need or opportunity to develop new hardware technology. In fact, the absence of new technology is central to our low-risk philosophy for the mission instrument components (see Table 3-1 for our assessment of the SCORE instrument maturity).

❒ The SHARPP investigation does explore new territory in two areas. First, an Application Specific Integrated Circuit (ASIC) will be developed to perform hardware image compression, CCSDS packet formatting and SpaceWire protocol generating. Secondly, the boom/occulter on ECOR can be replaced with a new occulter concept.

3.1.1 Advanced Technology for Visualization and Analysis. NRL will develop an ASIC to perform the image processing tasks required by each CCD control card. This approach minimizes size, mass, and power. As part of the ASIC development, a Xilinx programmable gate array supports ASIC prototyping and debug. The FPGA is fully tested to verify functionality. After verification, we commit to ASIC fabrication, and included three ASIC fabrication runs in our cost. If we do not obtain a satisfactory ASIC run, we incorporate the FPGA as a descope option with only a small mass and power penalty.

3.1.2 ECOR. ECOR was not selected for the SDO mission.

3.2 SB/SDB/WOSB Plan. NRL is committed to providing the maximum practicable business opportunities for Small Businesses, Small Disadvantaged Businesses, and Women-Owned Small Businesses. Established NRL programs provide assistance for socially and economically disadvantaged firms to conduct business with each organization. Through these programs, we pursue SB/SDB/WOSB firms capable of furnishing goods and services for this investigation. We are committed to increasing SB/SDB subcontracting and procurement opportunities commensurate with the AO's goals.

Table 3-1. NASA Technology Readiness Level Assessment

Level & Definition		Item
1	Basic principles	
2	Technology concept	
3	Analytical "proof-of-concept"	
4	Breadboard in lab	• ASIC for Visualization & Analysis
5	Breadboard in simulated environment	• Camera Electronics (similar to SECCHI)
6	Prototype demo in simulated environment	• SHEB (Reuse of SECCHI processor) • CCDs
7	Prototype demo in space	• Guide Telescope (TRACE, EIT) • ECOR (Similar to EIT) • KCOR (Similar to LASCO)
8	"Flight qualified" via on-orbit test & demo	• Doors and Mechanisms (Similar to LASCO)

❒ *Acquisition Approach:* The PI will be responsible to assess and supervise the SHARPP acquisition program and to establish SB/SDB subcontracting goals. Detailed records will be maintained concerning SB/SDB subcontracting and these will be available for NASA review. It should be noted that SDB/WOSB sources are not yet totally identified to meet the requested goal due to the nature of the proposal efforts. However, during Phase A, we will identity additional suppliers and subcontracts. During Phase B, it is our intent and commitment to identify further opportunities for SDB/WOSB to the maximum extent practicable to ensure the 8% AO goal is not only met, but also exceeded.

❒ *Past Performance*: NRL employs an aggressive SB/SDB program and more than 17% of NRL's FY01 contracts were awarded to SDB/WOSB, historically black colleges and universities, and minority institutions. These past results clearly exceed NASA's 8% target goal.

4. Mission Operations & Data Analysis

4.1 Health & Safety Monitoring. SHARPP flight software will monitor important parameters for instrument health and safety and will perform automatic safing procedures to protect the instrument. There is no catastrophic condition that is known at this time, however anomalies can occur. Excessive current draw, under voltage and pointing anomalies are examples of monitoring that will be performed in the flight software. On the ground, the operations software will perform a second level of autonomous monitoring of the instrument. This monitoring includes trending of various parameters to detect anomalies that are not serious enough to shut down the instrument, but could be indicative of a possible future failure. For example, monitoring mechanism performance could identify degradation before the failure. This would enable us to set the mechanism into a useful position and then disable any further commanding of that mechanism. Plots will be generated of the various parameters, reviewed daily, and published on the web. Alarm alerts will be automatically routed to the e-mail address and pager of the operations lead.

4.2 I&T S/W Reuse. During the integration and test (I&T) phases of the SHARPP development, the following software will be required: command generation, validation, transmission and archive; telemetry reception, translation, display, and archive for housekeeping parameters; and reception, decompression, reformatting, display, and archive of science data. We will use ITOS, a fully developed uplink and downlink telemetry handler, which is freely available from GSFC and which is being developed for SECCHI I&T. We only need to configure displays and databases using tools within ITOS. The SHARPP team will be able to use this package throughout I&T and operations by migrating the command database and packet decommutation database for each phase. The databases will be developed as part of I&T and will be available prior to mission operation. This is the same strategy that is being applied to the STEREO/SECCHI I&T reusability.

4.3 Science Planning.

4.3.1 Science Operations. The "science planning" function will be minimal after the commissioning phase, so only a small operations staff will be required. We will name a Lead Operations Scientist for the suite to interface with the other instruments, the Mission Operations Team, and other observers outside the SDO project. Additionally, an operations team consisting of three people will handle the primary operations tasks of commanding and monitoring health and safety of the suite, and pipeline data processing. The operations team will reside at the NRL Data Reductions and Analysis Facility (located at or near NRL), which will also house the science operations center for STEREO/SECCHI, thus allowing us to optimize personnel and equipment. For commissioning activities or special operations, the Lead Operations Scientist can relocate to the SDO Mission Operations Center, located at or near GSFC. Special operations such as bake-out of the CCDs or calibration pointings will be performed in consultation with the SDO hardware and software developers. Based on our SOHO experience, we expect that almost all anomaly flagging and diagnosis can be accomplished remotely via the Internet. An anomaly tracking system will ensure that the proper personnel are promptly informed of each anomaly. Health and safety alerts to operators will be built into the telemetry monitoring software as needed.

4.3.2 Mission phases. The SHARPP mission operations can be divided into two phases: (1) launch and commissioning and (2) nominal mission. Phase (1) will include a period of out-gassing and CCD bake-out, followed by initial operations to refine and calibrate the science exposures, over a period of 30-45 days following launch. During this phase the instrument engineers and scientists will be on hand to diagnose and verify the proper operation of SHARPP. We will require real-time commanding with a low ground delay (~1 min) and sufficient real-time telemetry to receive science image data (20 kbits/s). This telemetry mode would also be used in the event of anomalies or development of new observing techniques later in the mission. We believe that the "continuous operations" program should be instituted early in Phase (2) and then maintained throughout the mission life.

4.3.3 Planning and Command Generation. The maximum scientific return from the SDO mission will be accomplished by adopting a "fixed" observing schedule. Once this schedule has been op-

timized during the commissioning phase of the mission, it will be interrupted only for special operations or contingencies, such as CCD bakeouts, calibration maneuvers, etc. Note that the ability to schedule special campaigns will be available, but these will take place at well-defined times between the longer periods of "continuous operations." Our experience from SOHO is that frequent modifications of a schedule will reduce the overall effectiveness of the science return. However, the schedule can evolve to take advantage of optimized observing strategies.

The KCOR telescope will be a copy of the COR2 instruments flying on the two STEREO spacecraft, so we plan to use KCOR as the "third eye", providing synergy for NASA between the STEREO and SDO missions, and maximizing the scientific return for the community. Similarly, the AIA will provide the "third eye" for the SECCHI/EUVI images. This will be accomplished by synchronizing the science operations between the STEREO and SDO instruments. The SHARPP planning cycle will be staged in quarterly, monthly, weekly, and daily schedules. General guidelines and long-term constraints are introduced at the quarterly meetings; more detailed timelines are constructed on a monthly basis. The weekly schedule is the fundamental planning unit, and daily changes are expected to be only minor modifications to the weekly schedule. The weekly schedule will be the fundamental unit of planning for SHARPP in order to coordinate with SECCHI. Because of the "continuous ops" philosophy, there will be no need to respond to changing solar conditions on short time scales.

The Lead Operations Scientist and the operations team will be able to schedule any additional on board resources beyond those required by the synoptic program. Duties include preparation of the weekly plan during the week prior to execution, representing the SHARPP team at any daily status briefings, performing analysis of the quicklook data to ensure that scientific objectives are being satisfied, and acting as a point of contact for other observers. The SECCHI planning and scheduling software will be the basis for SHARPP, enabling us to easily synchronize exposures between the SECCHI and SHARPP instruments by accounting for light travel time and exposure time differences due to differing distances of the STEREO and SDO spacecraft from the Sun. The tool, written in IDL, will also manage SHARPP resources such as computer time, memory usage, and any observing constraints imposed by hardware or operational issues. The tool will provide both graphical and text displays of the observing timeline, which allows a planner to save and reuse observing sequences. Command sequences will be generated in conjunction with ITOS. Command generation and validation are summarized in Table 4-1. Automated tools with GUI operator interfaces always generate commands. ITOS will be used at all phases of the SHARPP program, from instrument development, through integration and test, during commissioning and anomaly diagnosis as well as normal operations. A consistent GUI software interface of the commanding and telemetry displays will minimize operator error and be easy to implement because software tools within ITOS will be used to rapidly generate displays. Critical commands are protected from accidental transmission by passwords and require special software not part of the routine command software. Validation is done by (1) the operator watching the HK telemetry; (2) a command file translator, which converts the command load to human readable form; or (3) an automated and limited command subset built into the planning tool. After commissioning, the planning and scheduling tool will be the nominal method of generating command sequences.

Table 4-1. Ground Software Requirements

Command Generation	Validation Method	Usage
ITOS Operator GUI Control Panel	HK Telemetry	Development, Anomaly Diagnosis
Recorded Operator GUI Commands	Scenario File Parser and Translator	Development, test and calibration procedures, Anomaly diagnosis
GUI Planning and Scheduling tool	SHARPP Simulator	Nominal Operation

4.4 Open Data Policy. The SHARPP data will be completely accessible to the community. This is the SDO policy but it has also been our policy on SOHO and is the policy on STEREO. We will not only provide the data formatted into images, but also all the calibration data and procedures to the community to convert the data into calibrated brightness units. The uncalibrated images and

movies will be sufficient to meet the needs of most users, but the calibration tools will also be available. A standard acknowledgement will be requested of those who use the data in publications as well as a copy for the publications listing.

4.5 Data Reduction & Analysis. The SHARPP requirement of multi-channel continuous high-resolution imaging creates a tremendous increase of down-linked science data, by more than two orders of magnitude compared to the previous generation of instruments. One of the biggest challenges for the success of SHARPP will be the exploitation of the image archive by the prospective users. We will implement automated image-processing and visualization tools to condense raw image information into a reduced set of high-level data products. A subset will be made available near real-time to support space weather (SW_x) forecasting, while the rest of the data products will be produced with a slightly longer delay.

4.5.1 Pipeline Processing. We envision the implementation of a pipeline processing architecture, continuously fed with raw images. A Beowulf cluster, consisting of multiple computers, is being considered to perform the processing in order to distribute the workload. The processing will involve reformatting the science telemetry stream into images, cataloguing the images, processing and cataloguing the housekeeping telemetry, and performing event detection, anomaly detection, and trend analysis. After this first stage, a second stage of processing will be invoked that combines multiple images into products, such as polarization brightness images, temperature ratios, etc. All of the routines will be written in IDL and will be available in the SolarSoft tree.

4.5.2 Real-Time Space Weather Products. Two types of SW_x oriented data -movies and event lists- will be available within about 10 minutes of their acquisition. To achieve realistic transfer times, reduced cadence (2-5 min) and resolution (1024^2) movies of the latest SHARPP data will be available for browsing over the Internet. A four-panel movie consisting of KCOR total brightness images and AIA images in 195 Å, 304 Å, and 335 Å, will provide a concise real-time overview of the state of the solar atmosphere, facilitating the detection of explosive events and their source regions for SW_x forecasting purposes. We will also produce lists of eruptive events (CMEs, coronal waves, particles). Autonomous transient detection algorithms developed and qualified on LASCO/EIT and SECCHI data will be used to continuously update these lists.

4.5.3 Science Data. Less time-critical data products for use in scientific investigations and model development will be produced within about 30 minutes of data acquisition. These datasets will include products such as KCOR total B and pB images, AIA line-ratio and temperature maps, integrated spectral irradiance plots, differential emission measure (DEM) maps, etc. The DEM is the physical quantity, as a function of temperature, which is needed to calculate the intensity of any individual line, or the intensity through a defined instrumental wavelength passband, where the emission is optically thin and arises in a steady state equilibrium from model ions populated by collisions and radiative transitions (not photoionization or recombination). With our DEM maps we can calculate an intensity image on the disk and above the limb (to the limits of the AIA field) for any optically thin line formed at a temperature, from approximately 50,000 K (He II 304 channel) to 3.5 M K (Fe XVI 335 channel). The power of the DEM is illustrated by the wide range of studies that can be directly performed given the DEM, for example: (1) solar absolute intensity or full disk irradiance maps of optically thin emission lines, (2) investigation of the thermal structure of the solar atmospheric energy balance, and (3) model radio thermal bremsstrahlung emission.

Calculation of the DEM curve using EIT observations has been discussed in Cook et al. (1999a, 1999b). This technique can be extended (and greatly improved due to the well chosen temperature complement of lines) in the AIA. Figure 4-1 shows the temperature contribution functions for the five EUV filtergraph channels. These are supplemented with the SPECTRE OV channel with a peak temperature response at 250 K. These figures clearly demonstrate our extensive temperature coverage.

A DEM map is an individual pixel by pixel DEM curve, which reproduces the intensities in the 6 optically thin AIA (not Lyman-α) channels for that pixel. We have used the existing CHIANTI (Dere et al. 1997) program, which computes a

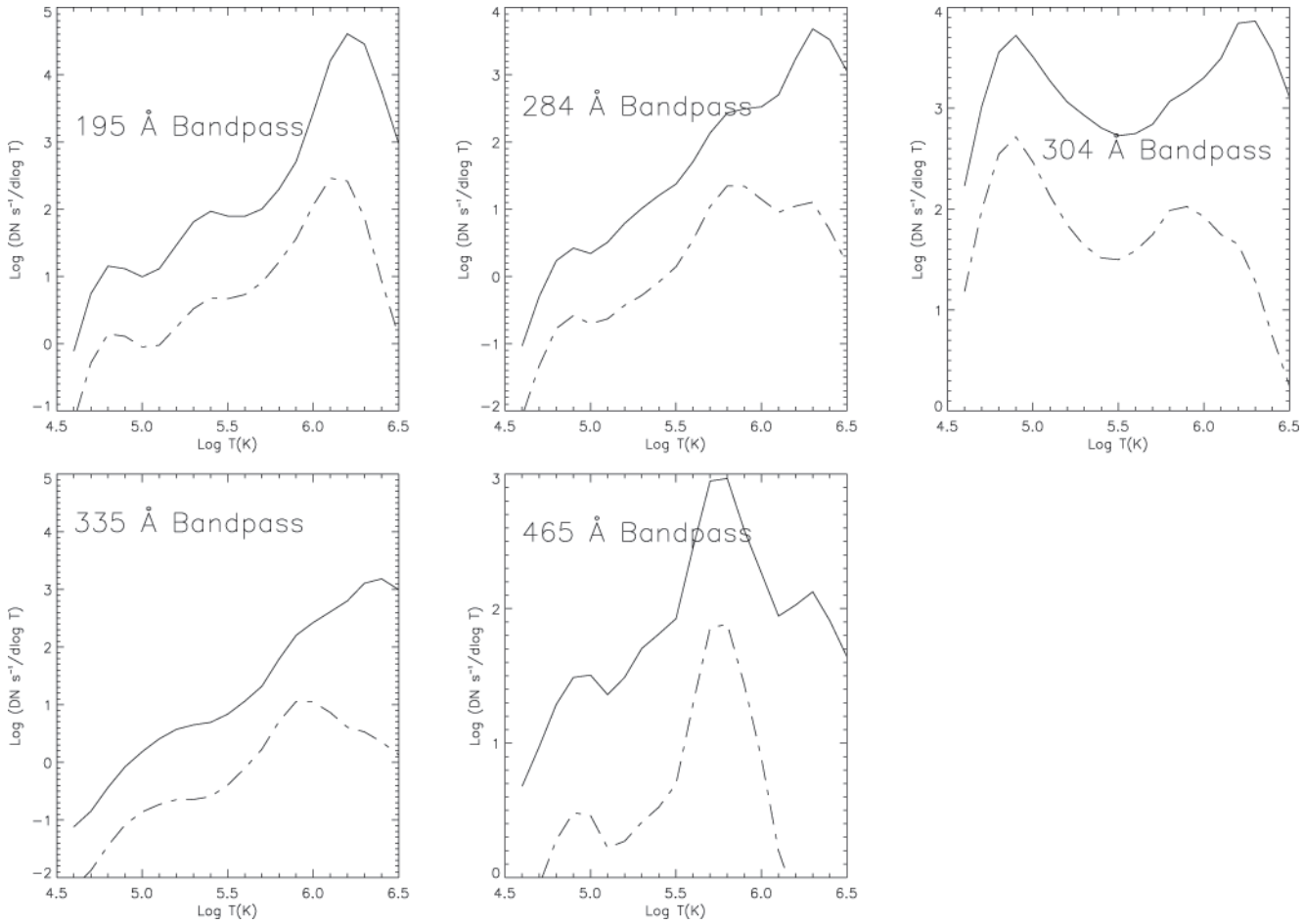

Figure 4-1. The contribution functions for the five EUV channels, giving DN s^{-1} contribution vs. Log T to the total channel intensity, for both the CHIANTI QS (dashed line) and AR (solid line) DEM curves

model spectrum using an arbitrary DEM curve and a large bank of atomic data, to compute intensities observed through the four channels of SOHO EIT for each pixel. We have previously used our DEM modeling tool to calculate full disk EUV irradiance over the SOHO mission lifetime. A comparison to the SOHO SEM (Newmark et al. 2002, Thompson et al. 2002) and SOHO CDS (Thompson et al. 2002) data is used as a test of our model assumptions. An important advantage of our DEM model intensities is the spatial resolution on the solar surface. We will provide a public database of daily, full disk, full resolution, DEM maps based upon the AIA data. Software tools will be made available in order to extract calibrated spectra (using the CHIANTI atomic physics package and out DEM model) for the full disk, full disk average, or average within any area, over the entire FOV. This is a valuable tool, which can be used by instruments such as the SIE in their conversion of signal to absolute irradiance, or to determine the spatial origins of the flux in irradiance measurements. Additionally, this has direct applicability to a multitude of solar physics studies, e.g. statistical studies across the solar surface of the atmospheric energy balance. The development of robust software and documentation will greatly help the novice user.

4.5.4 STEREO. Since SHARPP/KCOR and AIA are similar, if not identical, to the SECCHI/COR2 and EUVI on the STEREO mission, SHARPP complements the STEREO observations nicely. Currently, the SDO launch is about 2 years after the STEREO launch, at which time the STEREO-Sun-SDO angle will be about 45°. Thus, SHARPP will be able to contribute significantly to the STEREO mission by providing a third viewpoint. This will aid in the 3D deconvolution of the optically

thin corona by removing some of the indeterminacy.

4.6 Data Reduction and Archive Facility. The SHARPP data will be available over the web after routine processing has been completed. Under normal conditions, it is expected that this will take place within 30 minutes of receipt. In the case of space weather products, especially derived alerts, the space weather processing will be given high priority allowing the production of time sensitive determinations within 10 minutes or less. Calibrated data will be produced through the use of calibration routines written in IDL and publicly available in the SolarSoft library. The calibration data will be updated throughout the mission.

4.6.1 Computing Facilities. Standard UNIX workstations will be acceptable for the data reduction facility. The SHARPP GSE equipment used during I&T will be incorporated into the facility as well. Redundancy will be incorporated into the overall system design and implementation ensuring that down time is kept to the absolute minimum. The processing power of computers has been strongly advancing and so, although specific hardware and vendor choices are not made at this time, the acquisition of needed processing power should not be difficult or overly expensive. Because we are building on the LASCO data processing system model, we are confident that the system is sufficiently flexible so that additional processors and mass storage hardware are easily added. Each of the production systems will have access to the catalog database and the mass storage system.

4.6.2 Data Archive. The SHARPP mass storage system will consist of one or more RAIDs indexed by a relational database that is configured to be the data catalog. Routine processing and validation checks are performed automatically, triggered by the arrival of the data. As the volume of SHARPP data is very large, only raw images will be stored in the archive and all image corrections and calibrations will be implemented through validated software procedures accessible to the general user. The calibration software and the corresponding parameter calibration files will result from detailed instrumental analyses conducted by the SHARPP team. This software will be developed in the IDL language as part of the SolarSoft library.

4.6.3 Data Archive Architecture. The total amount of SHARPP raw data expected over the six-year mission is quite large, about 1800 TB, compressed. Mass storage technology has been advancing so rapidly it is impossible to predict with certainty the optimal storage solution for SHARPP. We have baselined the use of magnetic disks, a large RAM cache, and either a juke box of DVDs or a magnetic tape silo for backup and extended on-line storage. The actual mass storage solution will be selected closer to launch. Solar scientists will want to group and explore the SHARPP data in a wide variety of ways. The key element for locating desired data is a database query program that returns 2D images based on user search criteria over values contained in 2D image header fields. A similar query engine was used for LASCO and EIT data and is publicly available. Annotations (metadata) produced by the SHARPP science team are included in the database furthering its usefulness. The archive generated at the NRL SHARPP Data Reduction and Analysis Facility (DRAF) will be duplicated at several sites within Europe: Belgium (ROB), France (IAS), and the UK (RAL).

4.6.4 Data Distribution. Distribution to the scientific community will be electronic. Users may download data via a web interface that will allow users to select and "order" the desired data in much the same way that they do now for LASCO and EIT data from SOHO. It is expected that the web interface developed for LASCO and EIT will be modified for SHARPP. Other higher-level products, to be defined more fully at a later time, will also be available. We expect that a dedicated line from the NRL DRAF to Europe will be established to facilitate the transfer of data from the US to Europe. Within the DRAF, we will have some limited space for visitors to come and work with the data, however, we will also provide extensive online help files and data analysis tools to enable off-site users to easily access and utilize the data. The data centers in Europe will also have limited space for visitors.

5. Management and Schedule

The SHARPP Management Plan builds on the organization shown in Figure 5-1. The investigation team is lead by the Principal Investigator (PI), Dr. Russell Howard, of the Naval Research Laboratory (NRL) Solar Physics Branch. He is chartered with overall responsibility for the investigation, and he has assembled a world-class consortium for SHARPP. The management approach is an extension of the successful approach used on SECCHI, Solar-B EIS, LASCO and EIT. The SHARPP instrument suite represents the coordinated efforts of twelve institutions comprising the developmental team and supporting the scientific program. NRL, located in Washington, D.C., is the home institution for the overall management and system engineering of the SHARPP instrument suite. NRL is a world leader in the design and development of scientific instrumentation and missions, with over 40 years of experience with high-altitude and spaceflight solar physics instrumentation, including SECCHI, Solar-B EIS, SOHO's LASCO and EIT, and a number of sounding rocket missions. Key aspects of the our plan include:

❒ The SHARPP Instrument Project Office (S-IPO) is directly coupled to NRL and to the consortium technical infrastructure, and it fully supports the SHARPP PI in the management of the project. The S-IPO core is comprised of the SHARPP PI, the Instrument Project Manager (S-IPM), Mr. Steve Myers, and the Instrument Systems Engineer (S-ISE), Dr. Tim Carter. Additional electrical and mechanical systems engineering support is provided by Ms. Amy Hurley and Mr. Vince Stephens. Clear lines of authority, responsibility, and reporting are established (see Figure 5-1).

❒ Direct accountability for all project aspects to the S-IPO core team is provided by a proven Project Management Control Process (PMCS) evolved from SECCHI, Solar-B EIS, LASCO and EIT (see Sect. 5.2.3). It provides all essential elements, including planning, monitoring and control of all project aspects, and the motivation of all those involved to achieve the project objectives on time and to specified cost, quality and performance metrics. Furthermore, communication among the participants is focused to maintain good managerial insight, reporting, and control among the respective instrument teams.

❒ A WBS, developed in concert with the team member institutions, serves as the cost breakdown structure, and it also defines the limits of authority relative to requirements, cost, and schedule. It serves as the main formal management tool to control the project (see Sect. 5.8).

❒ Adequate technical and programmatic reserves are budgeted and baselined. Their allocation is centrally managed by the S-IPO and is formally distributed (see Sect. 5.5.2).

❒ The S-IPO (S-PI, S-IPM, and S-ISE) meet monthly with the foreign Consortium management as a part of the project review process. These meetings facilitate the NRL role of program control and technical support, and the process serves as an "early warning" system to detect and resolve emerging problems.

❒ Most importantly, our Management Plan is built on the dedication and personal commitment of each team member, with the full support of his/her institution. These team characteristics are demonstrated by the success of collaborative efforts on the SECCHI, Solar-B EIS, LASCO and EIT missions. Key performing personnel are identified in Figure 5-1 and in Table 5-4.

❒ Ultimately, the multi-institutional SHARPP investigation builds on the existing foundation of an effective project organization developed and managed through the NRL. Importantly, there is significant and relevant experience with all of the major foreign partners from past project. Finally, each member of the team brings a combination of experience with a relevant science perspectives, focused spaceflight instrumentation, and with technologies suitable for the application.

5.1 Management Organization. Our project framework captures the strengths of an international, multi-disciplinary consortium, and it also addresses potential risks associated with multi-institutional instrument development.

5.1.1 Organizational Structure. The reporting structure, based on the WBS for the SHARPP instrument suite (see Table 5-1), unequivocally defines the flowdown of roles and responsibilities to all subsystems and team member organizations. Our management approach focuses on the investigation elements and instrument subsystems as opposed to the consortium institutions. This process intensity provides clear insight into development

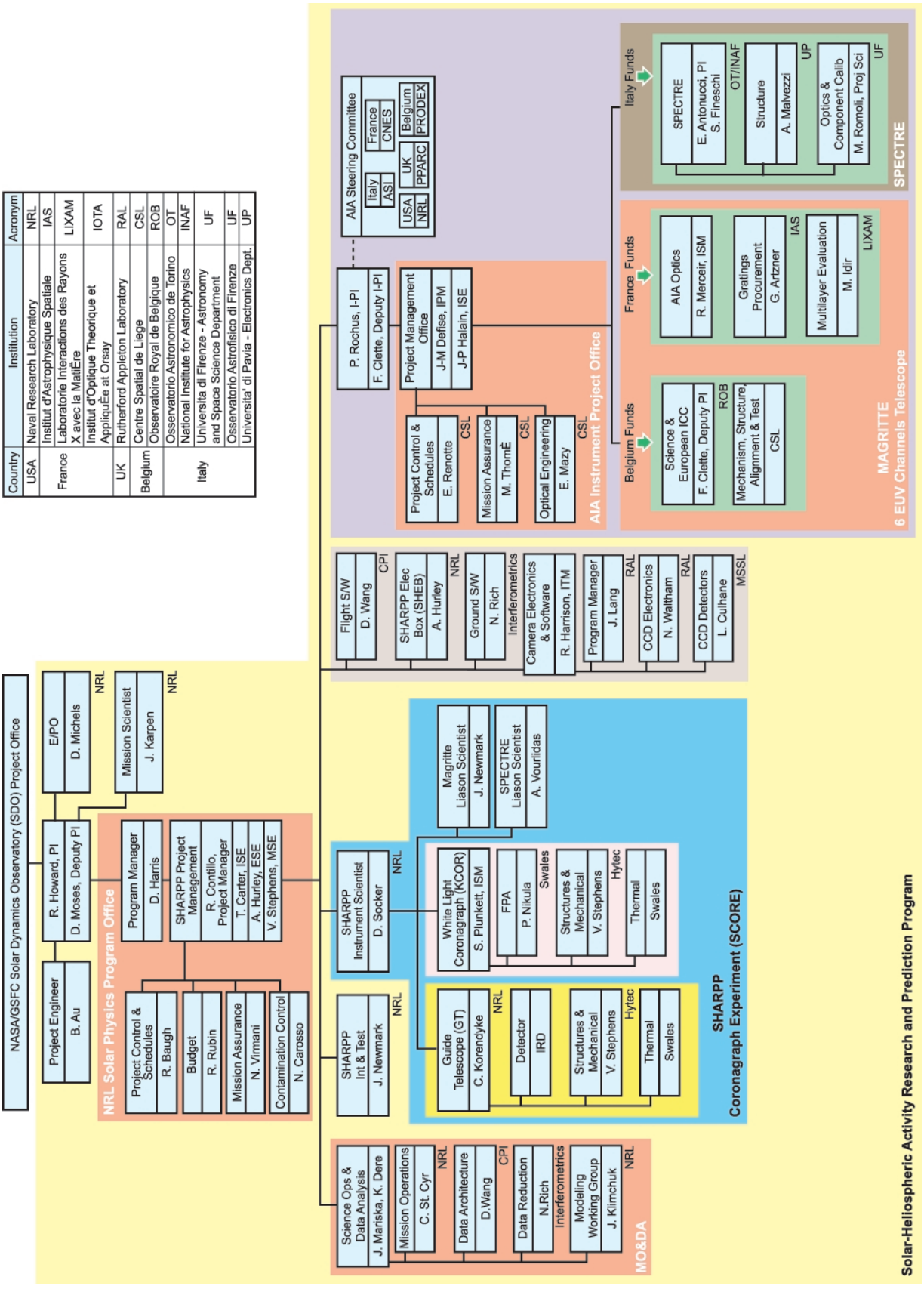

Country	Institution	Acronym
USA	Naval Research Laboratory	NRL
France	Institut d'Astrophysique Spatiale	IAS
	Laboratorie Interactions des Rayons X avec la MatiEre	LIXAM
	Institut d'Optique Theorique et AppliquEe at Orsay	IOTA
UK	Rutherford Appleton Laboratory	RAL
Belgium	Centre Spatial de Liege	CSL
	Observatoire Royal de Belgique	ROB
Italy	Osservatorio Astronomico de Torino	OT
	National Institute for Astrophysics	INAF
	Universita di Firenze - Astronomy and Space Science Department	UF
	Osservatorio Astrofisico di Firenze	UF
	Universita' di Pavia - Electronics Dept.	UP

Figure 5-1. The SHARPP Organizational structure provides clear lines of authority and well defined responsibilities among key institutions and personnel

processes allowing objective insight and analysis of the technical and programmatic status of each WBS element throughout the life of the project.

5.1.2 Organizational Responsibilities. The S-PI has the overall and ultimate responsibility to NASA and within the project team (see Figure 5-1) for the scientific and engineering integrity of the SHARP Investigation. Decision-making authority flows from the S-PI to the S-IPM by delegation of all day-to-day decision-making and authority with regard to management of technical, cost, and schedule issues. He coordinates the efforts of the collaboration science team. Advice concerning the day-to-day scientific direction of the project is provided to the S-PI by the Deputy PI. The S-PI is responsible and accountable to NASA for accomplishing the mission within defined costs and schedule constraints. Finally, the S-PI has delegated the day-to-day management of the SHARPP instrument suite development to the S-IPM using the full capabilities and talents of the S-IPO. Table 5-2 lists key S-IPO participants.

5.1.3 Institutional and Organizational Relationships. The investigation captures the strengths of both domestic and foreign technical institutions, university-based technical organizations, and four foreign funding agencies. Figure 5-1 illustrates these relationships, along with the flow of funds and technical direction to all supporting organizations. Note that when direct contracting mechanisms are not appropriate (as in the case of the non-U.S. contributions), institutions are linked by Memoranda of Agreement (MOA). Further, an Interagency Agreement between NASA and DoD provides the funding vehicle for NRL. The NASA funds are processed by the NRL business system which is currently performing the same processes for SECCHI and Solar-B EIS.

5.1.4 Teaming Arrangements. Each SHARPP member or consortium institution has demonstrated and traceable experience to perform their responsibilities. Furthermore, each brings flight instrument knowledge on a scale similar to SHARPP, proven familiarity with technologies relevant to SHARPP, and recent experience with the successful implementation of large, complex projects that are both multi-institutional and international in scope. Collectively, the consortium institutions bring a considerable history of success-

Table 5-1. The WBS, detailed to Level 4 and aligned with the responsible performing institution, explicitly defines all task elements and work packages.

WBS	Task	Lead	Supporting
1.0	Instrument Development	NRL	
1.1	Prelaunch Science Sprt.	NRL	
1.2	Instrument H/W & S/W	NRL	
1.2.1	Detector & FPAs	NRL	
1.2.1.1	CCDs	NRL	
1.2.1.2	Camera Electronics	RAL	
1.2.1.3	Compression/Packet	NRL	
1.2.1.4	SCORE FPA	NRL	
1.2.1.5	AIA FPA	CSL	
1.2.1.6	GT detector	NRL	
1.2.2	Optics	NRL	
1.2.2.1			
1.2.2.2	KCOR Optics	NRL	
1.2.2.3	AIA optics	CSL	IOTA
1.2.2.4	SPECTRE optics	OT	UF, UP
1.2.2.5	GT optics	NRL	
1.2.3	Mechanisms	NRL	
1.2.3.1	SCORE Mechanisms	NRL	
1.2.3.2	AIA Mechanisms	CSL	
1.2.4	Power distribution	NRL	
1.2.5	Structure	NRL	
1.2.5.1	SCORE structure	NRL	
1.2.5.2	AIA structure	CSL	OT
1.2.5.3	GT structure	NRL	
1.2.6	Electronics	NRL	
1.2.7	Other		
1.2.8	Integ., Assembly, & Test	NRL	
1.2.8.1	KCOR	NRL	
1.2.8.2			
1.2.8.3	AIA – multilayer	CSL	IAS
1.2.8.4	AIA – SPECTRE	OT	UF
1.2.8.5	GT	NRL	
1.2.8.6	SHARPP I&T	NRL	CSL, OT
1.2.8.7	Observatory I&T	NRL	CSL, OT
1.2.9	Software	NRL	
1.2.9.1	Flight software	NRL	
1.2.9.2	Ground software	NRL	
1.3	Prelaunch MO&DA, Algorithm Dev'l.	NRL	JPL, ROB, OT, UF, RAL, MPAE
1.4	Special Launch Services		
1.5	Ground Data System	NRL	ROB, RAL, IAS
1.6	Reserves	NRL	
2.0	Science Ops & DA	NRL	ROB, RAL, IAS, MPAe, OT, UF
2.1	Postlaunch Science Ops	NRL	
2.2	Postlaunch Analysis	NRL	
3.0	E/PO	NRL	
3.1	Prelaunch	NRL	
3.2	Postlaunch	NRL	

Table 5-2. SHARPP Instrument Project Office (IPO) Overview

Instrument Project Manager (IPM), Mr. D. Harris - Manages the engineering development and delivery of the SHARPP instrument suite and insures compliance to cost, schedule, and technical performance. He performed similar duties on STEREO SECCHI.
E/PO Coordinator, Dr. D. Michels - Reports directly to the SHARPP PI and executes the SHARPP E/PO program. He performed similar tasks on SECCHI and SOHO LASCO/EIT.
Instrument Technical Manager (ITM) as shown in Figure 5-1.- Instrument development responsibility via the Integrated Product Development Team (IPDT) which the ISE chairs.
Integrated Product Development Team (IPDT) shown in Figure 5-1 - Responsible to control the coordinated design, fabrication, integration, testing, and support of the designated Instrument Suite elements. Its membership includes the ISE, ITMs, Instrument PIs, and key engineering personnel.
Instrument System Engineer (ISE), Dr. T. Carter - Establishes and maintains performance specifications, verification and test plans, ICDs, and technical metrics and reserves; allocates and maintains these by instrument elements. He is assisted in this activity by an Electrical Systems Engineer, Ms. A. Hurley and by an Mechanical Systems Engineer, Mr. V. Stephens. Each performed similar duties on SECCHI.
Project Control Manager (PCM), Ms. R. Baugh - Manages the budget and reserve control system for cost, schedule, and technical performance, and executes the change control management of all performance parameters for the project. Serves as primary financial interface in the S-IPO for all consortium institutions reporting processes.Contractual and financial interfaces are handled by Mr. Richard Rubin. Both performed similar duties on SECCHI and Solar-B EIS.
Mission Assurance Engineer (MAE), To Be Named - Reports directly to the IPM, with responsibility for the development and execution of QA, safety, and environmental activities.

ful collaboration. This collaboration has long existed as a loosely-knitted team of institutions. Each shares a common set of scientific goals, and maintains a strong interest in continuing solar observations measuring those parameters necessary to provide a deeper understanding of the mechanisms regarding solar variability. As the collaboration has evolved, a strong fabric of cooperation has developed. At the time of this proposal, the WBS and subsystem responsibilities and teaming arrangements are firmly established, and creation of the draft MOAs between NRL and Non-U.S. partners are in-process.

5.1.4.1 Atmospheric Imaging Assembly Consortium. AIA is built by a consortium of institutes from Europe and USA (see Figure 5-1). The consortium represents the coordinated efforts of the twelve groups comprising the AIA Instrument Suite development team, and additional institutional groups supporting the scientific program after launch. A project team supervised and directed by scientists of the consortium institutes, is now defined and will be established to coordinate instrument development after contract award.

5.1.5 Experience and Capabilities of Team Member Organizations. The S-PI selected a strong science team and an experienced implementation team. All members have worked together on previous missions, interleaving science and design implementation to assure a balanced approach to mission success. Table 5-3 summarizes the responsibilities and relevant experience of select personnel and institutions, along with the relevant investigation responsibilities.

5.1.6 Key Personnel. Table 5-4 describes key personnel qualifications and expertise. Additional background and previous experience for science team members (both funded and unfunded) are described in the Curriculum Vitae (CV) contained in the Appendices to the proposal. The following paragraphs provide additional information on key personnel supporting instrument design, fabrication, integration, and test.

5.1.6.1 Key Personnel, Shared Subsystems. The SHARPP instrument contains H/W and S/W subsystems common to both the SCORE and AIA Instruments. Development responsibility for these items is under the direct supervision of Mr. B. Au. Supporting him in this task is a development team of NRL (SHARPP Electronics Box), Interferometrics (ground S/W), Computational Physics (Flight S/W), and RAL (Camera Electronics and S/W). Each of these organizations have worked together performing similar tasks on the SECCHI and similar scientific spaceflight instrumentation missions.

5.1.6.2 Key Personnel, SCORE Instrument. Refer to Figure 5-1 for the SCORE developmental team organization. Under the direct supervision of D. Socker (the SCORE I-PI), A. Vourlidas is the KCOR ITM and S. Plunkett is the ECOR ITM. Each is supported by a team with specific expertise in the relevant technologies. An industry team consisting of Swales (contamination control, FPAs, thermal, fabrication), and Hytec (structures and mechanisms) supports specific design engineering and implementation tasks. S. Bajt or LLNL supports the multilayer tasks. Each of these organiza-

Table 5-3. SHARPP has implemented well-defined roles, responsibilities, and commitments with experienced partners

Institution			Mission Responsibilities	Point of Contact	Experience
SHARPP	United States	NRL	• Home Institution for SHARPP PI & IPM for Phase A/B/C/D • Lead for Project Mgmt. & Reporting, Mission Assurance, Contamination Control, Systems Engineering, SR&QA, & Config. Mgmt. • Lead for SHARPP structure design & analysis via Hytec, Inc. • Lead for SHARPP mechanisms via Swales, Inc. • Lead for SHARPP Elec. Box (SHEB), harnessing, & supporting EGSE and development of image processing chipsets • Lead for flight & ground S/W on SHARPP Instrument Suite • Lead for SHARPP Instrument Suite integration & test with the S/C, CPET, calibration, delivery, & commissioning • Via SDO Mission Project Office, supports GSFC SDO S/C CPET, S/C-to-L/V integration process, & MO&DA • Lead for prelaunch MO&DA Ground Data System (GDS) Development & Phase E MO&DA • Leads the E/PO Program	• R. Howard, S-PI • D. Moses, Deputy PI • D. Harris, S-IPM • T. Carter, S-ISE • A. Hurley, E-SE • V. Stephens, M-SE • R. Baugh, PCM • R. Rubin, Contracts & Finance • D. Michels, E/PO Coordinator	• SECCHI • EIS • EUV Telescope (EIT) aboard SOHO • Large Angle Spectrometric Coronagraph (LASCO) aboard SOHO • EIT calib. on rocket launchs • High Resolution Telescope & Spectrograph (HRTS) on 10 flights since 1975 & on STS Spacelab 2
SCORE			• Lead for KCOR & Guide Telescope unit	• D. Socker, SCORE PI • S. Plunkett, ECOR ITM • A. Vourlidas, KCOR ITM • D. Moses, Deputy PI	
AIA			• Lead for AIA EUV Al filters & Lyman-alpha filters; Science support for screen & verification of detectors (i.e., back illuminated CCD & Lumogen CCD (Lyman-alpha).		
AIA	Belgium	CSL	• Home Institution for AIA Instrument PI • Lead for AIA systems engineering, project control, & mission assurance. Design & fabrication of Mechanisms (cover & filter cover), Structure, Thermal Design; H/W, & MLI; Performs alignments (e.g. optical quality & instrument pointing), Design Qualification Tests (Vibration & Thermal) & Acceptance Tests. Design & fabrication of Mechanical GSE (shipping container, purge system, lifting tools), Thermal GSE, & Optical GSE • Unique facilities for stray light & environmental qual tests.	• P. Rochus, AIA PI • J.M. Defise, AIA IPM • E. Renotte, Proj. Control • M. Thomé, Msn Assurance • J-P Halain, ISE	• SECCHI • EIT
		ROB	• Support to AIA calibration	• F. Clette, AIA PS	
AIA, SPECTRE	Italy	OT/INAF	• Lead Institution to design, fab, test & deliver SPECTRE, the OV channel & Lyman-alpha combined telescope instrument	• E. Antonucci • S. Silvanno	• UVCS
		UF	• Design of Optics & component level calib. tests	• M. Romoli	
		UP	• Multilayered Aluminum Filters	• A. Malvezzi	
AIA	France	IOTA	• Acquisition of optics, blanks, & figuring (EUV & Lyman-alpha); EUV multi-layered coatings.	• R. Mercier, Proj. Mgr • M-F Ravet • F. Delmotte	• LASCO, EIT • GOLF • SUMER
		IAS	• Gratings acquisition (O V channel) from Jobin Yvon; Camera CCD radiometric & flat field calibration; calib.on mirror pairs & end-to-end on spare telescopes, Partial support to measurement campaigns, & calib. at subsystem levels; filter calib.	• J-P Delaboudiniere, Optics Scientist	
		LIXAM	• Calib. of mirror multi-layers, samples, & witnesses	• M. Idir	
AIA	UK	RAL	• Lead Institution to design, integrate, test & deliver the camera electronics subsystem & camera S/W (excluding CCD acquisition performed by NRL). • Supports MO&DA during Phase E	• R. Harrison, Inst. Lead	• SECCHI • SMEI • CDS • Yohkoh/BCS
		MSSL	• Lead institution for providing CCDs for AIA & SCORE • Supports MO&DA during Phase E	• J.L. Culhane	• XMM • EIS

Table 5-4. Key Personnel Qualifications

	Name, Organization, Role, and Relevant Experience
SHARPP	R. Howard, NRL, SHARPP PI: PI for the SECCHI Program. PI and Program Scientist for LASCO coronagraph. Performed SOLWIND coronagraph test and calibration. Research on the physics of CMEs in terms of initiation, propagation, and eventual interplanetary effects. Developed LASCO's CCDs and CCD cameras and received the NRL Royalty Award. Participated in the LASCO/C3 telescope development, led LASCO/EIT flight S/W and its ground support system development. Led the effort to integrate, calibrate, and test the LASCO instrument. CoI on numerous NASA projects.
	J. D. Moses, NRL, Deputy PI: Authority on high resolution solar physics, EUV imaging, and spectroscopic instrumentation. Experienced in solar data analysis and detector development. Major role in NRL's SECCHI, LASCO and EIT. PI on four successful NASA suborbital program efforts. PI or CoI on numerous NASA and Navy sponsored spaceflight H/W development, data analysis, and advanced instrument development research efforts
SCORE	D. Socker, NRL, SCORE Instrument PI: Scientist**:** Head of NRL's Solar Spectroscopy Section. CoI for HRTS 4-HRTS 6 sounding rockets. CoI and section responsibility for HRTS 7-HRTS 10 sounding rockets. Project scientist and CoI for HRTS/Spacelab-2, project scientist for HRTS/OSL, and CoI for LASCO/SOHO. Team leader for LASCO/SOHO tunable Fabry-Perot filter, CoI for diamond UV imaging detectors for astronomy, and PI for High Resolution P-channel XUV CCD.
AIA	P. Rochus, CSL, AIA PI: International Program manager of EIT on SOHO; Director of R&D for EIT on a NASA sounding Rocket, Optical Monitor on XMM, Optical support of MERIS on ENVISAT, Optical Transient Camera for INTEGRAL, Far UV SpectroImager on IMAGE (MIDEX), and PACS on FIRST.
	F. Clette, ROB, AIA Deputy PI: SOHO EIT calibration campaign leader involving SOHO (EIT, MDI, CDS, SUMER), YOHKOH (SXT) and TRACE; EIT Science Planner at the SOHO EOF; Science coordinator of Belgian eclipse expeditions and TECONet project of JOSO.
	J.M. Defise, CSL, AIA Instrument PM: System engineer for SOHO EIT; PM for EIT Calibration rocket (CALROC); Local PM for OMC on INTEGRAL S/C.
	R. Harrison, RAL, UK Lead for AIA and Camera Electronics: Co-I on SMM and TRACE; PI for CDS on SOHO.

tions performed similar tasks on SECCHI and other similar missions.

5.1.6.3 Key Personnel, AIA Instrument. Refer to Figure 5-1 for the AIA management team organization. Under the supervision of P. Rochus (the AIA PI), the AIA management team is lead by Jean-Marc Defise (CSL) designated as the AIA PM. He is supported by E. Renotte for project control matters (e.g., CM, documentation control, planning, schedule control, cost control). M. Thomé coordinates all Product Assurance activities, and is responsible to supervise all related PA/QA matters of consortium institutes and subcontractors. The systems engineering task is lead by J-P Halain. To give him quick access to all technical matters at institutes beside CSL, the project manager is supported by the local managers of the partner institutes. E. Mazy performs optical engineering for AIA at CSL and supervises the optical engineering of the partners and at the subcontractors. Silvano Fineschi is technical lead for the "soft EUV channel" at 625 Å (OV). Local managers on each partner institute serve as interface point in all matters of the AIA management, design and development. They are supported by management and engineering personnel from their institutes.

5.1.6.4 Key Personnel, Science Operations and Data Analysis. This team, lead by J. Newmark, is chartered to produce browse products, calibrated data, and analysis software. These products will be publicly available shortly after launch. The data volume is much larger than any previous solar space missions. To meet this need, a formal Data Operations Working Group (DOWG), headed by the SHARPP Mission Scientist, J. Karpen, is established early in Phase B. This group develops approaches enabling public access to the SHARPP data using straightforward web-based tools

5.1.7 Business Relationships. The relationships among the SHARPP team institutions are governed by Memorandum of Agreements (MOA) between NRL and each performing institution. NRL, as a Governmental entity, is uniquely positioned to execute these agreements (see Sect. 5.1.8) with recent experience using similar MOAs on missions like SECCHI, Solar-B EIS, LASCO and EIT. These have served past projects well by establishing concise SOWs and responsibilities for each team institution, along with management, authority, and reporting needs.

5.1.8 International Information Exchange. The development, fabrication, and operation of the SHARPP Instrument Suite and the resultant science investigation adhere to all applicable U.S. laws and regulations concerning the import and export of technical information and materials. Compliance with these laws and regulations is written into all MOAs with foreign collaboration partners. We have recent experience with International Traffic In Arms Regulations (ITAR), based

on work on SECCHI and Solar-B EIS, including exports to International partners controlled under the ITAR. On-board staff are familiar with "taming the ITAR beast" and these same personnel are supporting other NASA programs involving extensive international collaboration. Ongoing development of draft MOAs among the consortium members serves as the framework to support industry Technical Assistance Agreement (TAA) development after contract award. We work in concordance with NASA Space Science and Aeronautics Division Office of External Relations during the preparation of the Phase A concept study to develop international cooperation requirements regarding export control, and document these as an annex to the SHARPP Project Plan.

5.2 Management Processes. The SHARPP Investigation operates in a management mode reflecting the overarching importance of containing costs within the agreed limits. During Phase A, we set realistic requirements that satisfy the basic science investigation and that we have a high confidence of meeting with low cost and schedule risk. We use a hierarchical WBS, with all work packages and budgets captured in an Integrated Master Schedule (IMS). System and subsystem technical requirements are baselined and managed through formal Change Control Board (CCB) process responsible to review and control all proposed changes of scope, requirements, design, and schedule (see Sect. 5.2.2.5). The SHARPP PI reviews for approval any CCB recommendations affecting performance, cost, or schedule.

5.2.1 Decision-Making Processes. The WBS and the organizational structure define the limits of individual authority and responsibility relative to cost, schedule, and technical requirements. The SHARP PI is the final authority regarding changes affecting project scope while the IPM is the final authority on the allocation of resources, schedules, and requirements among the second level WBS elements. System and subsystem specifications, ICDs, the IMS, and WBS budgets define the scope of each second level element.

5.2.2 Systems Engineering. We apply proven systems engineering methods and existing processes to accomplish the investigation's objectives. Our approach includes formal requirements development, design baseline management, verification

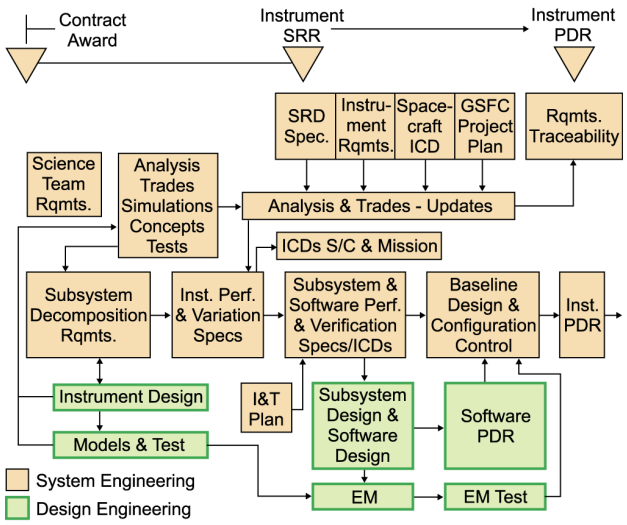

Figure 5-2. A formal Systems Engineering process is established during Phase B to capture all requirements

compliance matrix, technical performance metrics, peer reviews, detailed schedules, and weekly status meetings. The S-IPO ensures a formal system engineering process is implemented for Phase A and B (see Figure 5-2). The technique exercises all applicable design criteria, analysis, support, test precedents, lessons learned, environment and safety procedures and a distributed collaborative engineering methodology. We emphasize science benefit in the further development of the instrument requirements, formalize the products and processes needed to deliver the instrument, and place these under configuration control, while working under the constraints of "design-to-cost". The ISE is accountable for system trades, decomposition of requirements, developing instrument specifications and, in conjunction with subsystem engineers, developing the subsystem specifications and design verification plans and ICDs among subsystems. All requirements are formalized, documented, traced, and verified with a requirements traceability S/W tool. In a similar manner, the systems engineering activities continue during Phase C/D, as shown in Figure 5-3.

5.2.2.1 Requirements Development and Allocation. The science requirements flow-down is defined during Phase A as part of the GSFC SDO Project Mission Requirements Document (MRD).

❒ *Science Requirements*: A SHARPP Science Requirements Document (SRD) defines the Level 2 Requirements. These requirements are traceable through to component or subsystem specifications

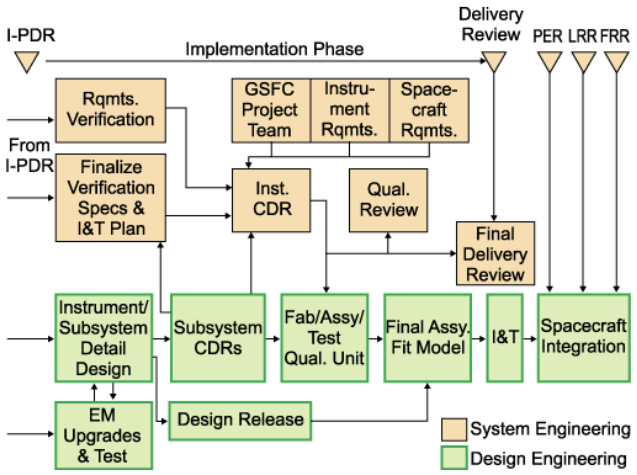

Figure 5-3. The formal Systems Engineering process extends throughout Phase C/D to verify all requirements

and test verification matrices. The SRD contains specific Level 2 objectives, design criteria for the full range of mission needs, and key referenced documents or agreements. The SRD is initiated during Phase A, baselined at PDR, and maintained throughout the program to reflect design changes. The mission design process follows the guidelines outlined in NASA's NPG 7120.5, including mission analysis and definition, requirements analysis and allocation, design, development, fabrication and manufacturing, test verification, and operations. Project review milestones allow external readiness assessments.

❒ *Analysis and Definition:* During Phase A, the ISE analyzes the requirements to determine the functional and performance requirements for each primary mission function and interface. These design requirements are synthesized during Phase B to: (i) define and allocate functions to the system elements; (ii) finalize internal and external interfaces; (iii) identify critical parameters; (iv) define system and element solutions to a level that enables verification; and (v) translate the architecture into final specifications and a configuration baseline. Major trade studies are defined, conducted, and documented. Significant life cycle cost impacts are provided to the IPM.

❒ *Requirements Documentation:* The S-IPO ensures the creation of project-level documents, risk management plans, and size/mass/power/data parameters. These documents are made available during all Peer and Technical Reviews. Working with the science team, the ISE integrates technical and performance goals with the IPM's cost and schedule goals, to provide cost-effective identification of conflicting interfaces, requirements, design products, and schedules.

5.2.2.2 Mission Assurance. During Phase A, a formal Safety, Reliability, and Quality Assurance (SR&QA) system is defined in a program-level document and implemented during Phase B. It uses existing processes and procedures to address mandatory SR&QA elements with special consideration given to contamination control and cleanliness needs. Our SR&QA process ensures that flight instrument H/W, S/W, and GSE are designed, manufactured, and tested to flight standards and that drawing and specification requirements are met. NRL manages the SR&QA program and reviews all team member processes. NRL designates a Mission Assurance Engineer (MAE) to work within the SHARPP IPDT structure and develop SR&QA implementation plans. Similarly, designees at our international partners are responsible for their SR&QA processes. NASA has the authority to review and approve the SR&QA approach. Additional discussion on this topic is contained in Sect. 5.6.

5.2.2.3 Technical Performance Metrics. The ISE and the IPDT mutually establish technical performance metrics (TPMs) for instrument development during Phase A. These critical parameters are reviewed at the SRR, formalized, and placed under CM. Typical metrics include size/mass/power/data parameters, processor throughput and memory usage, and pointing (including error budgets). Metrics are baselined at PDR and updated as the project evolves. If the margin required for a given project phase is not maintained, the PM and the PI take corrective action, including exercising descope options. TPMs represent the key performance requirements which must be met to ensure that the mission objectives are met. The criterion for selection of a TPM parameter metric is, if it exceeds a critical value, it will result in an impact to science, cost or schedule, requiring the implementation of a descope option, an increase to mission cost, or a slip in schedule to accommodate the variance. System-level metrics are flowed down and budgeted to the subsystems by the ISE and IPDT. All subsystem metric budgets are analyzed at project control meetings to ensure that problems

are quickly identified and appropriate corrective actions are developed.

5.2.2.4 Acquisition Management. Each institution's procurement responsibility resides with the designated ITM (see Figure 5-1).

❒ *Make/Buy*: Decisions for major instrument elements are based on trade studies by the S-ISE. Major items procured by project funds are selected via competitive procurements that meet FAR requirements. Existing support contracts provide many of the technical services, suppliers, and materials. We use a variety of contract mechanisms, including FFP, CPFF, and CPAF, with level-of-effort support clauses for out-of-scope efforts.

❒ *Vendor Selection*: The ITM, working with the S-IPO develops a procurement strategy, list of suppliers, a statement of work and procurement specification (containing QA requirements) and proposal evaluation criteria, all of which support the acquisition process.

❒ D*esign Specifications:* Commercial standards are preferred, and NASA/Military standards are used if industry standards are not available or acceptable for procured items.

❒ *Procurement Support*: The Mission Scientist and the ISE are chartered to provide scientific and technical support to acquisitions, each of which is managed by a designated Contract Officer. Conformance to specification is monitored via design reviews, audits, and acceptance tests. Performance assurance personnel visit suppliers to verify that all technical, reliability, and quality requirements are being met within cost and schedule.

❒ *Oversight*: The ITM maintains oversight of major procurements and contract schedules and reports on the status monthly to the S-IPO. Critical subcontracts are subject to S-IPM approval. Suppliers must have a proven record of meeting cost and schedule constraints. Deviations in schedule, cost, or performance are flagged for management attention.

5.2.2.5 Configuration Management. CM is the process by which the project documents the instrument's functional and physical characteristics during its lifecycle, controls changes to those characteristics, and provides information on the state of change action. Our CM process allows all engineers to design to the same set of requirements, provides visibility into the design interfaces, and supports the production of a design that meets the requirements. The S-IPO starts placing requirements and design documents under CM shortly after the SRR. Initially, the top-level instrument requirements and key instrument design parameters are baselined. These are then allocated to subsystem requirements, and interface design within the SHARPP instrument suite. Early establishment and subsequent control of the product baseline minimizes program costs and contribute to schedule control through: (i) systematic and documented approach to change control; (ii) careful evaluation and timely disposition of proposed changes; (iii) immediate communication by providing change disposition to all affected personnel; and consistent program documentation by establishing an internet-accessible database to provide a central point for controlling all H/W and S/W documentation. During Phase B, we establish a CM system using guidelines from MIL-HDBK-61 and EIA/IS-649 (hardware) and EIA/IEEE J-STD-016 (software). Team members and subcontractors implement their own CM systems meeting these guidelines under NRL oversight. The ITMs are responsible for instrument baseline control, while the S-IPO is responsible for program-level CM processes. H/W and flight S/W configuration is managed throughout development, integration, test, and launch to ensure a seamless transition to Phase E MO&DA with minimal impact. NRL maintains a secure, password-protected CM database to provide access and status documents via the Internet. NRL is responsible for defining and maintaining the configuration baseline and the Configuration Change Board (CCB). Class I changes include all instrument-to-S/C interfaces and mission performance requirements. Class II changes are internal to the instrument and are transparent to, or do not affect, external interfaces or performance. We submit a CM plan at PDR for NASA review and approval.

5.2.2.6 Integration, Verification, and Qualification. The S-IPO implements a thorough integration, verification, and qualification plan during Phase B, based on requirements established within the I&T Plan and the Systems Verification Plan (see Figure 5-3). The ISE and ITMs identify test and verification requirements at PDR and baseline these results at CDR. The ISE ensures that system-

Assembly / Subsystem Description	Subsystem Type					Hardware					Environmental Tests										Functional/Performance Tests						
	Assembly	Structure	Telescope	Electronics	Mechanism	BB	DM	QM	FM	FS	Random Vibration	Sine Vibration	Thermal Cycling	Thermal Vacuum Cycling	Thermal Balance	EMI/EMC	Electrostatic	Magnetics	Acoustic	Radiation	Functional Tests	Performance Tests	Life Cycle Vacuum	Alignment	Stray Light Rejection	Light Leak	Jitter
Camera Shutter					X			1	9	3	U	U		A		A					U	U	U				
Hollow Core Motor					X			1	2		U	U		A		A					U	U	U				
SCORE Instrument Mounts					X				6	3	A	A		A		A					U	U					
SCORE Spacecraft Mounts					X				3	3	A	A		A		A					U	U					
SCORE Focal Plane Assy					X		2	1	2	1	U	U		U	U	A					U	U		U			
AIA Filtergraph Focal Plane Assy					X		1	6	6	2	U	U		U	U	A					U	U		U			
AIA SPECTRE Focal Plane Assy					X		1	1	1	1	U	U		U	U	A					U	U		U			
SHEB				X			1		2		U	U	U	A	A	U	A	A			U	U					
Harness				X				1	1		A	A		A		A					U						
GT			X				1		1		A	A		A		A					U	U		U		U	U
KCOR			X			1	1		1		U	U		U							U	U		U	U	U	
ECOR			X			1	1	1	1		A	A		A		A					U	U		U	U	U	
SCORE Structure		X					1		1		A	A		A								U		U			
SCORE Assembly	X						1		2		A	A		A	A	A	A	A			A	A	A	A	A	A	A
AIA Filtergraph Cover Assembly					X		1	1	6	2	U	U		U		A					U	U	U				
AIA SPECTRE Assembly					X		1	1	1	1	U	U		U		A					U	U	U				
AIA Filtergraph Instrument Mounts					X				18	6	A	A		A		A					U	U					
AIA Filtergraph Spacecraft Mounts					X				3	3	A	A		A		A					U	U					
AIA SPECTRE Instrument Mounts					X				3	3	A	A		A		A					U	U					
AIA SPECTRE Spacecraft Mounts					X				3	3	A	A		A		A					U	U					
SCORE CEB				X			1		1		A	A	U	A	A	A	A	A			U	U					
AIA CEB				X			1	1	1		A	A	U	A	A	A	A	A			U	U					
AIA SPECTRE			X				1	1	1		A	A		A	A	A	A	A			A	A		A	A	A	
AIA Filtergraph Structure		X					1	1	1		A	A		A	A	A	A	A			A	A		A			
AIA Filtergraph Assy	X						1	1	1		A	A		A	A	A	A	A			A	A		A	A	A	

Responsible Institution: NRL, CSL; OT / UF / UP, IOTA/ IAS, RAL; Hytec, Swales

Hardware: BB Breadboard Model; DM Development Model; QM Qualification Model; FM Flight Model; FS Flight Spares

Test Performed at: Unit-Level U; Assembly-Level A

Figure 5-4. Preliminary Verification Test Matrix for SCORE and AIA Instruments will be finalized during Phase A

level analyses, including performance, reliability, risk, contamination, EMI/EMC, spacecraft and launch vehicle compatibility, and Failure Modes and Effects Analyses (FMEA) are accomplished. Contamination control and EMI/EMC guidance are established before PDR and preliminary design analyses are provided at PDR with CDR updates. A formal verification compliance matrix database captures the totality of analyses and test results to verify SHARPP's capability to meet specified performance and operational requirements.

❒ *Verification Test Approach*: During our proposal, we identified a preliminary test approach (shown in Figure 5-4) that will be refined during Phase B and used to develop verification plans, and traceability matrices that include verification criteria for all requirements. A formal test and verification plan covering all levels of hardware and software results from this process. The ISE verifies that engineering products satisfy requirements (including interfaces) from the lowest level and that they can be implemented.

❒ *Design Verification Testing:* The structural qualification approach uses extensive computer modeling and validation testing based on guidelines from the GSFC GEVS document and the S/C developer. The AIA and SCORE primary structures are qualified by Structural Model (SM) testing using mass simulators. Similarly, thermal modeling is performed using specified S/C environments. Combined TVAC and thermal balance testing of the SHARPP Flight Model suite is conducted prior to S/C installation. EMC/EMI testing will be conducted on the SHEB and the total SHARPP suite.

5.2.2.7 Mission Operations and Sustainment Processes. As activities flow from design to development, to integration and test, and then to operations, responsibilities migrate from the ITMs to the MO&DA operations team. The Mission Scien-

Table 5-5. An Integrated PCMS Proven on SECCHI & EIS

The Project Management Control System (PCMS):
• Establishes an integrated cost and schedule baseline;
• Provides for the orderly and systematic authorization of work and project budget;
• Develops and publishes timely management reports which display cost, funding and schedule status to baseline plans;
• Measures actual and forecasted cost and schedule status against the performance measurement baseline to determine the current and forecast future performance;
• Maintains a clearly documented audit trail of all changes to the performance measurement baseline through the WBS;
• Identifies potential problems in time to implement proper management actions; and
• Provides the IPM with the necessary visibility to analyze progress and identify any significant problems and issues to establish and implement corrective action.

tist and her MO&DA science team are involved in early development project stages to assure that mission operations are given consideration during development and that engineering support is available after launch.

5.2.3 Project Management Control. The S-IPO establishes an integrated Project Management and Control System (PCMS) that fully supports the S-IPM. It monitors and assures compliance with cost and schedule baselines, and is implemented by an experienced PCM charted with the responsibility for schedule, cost, contract, financial and data management, variance analysis, CM, and monthly project reporting. Table 5-5 lists the capabilities of this process.

5.2.4 Reporting and Reviews.

5.2.4.1 Programmatic Reviews. As described in Sect. 5.2.3, our PCMS generates monthly and quarterly reports using the process shown in Figure 5-5. Our formal review process was used during the execution of past projects (e.g., SECCHI, Solar-B EIS) at NRL, both as a tool to manage the project, and as a consistent formal feedback mechanism for GSFC and MSFC Project Office management.The PCM maintains accessible databases of the cost, schedule and performance baselines. The GSFC Project Office receives formal written monthly cost and schedule reports. On a quarterly basis, the SHARP PI and the S-IPO holds a project review with the GSFC Project Office that encompasses programmatic and technical progress, including accomplishment narratives, budgets, schedules, and issues, as well as configuration changes that have been approved/disapproved by the SHARPP IPO.

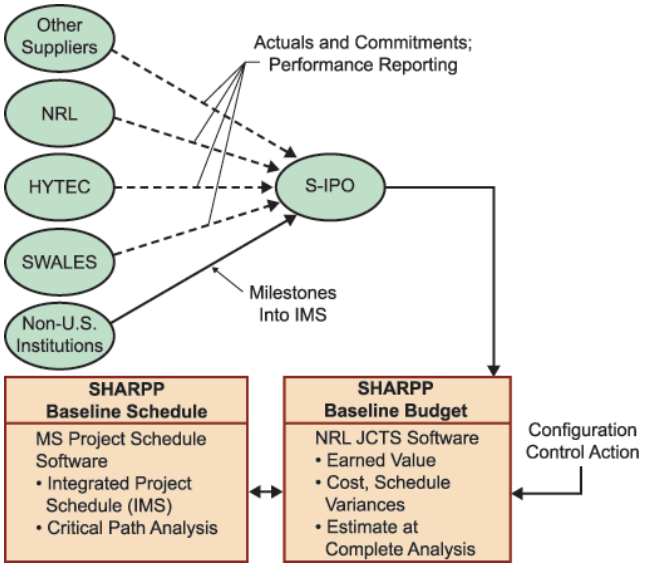

Figure 5-5. A proven PCMS process supports monthly and quarterly reviews with GSFC Project Office

NRL submits monthly (533M or equivalent) financial management reports as described in NPG 9501.2B, using the WBS and cost element structures shown in Table 5-1, or as mutually agreed upon. Financial management reporting is provided at WBS Level II and WBS Level III. Reporting is required for first-tier contracts using NFAR Supplement guidelines. NRL provides contract funding profiles and explains variances between projected and actual costs.

5.2.4.2 Technical Reviews. The S-IPO institutes a multi-tiered system of technical reviews for the project. First, the S-IPO supports NASA Mission-level reviews, including PDR and CDR, with status reporting on the technical and programmatic progress. The next tier of reviews focuses specifically on the SHARPP instrument suite.

The review process starts with the System Requirement Review (SRR), a formal review to finalize the mission requirements. Its purpose is to assure the mission team that the goals and objectives of the mission are being accomplished by the requirements and the flow down that has been established by the S-IPO. Additional reviews, graphically shown in Figure 5-6, address the allocation, and design implementation of the SRR. For all instrument-level reviews, the S-IPO presents designs, test plans, and verification plans. The review team develops specific recommendations, actions, and concerns to the Project. These actions are

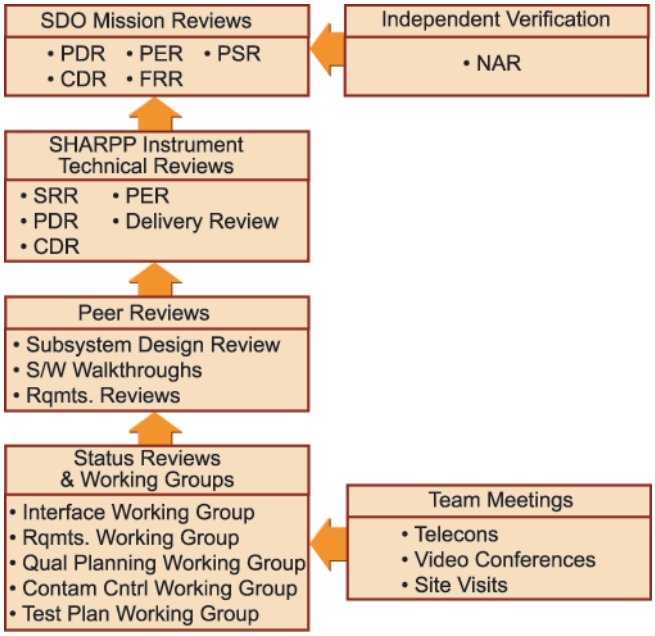

Figure 5-6. A formal Technical Review process is planned for all aspects of the SHARPP Instrument Project

tracked to resolution by the S-IPM to ensure closure and the closures are presented to the same review team at a subsequent review.

The second tier of technical reviews is comprised of, incremental "peer reviews" at the subsystem level. These occur on an ad hoc basis, convened and managed by the ISE as part of the process leading up to the formal reviews. For these reviews, technical experts from within the instrument subsystems engage in informal round table reviews of plans, designs, and implementations at key development stages. Formal notes and action items are taken at these peer reviews and are presented at the program review. We have already made extensive use of peer reviews during the SECCHI and Solar-B EIS design process.

5.2.5 Team Member Coordination and Communications. As discussed in Sect. 5.2.4, we have planned a number of reviews and coordination meetings to provide status reporting and guidance within the SHARP instrument team. These provide the formal structure of coordination within the team. We are investigating the use of video-conferences for both the monthly Project Control review, and the IPDT meetings to minimize travel costs. Communication within the instrument team is now being handled using a variety of available media. Specifically, the instrument already has in place an extensive array of web sites at most member institutions. These expand significantly at project start, when the S-IPO expands its web presence to include the latest schedule and cost data, as well as all documented and configuration-controlled requirements and design parameters. Action item lists are posted on the site along with the status and full explanation as to the resolution of the item. Events are posted to keep the entire team informed as to the latest status. Past experience at NRL on SECCHI has proven that these tools can, when applied by a strong and proactive IPO, yield a stable and dynamic team. There are two significant aspects to successfully managing such a dynamic project team. First, roles and responsibilities of all team members must be well defined. These are accomplished through a well-applied WBS structure, MOAs, and statements of work for all team member institutions. This empowers individuals and groups to excel in their work, while still maintaining clear accountability and management oversight for the project. Such a well-defined structure also works to minimize competition between organizations. Another critical aspect of successful management of such an international project is clear communication between team member institutions. The MOA formalizes these ties, and existing communications channels maintain strong project support at all institutions.

5.2.6 Multi-Institutional Management. The preceding sections describe the processes the S-IPO uses to guide the SHARPP Instrument Suite development. These processes, based on 'lessons-learned' on previous international projects, are tailored to support the international, dispersed project team elements of SHARPP. They rely heavily on the project WBS for clear definition of tasks, and on electronic communications for tight links among geographically diverse participants. Past NRL experience shows that these tools can, when applied by a strong and proactive IPO, yield a stable and dynamic teaming relationship.

❒ Two significant facets are required to manage such a dynamic team: First, all team member roles and responsibilities must be well-defined; this is accomplished though a well-applied WBS, clear SOWs, and established MOAs for each team member group and institution. This allows each member to excel at their work, while still maintaining

clear accountability and management insight for the project. This same approach also minimizes disruptive competition among organizations. Second, clear communication among team member institutions must be established. This is provided at the project-level by the planned tiered review and reporting system. At the institutional level, a strong commitment and comprehensive communications channel is required to ensure the project maintains adequate visibility.

❒ A key tenant of our Multi-Institutional Management approach is establishing the AIA Steering Committee (see Figure 5-1). Consisting of executive directors responsible for AIA institutional commitments, as well as NRL, this committee is responsible for the overall project direction, and agrees on all major policy and strategic decisions concerning AIA instrument development and task allocation. Comprised of the PI and one member from each of the participating countries, the members are senior figures representing the project within their own countries and before their national space agencies or direct representatives of their national space agencies. Each is chartered to ensure that the project has the necessary support from those agencies. In particular, they assist the PI in solving problems associated with funding and manpower resources within their countries. At the start of the project, each contributing nation commits to delivering an agreed package of work as described and signed off in the MOAs. This package can only be changed by agreement with the PI and the AIA Steering Committee. Within each country, attribution of resources between contributing groups is handled on a national level. The PI and the AIA Steering Committee are given visibility of such attributions. In the case of problems that cannot be solved within the Steering Committee, the matter is decided through the appointment of an ad-hoc group representing the appropriate national funding bodies. The PI serves as the AIA Steering Committee chairman. The AIA Project Manager is invited to attend the Steering Committee meetings.

5.3 H/W & S/W Acquisition Approach. Table 5-6 details the anticipated H/W acquisition approach, including the planned sources and equipment heritage.

5.3.1 KCOR / SHEB / GT Approach. The SHARPP Electronics Box (SHEB) is built and qualified at the NRL using a mix of laboratory and industry personnel. The KCOR instrument is built and tested at NRL. Final integration and test, including performance testing and calibration are conducted by NRL. NRL leads the systems engineering effort for the SHARPP instrument, including all documentation efforts. NRL is responsible for all interfaces with the S/C and the image compression chipset, SHEB and its S/W, the KCOR, and the Guide Telescope.

5.3.2 AIA Acquisition Approach. The "soft EUV channel" with 625 Å (OV) is built in Italy, with grating coming from France (JY) while the elements of the other channels (due to the similarity of their design) is built in Belgium and France.

5.4 Integrated Master Schedule. A SHARPP project Integrated Master Schedule (IMS) based on Figure 5-7 is fully developed during Phase A. It establishes task interrelationships, time phasing of events, critical path, and key activities. These activities and flows support an IMS developed in Phase B. Schedule sequences and durations are consistent with NRL and our team member's experience, and the planned staffing levels.

❒ *Process:* Our scheduling process ensures that the project schedules are integrated with the project cost estimates and authorized budgets. The IMS incorporates all project requirements and constraints that affect cost, schedule, and technical baselines. A Level 1 milestone schedule, jointly developed by the IPM, is approved by the PI during Phase B. All changes to Level 1 milestones are approved by NASA.

❒ *Tools*: By using MS Project Server, users are provided with a browser-based user interface, MS Project Web Access. Use of this tool assists not only in tracking schedule progress, but also support management of subsystem performance, variances against schedule, and corrective action.

5.5 Risk Management. Establishment and implementation of a structured Risk Management (RM) process, based on a thorough identification and analysis risks, is key to successful risk management; Figure 5-8 depicts our process methodology. During Phase A, we identify key risk elements, analyze and rank their potential impact based on the probability of the incident, and the final impact to

Table 5-6. Procurement Sources and Flight Heritage for AIA

	Item	Supplier or Designer	Flight Heritage
AIA	CFRP Structure & Bench	SONACA AEROFLEET	Spot 5, Mars Sample Return, & COROT Equip. Bay
	Kinematic Mounts	CSL	SOHO/EIT
	Cover Mechanism (Door)		SOHO/EIT, INTEGRAL/OMC, COROT
	Piezo Actuators	Micro-Mega Dynamics	ROSETTA/MIDAS, CEDRAT
MAGRITTE	EUV Optics	IOTA	SOHO/EIT, CALROC/EIT, STEREO/EUVI
	EUV Multilayers Calib.	LIXAM	
	EUV Filters	CSL, LUXEL	SOHO/EIT, CALROC/EIT, & STEREO/EUVI
	UV Optics	IOTA	TRC rocket instrument (R. Bonnet)
	UV Filters	Acton Research	
	Motors for Filter Covers	CSL FAULHABER	HERSCHEL/PACS granting launch lock
SPECTRE	Spectroheliograph	INAF	NRL Skylab instrument
	Mirrors & Coating		SOHO/UVCS spectrometer
	Gratings	IAS, Horiba Group (Jobin Yvon)	FUSE-Lyman (Jobin Yvon)
ECOR	The ECOR was not selected for the SDO mission.		
KCOR	Hollow Core Motor	Swales	STEREO/SECCHI
	Shutter		SOHO/LASCO-EIT, Solar-B EIS
	Polarizer	PolarCor	SOHO/LASCO-EIT, STEREO/SECCHI
	Kinematic Mounts	Swales	
	Cover Mechanism (Door)	Hytec	
	Structure (Tube), Optics, and baffles and similar to SECCHI COR 2	Swales, Tropel	
All	CCD Detectors	MSSL Marconi	STEREO/SECCHI & Vault heritage for Lumigen Coating
	SHARPP Elec. Box	NRL	SOHO/LASCO-EIT, STEREO/SECCHI
	Image Compression Chipset		New Development, Existing S/W
	Camera Elec. Box	RAL	STEREO/SECCHI
GT	Optics and Structure	NRL	STEREO/SECCHI, TRACE
	Detector	IRD	STEREO/SECCHI, TRACE

the SHARPP mission. Based on this process, we develop action plans, including a mitigation strategy, and at least two potential solutions.The first is a process to alleviate the risk using a planned implementation approach, and the second is an alternate solution to minimize project impact with established review and implementation dates.

5.5.1 Top Three Programmatic Risks. During our proposal process, we performed a preliminary risk analysis and mitigation process to identify the major factors affecting our proposed mission. (See Table 5-7). This listing is updated during Phase B.

5.5.2 Strategies for Reserves and Margins. All cost and schedule reserves are under the control of the S-IPM. Subsystem allocations may be made within the resources of the subsystem within the knowledge of the S-IPM and the PCM. Changes that affect other interfaces must be formally documented and approved by the CCB (see Sect. 5.2.2.5). Any changes affecting the science or programmatic requirements must be within the cognizance and concurrence of the S-PI. When actions impacting science (e.g., descoping), the S-PI must have the concurrence of the GSFC SDO project office. The allocation and release of all resources is under configuration control, and is monitored by the S-IPM. Cost reserves are held by the S-IPO and are not pre-allocated.

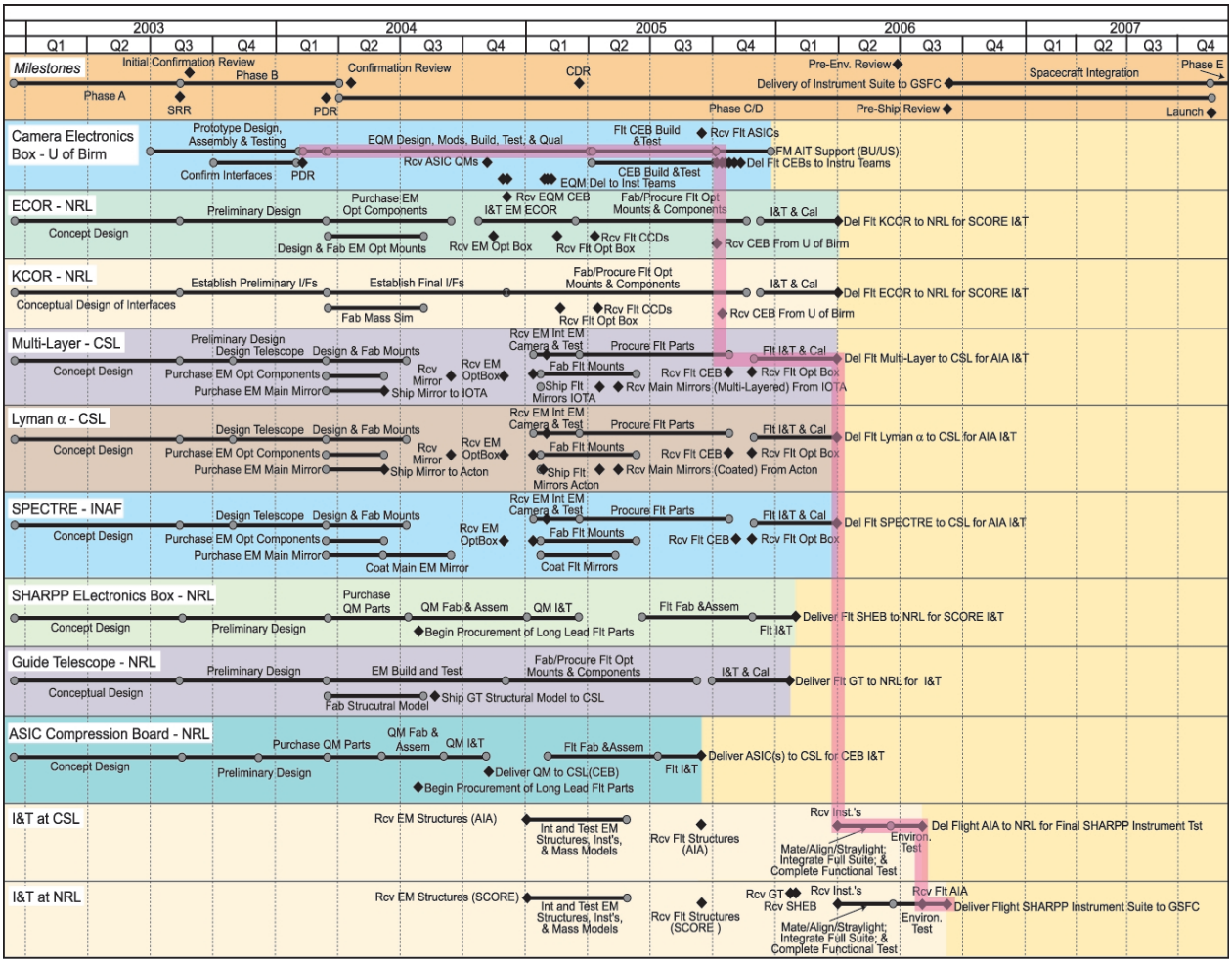

Figure 5-7. The SHARPP Integrated Master Schedule defines all Top-Level Mission and Instrument milestones, including allowances for long-lead item procurement and critical path.

5.5.3 Descope Plan. Our Risk Management Plan includes a descope strategy which is an integral managerial element. Descope is the action of last resort in the hierarchical approach to risk mitigation. The descope plan addresses mitigation of risk to four principal resources: cost, schedule, mass and power. Table 5-8 lists potential descope options and their impact on the mission. This table is refined during Phase B studies.

5.6 Performance and Safety Assurance. The S-IPO establishes, maintains, and monitors processes guiding performance assurance and safety assurance to ensure consistency of effort among all team members. The scope of the effort includes QA, material and parts selection/control, inspection, problem and failure reporting, reliability, S/W validation, and safety. Our process objectives are: operating the SHARPP instrument suite in a safe and environmentally sound manner; meeting science objectives and corresponding measurement requirements. To achieve these objectives, the S-IPO establishes formal programs to address the process to achieve safety and mission success.

5.6.1 Quality Assurance Process. QA is planned, implemented, and managed consistent with the requirements of ANSI/ISO/ASQC Q9001-1994, *Standard for Quality Systems*. Table 5-9 highlights our QA program objectives.

5.6.2 Reviews. The MAE supports a series of comprehensive system-level design reviews as conducted by the GSFC Project Office (see Sect. 5.2.4). These cover all aspects of the flight and ground H/W, S/W, and operations for which the S-IPO has responsibility. The S-IPO implements a series of peer reviews at the component and subsystems levels. The review teams are comprised of knowledgeable experts, as well as the ISE, MAE to evaluate system-level issues.

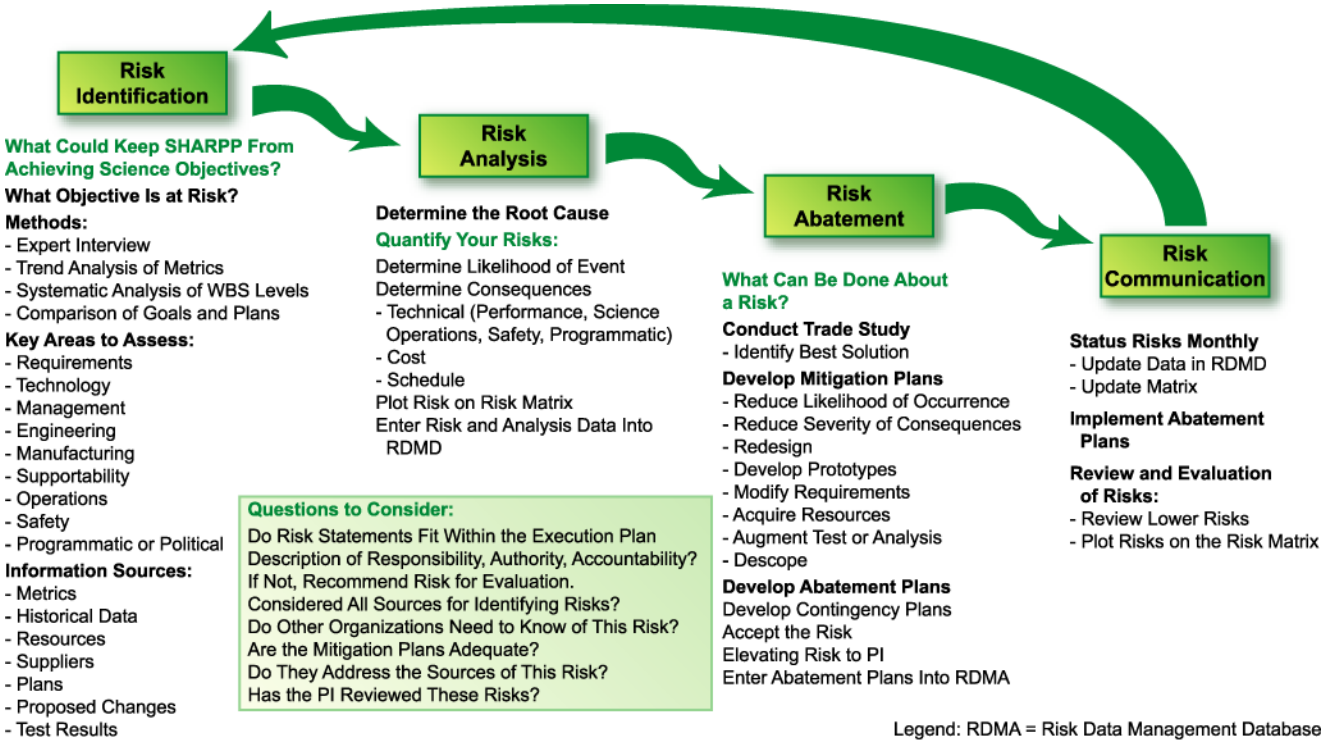

Figure 5-8. We implement a structured approach to identify project risks, including both implementation and project risks

Table 5-7. We have identified the top three programmatic risks for the SHARPP

#	Risk	Effect	Mitigation
1	AIA Instrument - Non-U.S. team institution's funding profile does not match NASA profile	Delays in delivery of critical CCDs for Camera Electronics contributed by non-U.S. source	Identified CCD procurement as most like candidate for funding delays; created contingency reserve of $2.3 mil in FY04 to mitigate potential delay.
2	Under-performing Non-U.S. institution	Delays in delivery or performance shortfalls	• Designed S-IPO to review Non-U.S. institutional status monthly with pre-defined milestones. • Implemented AIA steering committee comprised of senior executives from performing institutions to insure project visibility at high-level • Staffed S-IPO to provide technical support to critical activities
3	Problems or delays developing Image Compression chipset	Delays impact functional and performance test schedules	Design tests can be 'back-stopped' with FPGA-based image compression chipset.

Table 5-8. Potential Descoping Options and Mission Impact

Risk	Action	Performance or Parameter Loss	Science Impact	Resource Impact		
				Mass	Power	Cost ($)
Mass Growth	Eliminate redundancy in SHEB (single string design)	Lower reliability level for SHEB	None	~10 kg	-	
	Eliminate AIA Telescope (AIA_{max} => AUA_{min})	Loss of 2 channels	Reduced science data	~12 kg	~15 W	
	Delete Image Compression chip development & use off-the-shelf chipset	Lowered data rates	Reduce data flows from instrument suite	-	-	

Table 5-9. SHARPP Quality Program Objectives

• Define a fully integrated and functioning quality organization at all levels of the SHARPP instrument organization, • Assures quality requirements are identified and implemented through all phase of SHARPP instrument formulation and implementation, • Provide practical guidance on implementing a quality plan for critical project activities, • Assist in the implementation of project-wide quality measures with an emphasis on problem prevention, and • Integrate all subsystem and team member institution assurance activities.

5.6.3 Parts Selection and Control. We implement an Electrical, Electronic, and Electromechanical (EEE) Parts Control Program (PCP) to assure that all parts selected for usage in flight H/W meet specified mission objectives for quality and reliability. The PCP is developed prior to the PDR to facilitate the management, selection, standardization, control, and documentation of parts across all team and consortium participants. We use a Program Approved Parts List (PAPL). The PCP foundation rests on GSFC 311-INST-001 "Instructions for EEE Parts Selection, Screening, and Qualification". We implement a design review process that address parts derating, reliability assurance, materials and assembly processes, and thermal matching of materials.

5.6.4 Inspections. All flight components, piece parts, materials, and items that directly interface with flight H/W are subject to receiving inspection, in-process inspection, and final acceptance inspection. These documented procedures (e.g., instructions, procedures, travelers, inspection results) are used for inspection of quality characteristics during H/W processing. Data results are logged into a quality records database.

5.6.5 Workmanship. For all EEE parts and assemblies, the QA program rely heavily on proven NASA and Industry standards, and implement them as needed. These include NASA-STD-8739-2, 3,4,7 (Soldering, Staking/Conformal Coating, Crimping/Harnessing, Electro-Static Discharge), IPC-2221/6011/6012 (Printed Wiring Board Design, Performance, and Qualification), and NAS 5300.4 (Surface Mount Technology). For custom processes, new standards or processes are documented and subject to design review.

5.6.6 Problem/Failure Resolution. Problems or failures occurring during ground test of any flight H/W is identified, documented, assessed, tracked and corrected in an approved and controlled manner. We maintain a formal Problem/Failure Reporting system using a web-based database process. This approach is formalized prior to PDR. The system is monitored by the SHARPP MAE, and becomes effective with the first application of power at the component or subsystem level of flight H/W. For S/W items, the PFR becomes effective with the first use of the S/W with a flight H/W item.

5.6.7 Reliability. The S-IPO implements a formal reliability program that interacts effectively with all project disciplines, including systems engineering, H/W design, safety, and QA, is implemented.

❒ *Reliability Analysis:* During Phase B, reliability analysis is performed at the system and subsystem level to identify potential problem areas. At a minimum, a Failure Mode and Effect analysis is performed at a sufficient depth so that mission critical failure safe identified and mitigated. The analysis uses the GIDEP failure rate, failure mode, and replacement rate data. Additionally, information from the NASA Lessons Learned Information System (LLIS) is reviewed for applicability.

❒ *Flight S/W*: Verification and validation (V&V) activities are baselined to ensure that the flight S/W satisfies allocated functional, performance, and quality requirements. A varied sequence of testing, ranging from unit or element tests through integration tests and performance testing, as well as acceptance testing of the completed instrument suite is performed.

❒ *Safety and Hazard Mitigation:* We implement a system safety program that identifies and controls hazards to personnel, facilities, support equipment, and the flight system during all stages of instrument development. System safety requirements is derived from EWR 127-1, as well as the applicable safety requirements of the team members and the consortium.

5.7 Major Facilities and Equipment. The investigation requires no new major project-specific facilities or laboratory equipment. Estimates assume the reuse of in-place and unique optical facilities (used on successful solar programs like SECCHI, Solar-B EIS, LASCO, EIT) for all activities occurring during instrument development, system level test, and calibration.

Table 5-10. In-Place Optical Facilities

Org	Facility
NRL	UV Beamline (synchrotron) facility located at Brookhaven National Laboratory
	Coronagraph stray light test chamber
CSL	Vacuum facilities for AIA stray light tests
IAS	XUV calibration facilities

5.8 Work Breakdown Structure. As discussed in previous sections, the WBS provides the framework around which the management organization and plans are built. Cost and schedule control is delegated to the designated subsystem managers, and reporting of all subsystem performance from the lower levels of the WBS flows through them. The WBS defines all work packages for the SHARPP project. It was used for all budgeting and scheduling. Table 5-1 lists the WBS expanded to the fourth level.

5.9 Cost Plan. Cost budgets and estimates are presented in this section. Included is a first-order estimated cost for the SHARPP investigation encompassing all proposed activities, including Phase A/B/C/D/E, and contributions.

A. References

A.1 References.

Amari, T., et al. 2000, ApJ, 529, L49

Andrews, M. D. & Howard, R. A. 2000, Space Sci. Rev. 95, 147

Antiochos, S. K. 1998, ApJ, 502, L181

Antiochos, S. K., MacNeice, P. J., & Spicer, D. S. 2000, ApJ, 536, 494

Antiochos, S. K., & Noci, G. 1986, ApJ, 301, 440

Antiochos, S. K., DeVore, C. R., & Klimchuk, J. A. 1999, ApJ, 510, 485

Antiochos, S. K., et al. 1999, ApJ, 512, 985

Aschwanden, M. J., 2001, ApJ, 559, L171

Aschwanden, M. J., et al. 1999, ApJ, 515, 842

Aschwanden, M. J., et al. 2000, ApJ, 531, 1129

Aulanier, G., et al. 2000, ApJ, 540, 1126

Bailey, S. M., Woods, T. N., Barth, C. A., Solomon, S. C., & Canfield, L. R., 2000, JGR, Vol. 105, 27179

Banerjee, D., O'Shea, E. , & Doyle, J.G. 2000, Sol. Phys., 196, 63

Banerjee, D., et al. 2001a, A&A 377, 691

Banerjee, D., et al. 2001b, A&A 380, L39

Banks, P. M. & Kockarts, G. 1973, Aeronomy (New York: Academic)

Barrett 1990. TBD (from Sec. 1.3)

Bastian, T., et al. 1998, Ann. Rev. Astron. Astrophys., 36, 131

Beckers, J.M., and Argo, H.V., 1984, Proceedings SPIE, p. 312-317

Belien, A.J.C., Martens, P.C.H., & Keppens, R. 1999, ApJ 526, 478

Bentley, R. D., et al. 1994, ApJ 421, L55

Benz, A.O. & Krucker, S. 1998, Sol. Phys., 182, 349

Benz, A.O., Krucker, S., 2002, ApJ, 568, 413

Berghmans, D., & Clette, F. 1999, Sol. Phys., 186, 207

Berghmans, D., Clette, F., Moses, D., 1998, A&A, 336, 1039

Biesecker, D.A., Myers, D. C., Thompson, B. J., Hammer, D. M., & Vourlidas, A. 2002, ApJ, 569, 1009

Bornmann, P. L., Heckman, G., Hirman, J., Speich, D., Kunches, J., & Zwickl, R. 1996, in Solar Drivers of Interplanetary and Terrestrial Disturbances (ASP Conf. Series 95), eds. K. Balasubramaniam, S. Keil, & R. Smartt, p. 137

Brekke, P., et al. 1997, Sol. Phys., 175, 511

Brosius, J. W., et al. 1996, ApJ Supp, 106, 143

Brueckner, G. E., & Bartoe, J.-D. F. 1983, ApJ, 272, 329

Canfield, R.C., Hudson, H.S., & McKenzie, D.E. 1999, GRL, 26, 627

Cargill, P. J., & Klimchuk, J. A. 1997, ApJ, 478, 799

Carmichael, H. 1964, in AAS-NASA Symposium on the Physics of Solar Flares (NASA SP-50), ed. W.N. Hess, p. 451

Chae, J., Wang, H., & Goode, P.R. 2000, ApJ, 528, L119

Cook, J.W., et al. 1999a, Proc. 8th SOHO Workshop, Paris, Fr., ESA SP-446

Cook, J.W., et al. 1999b, "Coronal Thermal Structure from a Differential Emission Measure Map," AAS Meeting 194, #100.03

Cox 1999. TBD (from Sec 1.3)

Crooker, N. U., et al. 1993, JGR 98, 9371

Crooker, N. U., et al. 2001, JGR, 106, 15963

Dahlburg, R. B., Antiochos, S. K., & Norton, D. 1997, Phys. Rev. E, 56, 2094

Davila, J.M. 1987, ApJ, 317, 517

Delannée, C., 2000, ApJ, 545, 512

Delannée, C. & Aulanier, G., 1999, Sol. Phys. 190, 107

DeForest, C. E. et al., 1997, Sol. Phys., 175, 393

DeForest, C. E., Lamy, P. L., & Llebaria, A., 2001, ApJ, 560, 490

DeForest, C. E., & J. B. Gurman, 1998, ApJ, 501, L217

DeMoortel, I., Ireland, J., & Walsh, R.W. 2000, A&A 355, L23

Demoulin, P., et al. 2002, A&A 382, 650

Dere, K.D., Bartoe, J.-D.F., Brueckner, G. E., Ewing, J., & Lund, P. 1991, JGR, 96, 9399

Dere, K.P., Landi, E., Mason, H.E., Monsignori Fossi, B.C., and Young, P.R. 1997, A&A Suppl., 125, 149

Dobrzycka, D., Raymond, J. C., and Cranmer, S. R. 2000, ApJ, 538, 922

Dobrzycka et al. 2002, ApJ, 565, 621

Einaudi, G., & Velli, M. 1999, in ESA SP Series (SP-448), ed. A. Wilson

Einaudi, G. et al. 1999, JGR, 104, 521

Erdélyi, R., Ballai, I., & Goossens, M. 2001, A&A, 368, 662

Falconer, D. A., Moore, R. L., & Gary, G. A. 2002, ApJ, 569, 1016

Feldman, U., Cohen, L., & Doschek, G. A. 1982, ApJ, 255, 325
Fisk, L. A., Schwadron, N. A., & Zurbuchen, T. H. 1999, JGR, 104, 19765
Fletcher, L., & Hudson, H. S. 2001, Sol. Phys., 69
Fletcher, L., Metcalf, T. R., Alexander, D., Brown, D. S., & Ryder, L. A. 2001, ApJ, 554, 451
Forbes, T. G., & Isenberg, P. A. 1991, ApJ, 373, 294
Forbes, T. G. 2000, JGR, 105, 23153
Galsgaard, K., & Nordlund, A. 1996, JGR, 101, 13445
Gary, G. A., Moore, R. L., Hagyard, M. J., & Haisch, B. M. 1987, ApJ, 314, 782
Gopalswamy, N., et al. 1998, GRL, 25, 2485
Gopalswamy, N., et al. 2000, GRL, 27, 145
Gopalswamy, N., et al. 2001b, JGR, 106, 29207
Gopalswamy, N., et al. 2002, ApJ, in press
Gopalswamy, N., Yashiro, S., Kaiser, M. L., Thompson, B., & Plunkett, S. 1999, Proc. Nobeyama Symp., eds. T. Bastian, N. Gopalswamy, & K. Shibasaki, p. 27
Gosling, J. T., 1993, JGR, 98, 18949
Gosling, J. T. 1999, in Coronal Mass Ejections (Geophysical Monograph 99), eds. N Crooker, J. Joslyn, and J. Feynman (Washington:AGU), p. 9
Habbal, S.R., et al. 1997, ApJ, 489, L103
Habbal, S.R., Woo, R. & Vial, J.-C. 2001, Space Sci. Rev., 97, 5
Handy, B. et al. 1999, Sol. Phys., 190, 351
Harrison, R.A. 1997, Sol. Phys., 175, 467
Harra, L.K. & Sterling, A.C., 2001, ApJ., 561, L215
Hassler, D.M. et al. 1997, Sol. Phys., 175, 375
Hassler, D.M., et al. 1999, Science, 283, 810
Hinteregger, H. E., Fukui, K., & Gilson, B. R. 1981, GRL, 8, 1147
Hirayama, T. 1974, Sol. Phys., 34, 323
Hochedez, J.-F., Jaques, L., Zhukov, A. N., & Clette, F. 2002, in Proceedings of the SOHO-11 Conference "From Solar Min to Max: Half a Solar Cycle with SOHO", ESA SP-508, in press
Hollweg, J., & Yang, G. 1988, JGR, 93, 5423
Howard, R. A., et al. 1982, APJ, 263, L101
Hudson, H.S., Acton, L.W., & Freeland, S.L. 1996, ApJ, 470, 629
Hudson, H., S., & Cliver, E. W. 2001, JGR, 106, 25199
Hudson, H.S., & Webb, D.F. 1999, in Coronal Mass Ejections (Geophysical Monograph 99), eds. N Crooker, J. Joslyn, and J. Feynman (Washington:AGU), p. 27
Ionson, I. A., 1978, ApJ 226, 650
Innes, D., Inhester, B., Axford, W. I., & Wilhelm, K. 1997, Nature, 386, 811
Jorquera, C. et al. “Design of New Photodiode Standards for Use In the MISR In-Flight Calibrator”, Proc. of IGARSS, 1994, IEEE Catalog No. 94CH3378-7, 1998-2000 (1994)
Kahler, S. W. 1992, Ann. Rev. A&A 30, 113
Kahler, S.W., & Hudson, H.S. 2001, JGR, 106, 29239
Kahler, S.W., Reames, D.V., & Sheeley, N.R., Jr. 2001, ApJ, 562, 558
Karpen, J.T., Antiochos, S.K., & DeVore, C.R. 1995, ApJ, 450, 422
Karpen, J.T., Antiochos, S.K., & DeVore, C.R. 1996, ApJ, 460, L73
Karpen, J.T., Antiochos, S.K., & DeVore, C.R. 1998, ApJ, 495, 491
Karpen, J. T., Antiochos, S.K., Hohensee, M., Klimchuk, J. A., & MacNeice, P. J. 2001, ApJ, 553, L85
Klimchuk, J. A. 1996, 1996, in Magnetic Reconnection in the Solar Atmosphere (ASP Conf. Series 111), eds. R. Bentley & J. Mariska, p. 319
Klimchuk, J. A. 2001, in Space Weather (Geophysical Monograph 125), eds. P. Song, G. Siscoe, & H. Singer (Washington:AGU), p.143
Klimchuk, J. A., & Cargill, P.J. 2001, ApJ, 553, 440
Klimchuk, J. A., & Porter, L. J. 1995, Nature, 377, 131
Klimchuk, J. A. et al. 1994, in X-Ray Solar Physics from Yohkoh (Frontiers Sci. Ser. No. 10), ed. Y. Uchida, Te. Watanabe, K. Shibata, & H. S. Hudson (Tokyo: Universal Academy Press), 181
Kopp, R. A., & Pneuman, G. W. 1976, Sol. Phys., 50, 85
Korde, R. et at. “The Effects of Neutron Irradiation on Silicon Photodiodes”, IEEE Trans. on Nuclear Sciences, 1989, Vol. 36, 2169-2175
Koutchmy, S., et al. 1997, A&A, 320, 33L
Krasnoselskikh1, V., Podladchikova1, O., Lefebvre, B., & Vilmer, N. 2002, A&A, 382, 699
Krieger, A. S., Timothy, A. F., & Roelof, E. C. 1973, Sol. Phys, 29, 505

Krucker, S., & Benz, A. 1998, ApJ, 501, L213
Krucker, S., Benz, A.O., Bastian, T.S., & Acton, L.W. 1997, ApJ, 488, 499
Laming, J. M., Drake, J., & Widing, K. 1995, ApJ, 443, 416
Landi, E. et al. 1999, Proc. 8th SOHO Workshop, ESA SP-446, 417
LaRosa, T. N., & Emslie, A. G. 1988, ApJ, 326, 997
Lean, J. 1997, Ann. Rev. Astron. Astrophys., 35, 33
Lean, J. L., et al. 1998, ApJ, 492, 390
Lean, J. L., et al. 1995, GRL, 22, 655
Lean, J. L., Warren, H.P., Mariska, J. T., & Bishop, J. 2002, JGR., submitted
Leka, K.D., et al. 1996, ApJ, 462, 547.
Li, J., Rayond, J.C., Action, L., W., Kohl, J.L., Romoli, M., Noci, G., & Naletto, G. 1998, ApJ., 506, 431
Li, Y., et al. 2001, JGR, 106, 25103
Liewer, P. C., Hall, J. R., De Jong, E. M., Socker, D. G., Howard, R. A., Vourlidas, A., Crane, P., Reiser, P.,& Rich, N. 2001, JGR, 106, 15903
Linton, M. G., Dahlburg, R. B., & Antiochos, S. K. 2001, ApJ, 553, 905
Longcope, D. W. 1998, ApJ, 507, 433
Low, B. C., 1996, Sol. Phys., 167, 217
Low, B. C. 2001, JGR, 106, 25,141
Martin, S. F. 1998, Sol. Phys., 182, 107
Martin, S.F. & McAllister, A.H. 1997, in Coronal Mass Ejections (Geophysical Monograph 99), eds. N Crooker, J. Joslyn, and J. Feynman (Washington:AGU), p. 127.
Mason, H. E., et al. 1997, Sol. Phys., 170, 143
Matthews, S. A., Klimchuk, J. A., & Harra, L. K. 2001, A&A, 365, 186
McAllister, A.H., et al. 2001, JGR, 106, 29185
McClymont, A. N., & Canfield, R. C. 1986, ApJ, 305, 936
McComas, D. J., et al. 1991, GRL, 18, 73
McKenzie, D. E., & Hudson, H. S. 1999, ApJ, 519, L93
McKenzie, F.J., Banaskiewicz, M., & Axford, I. 1995, A&A, 303, L45
Meier, R.R. 1991, Space Sci.Rev., 58, 1
Meier, R.R., et al. 2002, GRL, in press
Mikic, Z., & Linker, J. A. 1994, ApJ 430, 898
Mikic, Z., Linker, Schnack, D. D., Lionello, R., & Tarditi, A. 1999, Phys. Plasmas, 6, 2217
Moore, R. L., & Roumeliotis, G. 1992, in Eruptive Solar Flares, eds. Svestka, Z., Jackson, B. V., and Machado, M. E. (New York: Springer-Verlag), 69
Moses, J. D., et al. 1997, Sol. Phys., 175, 571
Mullan, D.J., & Ahmad, I.A. 1982, Sol. Phys., 75, 347
Mullan, D.J. 1990, A&A, 248, 256
Neugebauer, M., et al. 1998, JGR, 103, 14587
Neugebauer, M. , Liewer, P. C., Smith, E. J., Skoug, R. M., & Zurbuchen, T. H. 2002, JGR, in press
Neupert, W.N., et al. 1998, Sol. Phys.. 183, 305
Newmark, J. S., Cook, J.W., Moses, J.D., & Floyd, L.E.2000, ' 'Solar EUV Variability as Measured by SOHO/EIT," AAS SPD meeting # 32.
Newmark, J.S., Cook, J.W., & McMullin, D. 2002, "Solar Model He II A and EUV Irradiances from SOHO/EIT Derived DEM Maps," in preparation
Nolte, J. T., Krieger, A. S., Timothy, A. F., Gold, R. E., E. C. Roelof, G. Vaiana, Lazarus, A. J., Sullivan, J. D. & McIntosh, P. S. 1976, Sol. Phys., 463, 303
Ofman, L. 2000, GRL, 27, 2885
Ofman, L., & Davila, J. M. 1996, ApJ, 456, L123
Ofman, L. , Klimchuk, J., & Davila, J. 1998, ApJ, 493, 474
Ofman, L., Nakanakov, V.M. & deForest, C.E., 1999, ApJ, 514, 441
Ofman L., Romali M., Poletto G., Noci G., & Kohl J.L., 1997, ApJ 491, L111
Ofman, L. et al., 2000, ApJ, 529, 592
Ofman, L., Nakariakov, V.M., & Sehgal, N. 2000, ApJ, 533, 1071
Ostrcil, D., & Pizzo, V. 1999, in Solar Wind Nine, ed. S.R. Habbal, R. Esser, J.V. Hollweg and P.A. Isenberg, p.661
Parenti, S., Bromage, B. J. I., Poletto, G., Noci, G., Raymond, J. C., & Bromage, G. E. 2000, A&A, 363, 800
Parker, E.N. 1983, ApJ, 264, 642
Parker, E.N. 1988, ApJ, 330, 474
Parker, E. N., 1991, ApJ, 372, 719
Patsourakos, S. and Vial, J.-C., 2000, A&A, 359, L1
Patty, S.R., & Hagyard, M.J. 1986, Sol. Phys., 103, 111

Pizzo, V., & Ostrcil, D. 1999, in Solar Wind Nine, ed. S.R. Habbal, R. Esser, J.V. Hollweg and P.A. Isenberg, p.665

Plunkett, S. 2001, "Two Classes of CMEs?", AGU Spring meeting 2001, SH31-C01

Plunkett, S.P. et al. 2000, Sol. Phys., 194, 371

Plunkett, S.P. 2001, Halo CMEs in the Rise Phase of Solar Cycle 23, EOS Trans. AGU, 82(47), Fall Meet. Suppl., Abstract SH12B-0745

Poedts, S., Toth, G., Belien, A.J.C., & Goedbloed, J.P. 1997, Sol. Phys., 172, 45

Porter, L. J., & Klimchuk, J. A. 1995, ApJ, 454, 499

Priest, E. R., 1999, AP & Space Science, 264,77

Priest, E. R., et al. 2000, ApJ, 539, 1002

Prinz, D. 1973, Sol. Phys., 28, 35

Raymond, J.C., et al. 1997, Sol. Phys. 175, 645

Reale, F. 2002, ApJ, submitted

Reames, D.V. 1999, Space Sci. Rev., 90, 413

Richardson, I.G. & Cave, H.V., 1993, JGR, 98, 15295

Rose 1948. TBD (from sec. 1.3)

Rozanov E., Egorova T., Frohlich C., Haberreiter M., Peter T., & Schmutz W. 2002, in Proceedings of the SOHO-11 Conference "From Solar Min to Max: Half a Solar Cycle with SOHO", ESA SP-508, in press

Rust, D.M. 1983, Space Sci. Rev., 34, 21

Rust, D.M., 1994, GRL, 21, 241

Rust, D.M., & Hildner, E. 1976, Sol. Phys., 48, 381

St. Cyr, O. C., Burkepile, J. T., Hundhausen, A. J., & Lecinski, A. R. 1999, JGR, 104, 12493

Schmieder, B., Demoulin, P., Aulanier, G., & Golub, L. 1996, ApJ, 467, 881

Schrijver, C.J. 2001b, ApJ, 547, 475

Schwadron, N. A., Fisk, L. A., & Zurbuchen, T. H. 1999, ApJ, 521, 859

Schwenn, R. et al. 2001, A Tool for Improved Space Weather Predictions: the CME Expansion Speed, EOS Trans. AGU, 82(47), Fall Meet. Suppl., Abstract SH12A-0739

Seaton, D. B., et al. 2001, ApJ, 563, L173

Sheeley, N. R. Jr., & Wang, Y.-M. 2001, ApJ, 562, L107

Sheeley, N. R., Jr., et al. 1997, ApJ, 484, 472

Sheeley, N. R. Jr., Walters, J.H., Wang, Y.-M., & Howard, R. A. 1999, JGR, 104, 24739

Sheeley, N. R. Jr., Knudson, T. N., & Wang, Y.-M. 2001, ApJ, 546, L131

Shibata, K. et al., 1992, PASJ, 44, L173

Smith, E.J. 2001, JGR 106, 15819

Solomon, S. C., Bailey, S. M., & Woods, T. 2001, GRL 28, 2149

Sterling, A. C. & Moore, R. L. 2001a, ApJ 560, 1045

Sterling, A C., Moore, R L., Qui, J., & Wang, H. 2001, ApJ 561, 1116

Sturrock, P. A. 1966, Nature, 211, 695

Sturrock, P. A. 1989, Sol. Phys. 121, 387

Suess, S.T., Wang, A.H., Wu, S.T., & Nerney, S.F. 1999, Space Sci. Rev. 87, 323

Suess, S.T., Wang, A.H., Wu, S.T., & Nerney, S.F. 1999, JGR, 101, 9957

Tobiska, W. K. & Eparvier, F. G. 1998, Sol. Phys., 177, 147

Thompson, B.J. et al. 1999, in Sun-Earth Plasma Connections (AGU Geophysical Monograph 109), ed. J.L. Burch (Washington:AGU), p.31

Thompson, W.T., Newmark, J.S., & McMullin, D. "Comparison of SOHO EIT and CDS Irradiance Measurements," 2002, SOHO Intercalibration - ISSI.

Title, A.M., & Schrijver, C.J. 1998, ASP Conf. Ser. 154, Vol.10, 345

Tsiklauris, D., & Nakariakov, V.M. 2001, A&A, 379, 1106

Tsuneta, S. 1996, ApJ, 456, 840

Uchida, Y., et al. 1992, PASJ, 44, L155

Van Aalst, M.K., Martens, P.C., & Beliën, A.J.C. 1999, ApJLet, 511, L125

VanBallegooijen, A., & Martens, P. C. H. 1989, ApJ, 343, 971

Veselovsky, I. S., Zhukov, A. N., Dmitriev, A. V., Tarsina, M. V., Clette, F., Cugnon, P., & Hochedez, J.-F. 2001, Sol. Phys. 201, 27

Vourlidas, A., Klimchuk, J. A., Korendyke, C. M., Tarbell, T. D., & Handy, B. N. 2001, ApJ, 534, 456

Vourlidas, A., 2002, in Proc. of COSPAR Coll., Sept. 2001, Beijing, China, in press

Wang, Y.-M., 1994, ApJ, 437, L67

Wang, Y.-M., 1998, ApJ, 501, L145

Wang, Y.-M., & Sheeley, N.R., Jr. 1992, ApJ, 392, 310

Wang, Y.-M., & Sheeley, N.R., Jr. 1993, ApJ, 414, 916

Wang, Y.-M., & Sheeley, N.R., Jr. 1995, ApJ, 446, L51
Wang, Y.-M., & Sheeley, N.R., Jr. 1995, ApJ, 452, 457
Wang, Y.-M., & Sheeley, N.R., Jr. 2002, ApJ, submitted
Wang, A.H., Wu, S.T., & Poletto, G. 1998, JGR, 103, 1913
Wang, Y.-M., et al. 1997, ApJ, 484, L75.
Wang, Y.-M., et al. 1998, ApJ, 508, 899
Wang, Y.-M. et al., 1999, GRL 26, 1203
Wang, Y.-M., et al. 2000, JGR, 105, 25133
Warmuth, A., et al. 2001, ApJ, 560, L105
Warren, H. P., Mariska, J. T., & Lean, J. 1996, GRL, 23, 2207
Warren, H. P., Mariska, J. T., & Lean, J. 2001, JGR, 106, 15745
Webb, D. F., 1995, Adv. Space Res., 16, 57
Webb, D. F. 2000, JAS-TP, 62, 1415
Webb, D. F. et al. 1999, JGR, 105, 27251-27259
Wilhelm, K., et al. 2000, A&A, 353, 749
Winebarger, A. R., et al. 1999, ApJ, 526, 471
Winebarger, A.R., DeLuca, E. E., & Golub, L. 2001, ApJ, 553, L81
Wolfson, R., & Dlamini, B. 1999, ApJ, 526, 1046
Wolfson, R., & Saran, S. 1998, ApJ, 499, 496
Woo, R., & Habbal, S.R. 1999, ApJ, 510, L69
Wood, B. E. et al. 1999, ApJ, 523, 444
Worden et al. 1999, ApJ, 511, 965
Wu, S.T., Guo, W.P, & Wang, A.H. 1995, Sol. Phys., 157, 325
Wu, S.T., Guo, W.P, & Dryer, M. 1997, Sol. Phys., 170, 265
Wu, S.T., et al. 2001, JGR, 106, 25089
Wu, S.T., Wang, A.H., Plunkett, S.P., & Michels, D.J. 2000, ApJ, 545, 1101
Yokoyama, T., & Shibata, K. 1999, in Solar Wind Nine, ed. S.R. Habbal, R. Esser, J.V. Hollweg & P.A. Isenberg, p. 61
Young, P. R., & Mason H. E., 1997, Sol. Phys., 175, 523
Yurchyshyn, V. B, et al. 2001, ApJ, 563, 381
Zhang, J., et al., 2002, ApJ, Submitted
Zirker, J. B., Engvold, O., & Martin, S. F. 1998, Nature, 396, 440

A.2 Acronyms.

ASIC	Application Specific Integrated Circuit
CCB	Change Control Board
CCB	Configuration Change Board
CUA	Catholic University of America
CV	Curriculum Vitae
DEM	Differential Emission Measure
DOWG	Data Operations Working Group
DRAF	Data Reduction and Analysis Facility
E/PO	Education and Public Outreach
EEE	Electrical, Electronic, and Electromechanical
EIT	Extreme-ultraviolet Imaging Telescope
FMEA	Failure Modes and Effects Analyses
GDS	Ground Data System
HRTS	High Resolution Telescope and Spectrograph
IMS	Integrated Master Schedule
IPDT	Integrated Product Development Team
IPO	Instrument Project Office
ITAR	International Traffic In Arms Regulations
ITM	Instrument Technical Manager
LASCO	Large Angle Spectrometric Coronagraph
LLIS	Lessons Learned Information System
LOA	Letter of Agreement
LOA	Letter of Agreement
MAE	Mission Assurance Engineer
MAE	Mission Assurance Engineer
MOA	Memorandum of Agreement
MRD	Mission Requirements Document
NRL	Naval Research Laboratory
PAPL	Program Approved Parts List
PCM	Project Control Manager
PCMS	Project Management and Control System
PCP	Parts Control Program
PI	Principal Investigator
PMCS	Project Management Control Process
PPARC	Particle Physics and Astronomy Research Council
RM	Risk Management
S/W	Software
SDO	Solar Dynamics Observatory
SEC	Sun Earth Connections
SECEF	Sun-Earth Connections Educational Forum
SHARPP	Solar-Heliospheric Activity Research and Prediction Program
SHEB	SHARPP Electronics Box
S-IPM	SHARPP Instrument Project Manager
S-IPO	SHARPP Instrument Project Office
S-ISE	SHARPP Instrument Systems Engineer
SR&QA	Safety, Reliability, and Quality Assurance
SRD	Science Requirements Document
SRR	System Requirement Review
SWx	Space Weather
TAA	Technical Assistance Agreement
TPM	Technical Performance Metrics
V&V	Verification and Validation

B. International Agreements

During Phase A, NRL will support the SDO Project Office in establishing a Letter of Agreement (LOA) with the UK (PPARC), Belgium (OSTC), France (CNES), and Italy (IAS). This appendix contains draft LOAs for three countries.

C. Compliance with U.S. Export Laws and Regulations

The Naval Research Laboratory (NRL) is the sponsoring institution and an instrumentality of the United States. It is exempt from certain licensing requirements imposed under 22 C.F.R. parts 120-130 and 15 C.F.R. Parts 730-774. All disclosures of information and deliveries of materials made to foreign participants identified in this proposal will be made in strict compliance with all applicable U.S. Navy and Department of Defense security regulations and procedures. Export controls employed in the SHARPP program will mirror those that have been successfully followed in the SECCHI component of the NASA Solar Terrestrial Probe STEREO mission where Letters of Agreement (LOAs) between NASA and its European partners have been implemented.

❒ As planned and implemented in Phase A, the SHARPP program will use formal Memoranda of Agreement (MOA) between the NRL and European consortium partners. These will define the terms of collaboration for development of non-cash contributions for SHARPP instrumentation.

❒ The MOA is a contractual/cooperative agreement between the NRL and a non-U.S. partners. While similar to the LOA, it is more detailed, and it is mandatory for all ITAR items to have a MOA in place prior to requesting an Export license or prior to shipping on a temporary basis. Table C-1 provides the critical elements of a MOA document.

Following approval within NRL, the MOAs will be submitted to the U.S. Department of Defense Foreign Affairs Office through the NASA SDO Project Office. As in STEREO, the MOA serves as a LOA and allows U.S. Government instrumentalities to accomplish specifically described exchanges with the signatory foreign institutions. Our recent and successful STEREO mission experience with processing Technical Assistance Agreements (TAA) for our U.S. non-government co-investigators reflects a DoD commitment to expedite the approval process for foreign collaborations.

Table C-1. Critical Elements of a Memoranda of Agreement

• Purpose
• Mission description and participation
• NRL responsibilities
• European partner responsibilities
• Program and project management
• Scientific investigations
• Funding or limits of obligation
• Data distribution
• Coping mechanisms for programs occurring in the development phase and any related schedule impacts or with anomalous in-flight behaviors
• Personnel accommodation
• Support Equipment
• Transfer of technical data and goods
• Inventions and patent rights
• Customs and taxes
• Public information
• Liability
• Registration
• Settlement of disputes
• Implementing arrangements
• Amendment
• Entry into force, duration and termination
• Software data exchange principles